Molecular Mechanism of Sphingosine-1-phosphate Action in Duchenne Muscular Dystrophy

Diem-Hang Nguyen-Tran

A dissertation

submitted in partial fulfillment of the

requirements for the degree of

Doctor of Philosophy

University of Washington

2013

Reading Committee:

Hannele Ruohola Baker, Chair

Raymond David Hawkins

Morayma Reyes

Program Authorized to Offer Degree:

Molecular and Cellular Biology

University of Washington

Abstract

Molecular Mechanism of Sphingosine-1-phosphate Action in Duchenne muscular dystrophy

Diem-Hang Nguyen-Tran

Chair of the Supervisory Committee:

Professor Hannele Ruohola-Baker

Department of Biochemistry

Duchenne Muscular Dystrophy (DMD) is a lethal muscle wasting disease. In *Drosophila,* a genetic increase of the bioactive lipid Sphingosine-1-Phosphate (S1P) and oral delivery of 2-Acetyl-5-tetrahydroxybutyl imidazole (THI), an S1P lyase inhibitor, suppresses dystrophic muscle degeneration. In dystrophic mice, up regulation of S1P by THI increases muscle force, fiber size and reduces fibrosis as well as fat deposition. S1P can exert extracellular and intracellular mode of function, acting as a ligand for mammalian S1P receptors and as a repressor for HDAC1 and HDAC2 activities. Since *Drosophila* lacks orthologues for S1P receptors and because muscular dystrophies correlate with increased HDAC2 protein levels, we tested whether the common molecular mechanism for the S1P effect in muscle involves HDAC inhibition. Here, we show that total nuclear HDAC activity, HDAC2 protein levels and HDAC2 activity are

increased in several *mdx* muscle types. Importantly, THI-treatment significantly increased nuclear S1P and decreased HDAC activity in injured *mdx* TA muscles. In un-injured *mdx* mice, a one-month THI treatment similarly increased muscle nuclear S1P levels, decreased HDAC activity and furthermore, increased H3K9, K18 and H2BK12 acetylation. In addition, we observed an increased expression of HDAC2 target genes. These effects correlate with reduced white blood cell number and diaphragm fibrosis in addition to an increased normal Titin pattern in the sarcomeres. We also demonstrate a significant decrease in gene expression of inflammation-related genes and an increase in metabolic genes; especially genes involved in fatty acid metabolism in THI-treated adductor muscles by using a microarray-based gene expression analysis. Finally, we show an increase in cellular S1P levels and a functional increase in mitochondrial activity, especially in fatty acid oxidation after THI treatment of differentiating C2C12 cells. This result supports our proposal that THI treatment is beneficial for the energy metabolism of *mdx* muscles.

Acknowledgements

I would like to give my sincere and deepest thanks to my supervisor, Dr. Hannele Ruohola-Baker, as without her, I would not have come this far in my graduate study. Her guidance, focus direction, motivation, and patience helped me learn a lot since I joined her laboratory.

I am also thankful to my committee members, Dr. David Hawkins, Dr. Morayma Reyes, Dr. Stephen Tapscott, Dr. Celeste Berg and Dr. Peter Byers for taking time out of their very busy schedules to help me along my research path. I am especially grateful to Dr. Hawkins and Dr. Reyes for spending time teaching me to do experiments and for being in my reading committee.

For their company through good and bad times, through laughter and tears, for their encouragement, instruction and help, I would like to thank my lab mates: Julie, Yalan, Kavitha, Henrik, Amy, Wenny, Karin and Mario. Special thanks goes to my old lab mate, also my first mentor in the US, Luther Davis, for his patience and kind instruction.

My best cousin, Christine Le deserves big thanks for her kind and sincere love, for always being there for me, for helping me survive and enjoy life in the US. I am also very lucky to have the support and love from my aunts, uncles and cousins who gave me “a home away from home”.

Above all, I thank my parents, siblings, nieces and nephews, for their unconditional love, support, encouragement and comfort. I thank my boyfriend, Don Pinto and the Pinto family for keeping me motivated along the way without giving up.

I thank God for blessing me and choosing me to become a scientist. I surely could not have come this far in my study without God's will. I thank Mother Mary for her peaceful love and for always being there to comfort me.

A house cannot be built without a foundation, likewise, I wouldn't have become who I am today without the education and orientation from my parents. Even though growing up in a small village in a developing country, I still had a chance to receive the best education conditions possible in our system. My dad brought me the best books he could find, my mom found me good tutors when I was a kid. Before he died, my dad asked my mom to make sure I would finish my PhD. My mom, being very old now, traveled all the way from Vietnam to the US to accompany me in my time of crisis. She stayed up as late as I did to watch me writing my thesis. She cried with me over my stress, and gave me the best comfort she could.

For their nurturing, tremendous caring, unfailing love, teaching, provoking my love for science, providing me with the best study conditions ever, I dedicate this dissertation to my parents.

Many thanks,

DIEM-HANG NGUYEN-TRAN

Table Of Contents

List Of Figures

List Of Tables

List Of Abbreviations

Abbreviation	Full name
2DG	2 Deoxy-D-glucose
CaM	Calmodulin
CaMK	$Ca^{2+/}$calmodulin-dependent protein kinases II
CaMKII	Calmodulin kinase II
CTX	Cardiotoxin
DGC	Dystrophin –associated protein complex
DHS1P	Dihydro sphingosine-1-phosphate
DHSph	Dihydro sphingosine
DMD	Duchenne Muscular Dystrophy
ECAR	Extracellular acidification rate
ECM	Extracellular Matrix
EDL	Extensor Digitorum Longus
ER	Endoplasmic Reticulum
ETO	Etomoxir
FAD	Flavin Adenine Dinucleotide
FCCP	Carbonilcyanide *p*-triflouromethoxyphenylhydrazone
Gastro	Gastronemius
HAT	Histone acetyltransferases
HDAC	Histone Deacetylase
HDACi	Histone Deacetylase inhibitor

MEF2	Myocyte Enhancer Factor-2
MHC	Myosin Heavy Chain
NAD^+	Nicotinamide Adenine Dinucleotide
NES	Nuclear export signal
NFAT	Nuclear factor of activated T-cells
NLS	Nuclear localization signal
nNOS	Neuronal nitric oxide synthase
NO	Nitric oxide
OCR	Oxygen consumption rate
PGC-1α	Peroxisome proliferator-activated receptor-γ coactivator-1-α
PLA	Plantaris
PPAP-δ	Peroxisome Proliferator-Activated receptor δ
S1P	Sphingosine-1-phosphate
S1PR	Sphingosine-1-phosphate receptor
Sph	Sphingosine
SphK	Sphingosine kinase
SR	Sarcoplasmic Reticulum
TA	Tibialis Anterior
THI	2-Acetyl-5-tetrahydroxybutyl Imidazole
WV	White Vatus

Introduction

Duchenne muscular dystrophy (DMD) is an inherited disease characterized by extreme muscle wasting that deprives the patients' ambulation by the age of 12 and leads to an unavoidable death in their twenties (Moser, 1984; Blake et al., 2002). The prevalence and severity of DMD requires immediate attention to find a cure for this lethal disease. DMD is caused by mutations in the gene coding for dystrophin, resulting in a total absence or trace levels of the dystrophin protein (Fairclough et al., 2013). To tackle these genetic mutations, gene therapy was proposed to replace the damaged genes with fully functional genes. This is an obstacle because delivering genes to non-dividing adult muscles that account for 40% body mass is very challenging (Wang and Pessin, 2013). Furthermore, because of its huge size (427KDa) (Koenig et al., 1988), full-length dystrophin is unable to be packed into a viral vector for delivery to the muscle fibers. To circumvent this issue, mini-dystrophin, containing functional domains of the protein, has been used instead, but it can only alleviate the disease to a small extent because most of other important parts of dystrophin have been removed (Fairclough et al., 2013). Compensating dystrophin by its related protein, utrophin is a promising strategy, but the current utrophin-increasing methods failed to raise utrophin above the benchmark level required for preclinical rescue (Tinsley et al., 1998). Alternatively, targeted gene correction (TGC) to fix the mutated gene is a potential approach to treat DMD. Although promising results are evident for TGC in a favorable condition model, practical applications in DMD patients still need a long time to resolve TGC side effects, among which cancer risk caused by off-target cleavage is the biggest problem (Chapdelaine et al., 2010). In an attempt to repair damaged muscle with healthy myogenic stem cells, the powerful cell-based therapy approaches have been tested. Disappointingly, no significant improvement in muscle function has been yet achieved using this

method (Spitali and Aartsma-Rus, 2012), suggesting that more research is required to develop a successful stem cell based therapy for DMD. To provide more options for tackling DMD, a number of pharmacological approaches have been tried, in which exon skipping gives the most encouraging outcome on dystrophin protein restoration and modest muscle function enhancement. However, the exon skipping method only addresses a particular proportion of DMD patients by targeting one of the many dystrophin mutations. Moreover, it requires life-long administration of exon-skipping oligos, raising the potential toxicity of these non-degradable oligonucleotides (Chapdelaine et al., 2010).

In summary, DMD treatments are en route to patients, however, how long we need to wait until the research behind these treatments are successfully applied in a clinical setting is an unanswered question. In the mean time, there is an urgent need for lengthening DMD patients' life span and improve muscle function. There have been a number of pharmacological strategies designed to tackle the disease progression, but not the genetic mutation itself. These approaches attempt to treat inflammation, fibrosis, fat deposition and calcium homeostasis (Engvall and Wewer, 2003; Mozzetta et al., 2009).

Currently, steroids are the only drugs that have been used to treat DMD for over two decades, and can extend the patients' ambulation for around two years. The main mechanism of action in steroids is characterized by suppressing inflammation and accompanied muscle damage and fibrosis, without increasing dystrophin level. To get extended ambulation for just 2 years, DMD patients face a number of steroid side effects that badly impact the quality of their lives. Young boys not only have to counter a problem with weight gain, where they must adopt a restricted

diet, but must also deal with hypertension that endangers their lives. Furthermore, their bones get demineralized and their physical features and behavior are also affected (Spitali and Aartsma-Rus, 2012). Because of the side effects associated with steroids, a safer and immediate alleviating therapy to improve muscle function and lengthen patients' lifespan is needed while waiting for gene and cell-mediated therapies to resolve their potential problems.

A number of research groups are working on finding immediate pharmacological strategies for DMD, among which is the Ruohola-Baker laboratory. A genetic suppressor screen in *Drosophila* revealed that mutants that should result in an increase in bioactive lipid Sphingosine-1-Phosphate (S1P) suppress dystrophic muscle defects in *Drosophila* (Kucherenko et al., 2008; Pantoja et al., 2013; Pantoja and Ruohola-Baker, 2013). Furthermore, increasing S1P levels by oral delivery of THI, a S1P lyase inhibitor also leads to suppression of dystrophic muscle degeneration in flies (Pantoja et al., 2013). In mice, administration of THI is beneficial in the recovery from acute muscle injury in the *mdx* dystrophic model (Loh et al., 2012; Ieronimakis et al., 2013). Treating *mdx* mice after acute injury with S1P promoted muscle regeneration by increasing satellite cell proliferation and myofiber size *in vivo*. THI treatment in dystrophic mice increased muscle fiber size, decreased fibrosis and fat deposition and significantly increased muscle force (Ieronimakis et al., 2013). THI is a non-toxic component of caramel food coloring approved for use by the FDA (Schwab et al., 2005). Intriguingly, there is no evidence of increased dystrophin level in THI/S1P-treated *mdx* mice, yet their muscle function is still significantly improved. My goal has been to explore the actions of S1P that benefit the muscles. S1P has been implicated in cell proliferation and differentiation (Neri et al., 2007; Neubauer and Pitson, 2013) and especially in promoting muscle regeneration via the activation of satellite cells (SC) (Loh et al., 2012). S1P

has long been shown to exert its action through extracellular function, acting as a ligand for mammalian S1P G-protein coupled receptors (GPCR). In a concomitant investigation of THI effects on *mdx* mice, the Saba group proposed that S1P promotes muscle regeneration by inducing satellite cells activation through S1PR2 (Loh et al., 2012). The Reyes group observed an up regulation of S1PR1 along with an increased regeneration in S1P-treated *mdx* mouse muscles (Ieronimakis et al., 2013). While this extracellular function of S1P nicely explains the regeneration aspect of S1P benefits on *mdx* mice, it fails to explain the actions on *Drosophila* that do not have orthologues for S1P receptors. Moreover, boosting regeneration should not be the only benefit of S1P, as it has been shown to decrease muscle degeneration as well (Pantoja et al., 2013). Furthermore, to be beneficial for DMD, S1P should have more functions rather than just enhancing muscle regeneration. My prediction is that S1P is involved in other mechanisms that help to alleviate muscle damage and protect contractile protein components. Ieronimakis et al. proposed another explanation for S1P action when observing an increased level of phosphorylated ribosomal protein S6 (P-rpS6) in THI-treated muscles (Ieronimakis et al., 2013). They suggested that the AKT-mTOR-S6 Kinase pathway is a potential mechanism that S1P employs to elevate protein synthesis, and thus increasing muscle mass. This is interesting to follow, but my prediction is that S1P acts on more than just muscle mass. THI was previously shown to inhibit S1P lyase, which is an enzyme located in the endoplasmic reticulum, with its active site oriented towards the cytoplasm (Saba and de la Garza-Rodea, 2013). As per this inhibition and the orientation of S1P lyase, the elevation of intracellular levels of S1P must take place prior to export. Recent discoveries have pointed out several intracellular functions of S1P, among which the *in vitro* inhibitory effect of S1P on HDAC2 in the nucleus came to my attention because muscular dystrophies correlate with increased HDAC2 levels and HDAC

inhibitors have been shown to be beneficial for the DMD disease (Minetti et al., 2006; Colussi et al., 2008; Consalvi et al., 2013).

Being fascinated by epigenetics that can regulate gene expression without altering the DNA sequence, with the wish to contribute in treating an inherited disease, I chose to employ gene expression profiling and HDAC activity assays to elucidate the molecular mechanism of S1P action on DMD. This dissertation will reveal interesting data demonstrating the intracellular function of S1P on inhibiting HDAC, especially HDAC2 activity and thereby increasing histone acetylation in THI-treated muscle samples. I will also present microarray data showing S1P induction of gene expression of beneficial-, insulin related-, metabolism-, Wnt-, slow-twitch muscle genes. I will also present the potential action of S1P on inducing shifts in the metabolic mechanism of muscle fiber types, which I find exciting. I will discuss in detail how this shift benefits DMD and how we can take advantage of it in treating DMD in the discussion chapter.

During my studies, other approaches have also revealed new, complementary compounds to treat DMD (Gehrig et al., 2012). THI and other new components are better suited than steroids for use in the current generation of dystrophic patients because of their predicted lower side-effect. Elucidation of the S1P action on dystrophic muscles will not only give a better understanding of the DMD disease at the molecular mechanism level, but will also provide a good interim solution to treat DMD that does not need to tackle the huge and problematic dystrophin protein itself, paving a more achievable path for DMD therapy.

Chapter 1: Background

1.1 Skeletal muscle

Skeletal muscles constitute more than 40% of the body mass of a given individual and play critical roles in locomotor activity (Wang and Pessin, 2013). Skeletal muscle tissues attach to the bone via tendons, and regulate movement under voluntary control. In the adult human, muscle fibers, which are elongated muscle cells with dimensions of 2-3cm in length and 100μm in diameter, are organized into bundles to form muscle tissues (Alberts et al., 2002). Muscle cells are unique in two main ways: (1) one muscle cell contains multiple nuclei, located in the periphery of the cell, and (2) the main components in muscle cells are contraction proteins, which are arranged in repeated contractile units called sarcomeres.

In our experiments, four types of skeletal muscle tissues were used: (1) diaphragm, (2) adductor, (3) gastrocnemius (gastro), and tibialis anterior (TA). The diaphragm separates the chest from the abdomen and plays an important role in respiration. Adductor muscles arise from the pelvis, and attach to the femur. Adductors stabilize the hip joint and help in pulling the leg towards the midline of the body. Adductor muscles include the adductor magnus, longus, brevis, minimus, pectineus, and gracilis. Gastro is the largest muscle of the leg calf and helps in maintaining body posture. TA runs from the tibia to the bones of the ankle and foot. It helps the toes to move up and down (Halmilton et al., 2001; Werner, 2004; Jenkins et al., 2007).

1.1.1 Skeletal muscle structure

Each muscle fiber is composed of thousands of parallel myofibrils, which are surrounded by the sarcoplasmic reticulum. Each myofibril contains myofilaments, including thin and thick

filaments arranged in repeating units called the sarcomere. Thin filaments consist of actin proteins with one end anchored to the Z disk of the sarcomere via a Z disk-bound protein while the other end is free to interact with thick filaments. Thick filaments are made of myosin proteins that are attached to the center of the sarcomere with the heads being free to interact with the actin strands in thin filaments. In a muscle contraction, the myosin heads slide longitudinally past the actin filaments (Campbell et al., 1999).

In addition to thin and thick filaments, muscle myofibril also has a large elastic filament composed of Titin proteins that span from the Z disk to the M line regions of the sarcomere. Titin has been shown to develop passive force when the muscles are stretched (Granzier and Labeit, 2006) and proposed to be involved in assembly and function of the muscle sarcomere (Tskhovrebova and Trinick, 2010).

1.1.2 Skeletal muscle contraction

When a stimulus for contraction is present, the brain transduces the signal to motor neurons. Each motor neuron can branch and control several muscle fibers. The neurotransmitter acetylcholine is then released from the motor neurons and diffuses across the neuromuscular junction, which causes the depolarization of the plasma membrane of muscle fibers. The depolarization triggers an action potential that travels into the T tubules of the muscle, changing the permeability of the sarcoplasmic reticulum (SR) and ultimately leads to the release of Ca^{2+} (Campbell et al., 1999). Calcium then binds to troponin protein, altering the troponin-tropomyosin interaction to expose the binding sites of myosin on actin molecules. The myosin head then hydrolyses ATP to ADP and an inorganic phosphate Pi. The hydrolysis of ATP provides the energy to switch the myosin head conformation to a high-energy configuration.

Myosin heads then bind to actin strands. ADP and Pi are then released, switching the myosin head conformation to its low-energy configuration, and as a result, pulling the thin filaments toward the center of the sarcomere, hence, shortening the sarcomere length. When a new ATP binds to a myosin head, it no longer interacts with actin and the cycle repeats. The pulling of many myosin heads results in sarcomere contraction. Simultaneous contraction of sarcomeres will shorten the myofibril, causing the muscle cell to contract. Many muscle cells contracting together will lead to movement. When calcium is pumped back into the SR, the calcium concentration in the cytoplasm drops, causing the myosin binding sites to be blocked and contraction stops (Campbell et al., 1999).

1.1.3 Muscle development and regeneration

Myoblasts are the precursors of skeletal muscle fibers. Regulatory factors belonging to the MyoD and MEF2 families regulate gene expression to impart mature muscle cells their unique characteristics, and establish memory of the committed state in myoblasts. Myoblasts continue to proliferate for a period then stop to differentiate into mature muscle cells. During the differentiation step, myoblasts fuse together to form a multinucleated muscle fiber. Once the cells complete differentiation, they stop dividing, and thus, to replace degenerated muscles, the body needs to mobilize muscle stem cells to differentiate (Alberts et al., 2002). The special skeletal muscle stem cells in the adult body are called satellite cells (Alberts et al., 2002). Satellite cells are located beneath the muscle basal lamina (Muir et al., 1965) and remain in a quiescent state in normal conditions. When there is a myotrauma, satellite cells are activated and proliferate. Among the proliferating population, some cells replenish the quiescent satellite cell pools through a self-renewal process while other cells migrate to the injured regions. There, depending on the severity of the injury, myoblasts either fuse to damaged myofibers or fuse to

themselves to produce new myofibers. Muscle regeneration results in central nuclei morphology in regenerating fibers, which will end up migrating to the peripheral position later (Hawke and Garry, 2001).

1.1.4 Muscle repair

When skeletal muscles get injured, inflammatory cells are recruited to the injured sites. There, inflammatory cells have two main tasks: first, they phagocytose cell debris; second, they release growth factor and cytokines to stimulate migration, proliferation and survival of other cell types. Growth factors are believed to activate satellite cells, resulting in muscle regeneration and muscle repair (Serrano and Munoz-Canoves, 2010). For successful fusion, satellite cells rely on scaffolds, which are composed of a basement membrane of necrotic fibers to maintain correct orientation. In addition, muscle repair requires increased levels of extracellular matrix (ECM) components, including fibronectin, collagen I and II, and proteoglycan. The major ECM producing cell is the fibroblasts (Mann et al., 2011). ECM components will be degraded after the regeneration process by the act of matrix metalloproteases (Serrano and Munoz-Canoves, 2010). In muscular dystrophies, degeneration exceeds regeneration leading to unrepaired muscles. This results in accumulation of ECM components that causes permanent fibrosis. After that, fat is infiltrated into the muscle tissues to replace the necrotic fibers. Fibrotic tissues can be detected by staining collagen, the ECM protein, with picrosirius red. Fat infiltration can be visualized with Oil Red O staining.

1.1.5 Muscle types

Muscle contraction is triggered by an action potential and maintained by elevated cytoplasm calcium concentration. The duration of contraction is an identifiable feature of slow twitch (type

I) and fast twitch muscles (type IIa-oxidative, glycolytic and IIb-glycolytic). As denoted by their name, fast twitch muscles have quick and short contraction time while slow twitch muscles have long contraction time (about five times longer than slow twitch). Slow and fast twitch muscle can also be distinguished by their distinct physiological characteristics, protein expression (the myosin heavy chain – MyHC isoforms), and especially metabolic activity. Slow twitch muscles contain more mitochondria and myoglobin than fast twitch muscles and use fatty acids as a main energy source, whereas fast twitch muscles rely on glucose (Campbell et al., 1999). Regarding distinct protein expression, at least two discrete isoforms have been identified for most of the contraction-involved proteins, such as MHC, myosin light chain, troponin I, troponin T, troponin C, actinin, etc. For example, MHCs have Myh7 for type I slow fibers, Myh4 for type IIb glycolytic fast twitch fibers, and Myh2 for type IIa fibers (Schiaffino and Reggiani, 1996; Pette and Staron, 2000; Soares et al., 2007; Simmons et al., 2011). Muscle tissues in our body are composed of a mixture of slow and fast twitch fibers, and are characterized by the percentage contribution of each muscle fiber type. Soleus, a muscle in the back part of the lower leg, which consists of 84% type I, 16% type IIa, 0% type IIb fibers is considered as slow muscle. On the other hand, extensor digitorum longus muscle (EDL), which includes only 3% type I, but up to 57% type IIa and 40% IIb is called fast twitch muscle (Song et al. 1999). The other fast twitch muscles are plantaris (PLA), and white vatus (WV) (Potthoff et al., 2007). More satellite cells have been found in the soleus than in fast twitch muscles in the limbs (Schmalbruch and Hellhammer, 1977; Kelly, 1978).

Slow and fast twitch muscle switch

Before birth, specific developmental cues determine the formation of fast- and slow-twitch muscles (Schiaffino and Reggiani, 1996). After birth, the adult myofiber phenotype can be

changed (Bassel-Duby and Olson, 2006; Simmons et al., 2011). The switch between fiber type components is regulated by the motor innervation pattern. The induction of shifting preexisting fast to slow twitch fibers is mediated by repetitive use such as aerobic exercise and a tonic, low frequency (10-20Hz) motor neuron stimulation along with high concentration of intracellular calcium (100-300mM). The reverse process of conversion from slow to fast twitch fibers is involved with decreased neuromuscular activity and phasic, high frequency (100-150Hz) myofiber stimulation. (Olson and Williams, 2000; Simmons et al., 2011). Regarding gene regulators, Nuclear factor of activated T-cells (NFAT), calcineurin, Ca^{2+}/calmodulin-dependent protein kinases II (CaMK), Peroxisome proliferator-activated receptor-γ coactivator (PGC-1α) and peroxisome proliferator-activated receptor delta (PPAPδ) have been implicated in upregulating fatty acid oxidation and slow-fibers specific gene expression (Chin et al., 1998; Delling et al., 2000; Naya et al., 2000; Wu et al., 2000; Lin et al., 2002). In addition, MEF2, a myocyte enhancer factor 2 transcription factor is activated in slow twitch muscles (Wu et al., 2000) and responds to a calcium-dependent pathway that induces the formation of slow twitch muscle (Wu et al., 2001). Lately, Peroxisome proliferator-activated receptor γ coactivator 1β (PGC-1β) has been identified as a potential factor in promoting fast twitch formation (Arany et al., 2007). Slow twitch fibers have been shown to be more sensitive to insulin than the fast ones (Song et al., 1999). After incubation with insulin, there was more response to insulin from all signaling intermediates in soleus than EDL muscles. In particular, there was quicker and higher up regulation of the activated form (phosphorylated) of insulin receptor (IR), insulin receptor substrate 1 (IRS1), insulin receptor substrate 2 (IRS2), protein kinase B (AKT), and an elevated level of the subunit of p85α and the lipid phosphatidyl inositol 3 phosphate in soleus compared to EDL.

1.1.6 Examining the metabolic profile

As the metabolic mechanism is the main distinguishable feature of slow and fast twitch muscle, it is important to understand how the cells utilize glucose or fatty acids to generate energy. Both glucose and fatty acids can produce energy for the body through a process called aerobic oxidation, known as glucose oxidation and fatty acid oxidation, respectively. However, only glucose can generate ATP in the absence of oxygen, through a process called anaerobic glycolysis (Lodish et al., 2007). Glycolysis is first initiated by mobilizing glucose from the blood or breaking down the glycogen polymer. Glucose is converted to pyruvate in the cytosol of the cell. Fatty acid oxidation starts with free fatty acid that the cell uptakes from the blood or from hydrolyzing triglycerides. The fatty acid is then converted into fatty acyl CoA in the cytosol. The conversion of glucose to pyruvate, and fatty acid to fatty acyl CoA is the first stage of aerobic oxidation. The three other stages occur inside the mitochondria. The mitochondria are organelles of the cells that function in cellular respiration. They have two membranes (outer and inner) and two subcompartments (the intermembrane space between the two membranes and the matrix surrounded by the inner membrane). Stage II of oxidation takes place in the matrix while stage III and IV occur on the inner membrane of the mitochondria (Lodish et al., 2007).

Pyruvate and fatty acyl CoA produced in stage I are transported into the matrix of the mitochondria to join stage II of the oxidation. In this stage, pyruvate and fatty acyl CoA are converted to acetyl CoA, with the formation of NADH, CO2 (for pyruvate) and Flavin Adenine Dinucleotide (FADH2) and NADH (for acetyl CoA). Next, Acetyl CoA enters the citric acid cycle where it is oxidized and generates reduced coenzymes carrying high-energy electrons: NADH and FADH2, along with GTP and CO2. The coenzymes move to the inner membrane

where stage III takes place. In stage III, electrons from NADH and FADH2 enter the electron transport chain and finally reduce oxygen to water. The released energy from electron transportation creates a proton-motive force that pumps protons from the matrix to the intermembrane space. This results in a proton gradient that is used by the ATP synthase to produce ATP from ADP and Pi in stage IV, which is also called oxidative phosphorylation (Lodish et al., 2007).

In the absence of oxygen, pyruvate undergoes anaerobic glycolysis where it is metabolized to lactate, producing only 2 ATPs. When oxygen is available, 36 ATPs are produced through glycolysis, and 48 or 144 ATPs are formed from the oxidation of a short 8-carbon fatty acid or a fat with three chains of this length, respectively. This clearly demonstrates that our body gets more energy by burning fat.

Seahorse Extracellular Flux analyzer

The seahorse extracellular flux analyzer is a special apparatus used to examine the metabolic profile of cells. It provides real-time measurement of two metabolic parameters: (1) oxygen consumption rate (OCR), an indicator of mitochondrial respiration level, and (2) extracellular acidification rate (ECAR), which measures glycolytic activities (Wu et al., 2007).

For the OCR value, seahorse measures the dissolved oxygen in the culture media to determine the level of oxygen the cells have used, denoting the degree of cellular respiration through mitochondria activity. In order to clearly visualize the difference in OCR between various treatments applied to the cells, the mitostress assay is employed. In this assay, mitochondrial ATP synthase is first inhibited by oligomycine (Chappell and Greville, 1961). Next, maximum

mitochondrial respiration is stimulated by adding a proton gradient discharger, carbonyl cyanide 4-(trifluoromethoxy) phenylhydrazone (FCCP) (Brennan et al., 2006). FCCP allows the electron transport chain to be used to its full capacity, without using energy to pump protons. Finally, maximum OCR change after FCCP addition is calculated as a difference between OCR values before and after adding FCCP, and the maximum turn over of the electron transport chain uncoupled from ATP synthesis is recorded.

To examine fatty acid oxidation capacity, we used a fatty acid oxidation stress analysis. In this assay, palmitate, an exogenous fatty acid substrate is injected into the cell medium, which enables us to record the maximum capacity of the cells to oxidize fatty acids. Afterwards, the fatty acid oxidation is stopped by adding etomoxir (ETO) – an inhibitor of CPT-1 (carnitine palmitoyl transferase) (Schrauwen et al., 2002). Maximum OCR changes due to ETO are then calculated and refer to fatty acid oxidation capacity.

For the ECAR value, seahorse measures pH-change by recoding the free protons produced mostly from lactic acid, an end product of anaerobic glycolysis. To get pronounced changes in ECAR values in different cell treatments, the glycolysis stress assay is used. The cells are first incubated with a glycolysis substrate, glucose, and maximum glycolysis is induced by adding oligomycine that blocks pyruvate from entering into the mitochondria to join the tricarboxylic acid cycle (TCA) for respiration. Finally, glycolysis is stopped by the action of a glycolysis inhibitor, 2 Deoxy-D-glucose (2DG) (Stafstrom et al., 2008). Maximum glycolysis capacity is then recorded by subtracting the lowest ECAR value obtained after adding 2-DG from the highest ECAR value obtained after adding Oligomycin.

1.2 Duchenne Muscular Dystrophy (DMD)

DMD is an X-linked recessive inherited disease occurring in 1 out of 3,500 male births (Blake et al., 2002). It causes progressive muscle wasting and eventually leads to death. DMD patients are clinically normal at birth, though having elevated serum creatine kinase. The first symptoms of DMD start showing in children between 2 to 5 years of age, which entail delayed motor achievement milestones and a waddling gait. Then, pseudohypertrophy starts to take place in calf muscles and the patients exhibit reduced strength in limb muscles. As muscular dysfunction gradually progresses, the boys end up confined to a wheelchair by 12 years of age and die in their twenties as a result of respiration or cardiac failure (Moser, 1984; Emery, 1991; McDonald et al., 1995; Blake et al., 2002; McDonald, 2002; Eagle et al., 2007; Bach and Martinez, 2011).

1.2.1 DMD pathologies

Regarding the histological aspect, DMD muscles are mostly normal in fetuses. After birth, muscle degeneration appears with a necrotic group, accompanied by inflammation (macrophages and CD4+ lymphocytes) and active regeneration, denoted by the central nuclei muscles. With time, regeneration fails to repair severe degeneration, resulting in muscle replacement by fibrosis and fat infiltration. At this point, pseudohypertrophy appears and later becomes atrophy. Progressive fibrosis and muscle loss cause muscle wasting and finally muscle weakness (Blake et al., 2002).

1.2.2 Causes of DMD

In 1987, mutations in the Dystrophin gene were shown to be causal for DMD (Hoffman et al., 1987). Dystrophin, located on the X chromosome, is one of the largest genes in the human

genome, spanning over 2.4 million base pairs. It is 90 times the size of most genes (Pichavant et al., 2011) and consists of 79 exons, coding for a 14Kb mRNA. Among the dystrophin mutations, 65% are caused by the whole-or-part-of-gene deletions (Fairclough et al., 2013), 83% by out-of-frame deletions (Mendell et al., 2010; Muntoni and Wood, 2011), and 15% by premature-termination codons (Flanigan et al., 2003). Exons 2-20 and 45-53 are the two "hot spot" regions for mutation in the dystrophin gene. These mutations result in undetectable or trace levels of dystrophin protein in DMD patients (Fairclough et al., 2013). Some other types of dystrophin mutations cause a milder dystrophy disease called Becker muscular dystrophy (BMD). BMD occurs mostly due to in-frame deletions of the rod domain of the dystrophin gene. This mutated dystrophin encodes for partially functional dystrophin proteins leading to variable disease course (Bushby and Gardner-Medwin, 1993).

1.2.2.1 Dystrophin-associated glycoprotein complex (DGC)

Dystrophin is a 427KD intracellular protein (Koenig et al., 1988), located beneath the sarcomere plasma membrane (Zubrzycka-Gaarn et al., 1988). It is expressed mainly in the skeletal and cardiac muscles, and to a lesser extent in the brain (Fairclough et al., 2013). Dystrophin has four main domains – NH2, rod, cysteine and COOH-terminal domains. The NH2 domain binds to the skeletal actin. The rod domain contains: (1) extra actin binding sites, (2) neuronal nitric oxide synthase (nNOS) binding sites, and (3) four hinge regions providing flexibility. The cysteine rich domain links to β-dystroglycan that binds to α-dystroglycan. The COOH-terminal connects to α-, β-, ϒ-syntrophin. Together, dystrophin, dystroglycan and syntrophin belong to the dystrophin-associated glycoprotein complex (DGC), along with many other proteins. Due to its connections, dystrophin provides a link of cytoskeleton actin to the extracellular matrix (Pichavant et al., 2011) and is assumed to keep the sarcolemma stable during contraction (Matsumura and

Campbell, 1994).

1.2.2.2 DGC in signaling

DGC performs as a scaffold for complexes of signal proteins that regulate muscle cell viability (Evans et al., 2009; Nakamura and Takeda, 2011). Four signal proteins associate with the DGC: calmodulin (CaM), calmodulin kinase II (CaMKII), growth factor receptor-bound protein 2 (Grb2), and nNOS. The interaction between dystrophin and utrophin with actin and the cell survival cascade, i.e., the phosphatidylinositol 3-kinase (PI3K)/Akt cascade and the calcineurin/nuclear factor of activated T cells (NFAT) pathway is regulated by CaM and CaMKII. Cell survival is promoted when Grb2 initiates the Ras/mitogen-activated protein kinase (MAPK) signaling cascade through the adaptor protein son-of-sevenless. nNOS produces nitric oxide (NO) to mediate vasodilatation during contractions, thereby reducing ischemic injury in skeletal muscles (Rando, 2001; Oak et al., 2003; Evans et al., 2009). NO also protects cells from apoptosis through the c-GMP-dependent cell survival pathways or cytoprotection (Rando, 2001). NO production is reduced in DMD patients and an up regulation of this free radical ameliorates dystrophic phenotypes in *mdx* mice (Wehling et al., 2001).

1.2.2.3 DGC in DMD pathology

The exact reason why the absence of dystrophin causes muscle necrosis is still unknown. However, several models have been proposed to explain the causative role of dystrophin in DMD. The first one is a pathogenesis model that emphasizes the role of dystrophin in muscle fiber membrane integrity, in which lacking dystrophin results in the loss of a shock absorber for the cell membrane under the rigors of contraction, leading to membrane fragility, then causing membrane damage and finally myofiber necrosis (Grounds, 2008). The second model focuses on intracellular calcium accumulation (Duncan, 1978). In this model, dystrophin deficiency causes

damage to the cell membrane, leaving the membrane highly permeable to calcium. When calcium gets into the cytosol, Ca^{2+} dependent proteases are activated and degrade the myofiber, leading to myofiber necrosis. The third model is about signaling for cell survival in which the absence of dystrophin causes the mislocalization of DGC that is important for cell survival signaling (Evans et al., 2009). This results in myofiber necrosis. In conclusion, many models have been proposed for the causative roles of dystrophin in DMD. All of the hypotheses are plausible. Elucidating the direct roles of the dystrophin protein in the pathologies of DMD is important to find a cure for this disease.

1.2.3 Animal models

Progress towards developing a novel drug to treat DMD requires research that utilizes animal models that sufficiently reproduce characteristics found in humans. Previous research studies used a number of dystrophic animal models, among which are *Drosophila*, the mouse, cat, and dog. *Mdx* mice (X-linked muscular dystrophy mice), dystrophic cats, and GRMD dogs (Golden Retriever Muscular Dystrophy) lack the dystrophin protein or have reduced function (Hoffman et al., 1987; Cooper et al., 1988; Carpenter et al., 1989). Among these models, dogs have the closest clinical phenotypes to DMD, with critical muscle degeneration and fibrosis that leads to movement incapacity due to gradual loss of muscle structure and motor functions. Mice and cats have much milder clinical phenotypes, but still exhibit DMD hallmarks in muscles, such as degeneration, necrosis, regeneration and hypertrophy. However, the mice and cats do not show as extensive fibrosis, fat infiltration or movement disability as seen in DMD patients (Partridge, 1991).

Dystrophic *Drosophila* is a good initial model to study DMD because of its simpler chromosomes and shorter life cycle. Dystrophic *Drosophila* also have disease phenotypes in muscle degeneration. This reduces their climbing activity, heart function and reduces their lifespan (Shcherbata et al., 2007; Taghli-Lamallem et al., 2008). *Drosophila* are good for studying gene interaction in diseases, however, to test a potential drug, a more thorough study should be conducted on higher-level models. GRMD dogs are the most appropriate animals as they have the closest clinical muscular weakness to DMD patients. However, due to their long generation times, leading to long and expensive experiments, dogs are best to use for translational research whereas basic research is easier to perform on mice or cats. As dystrophic cats are no longer available (Partridge, 1991), the available animals to use for basic research are *mdx* mice.

Mdx mice arose through a spontaneous point mutation in the C57BL/10 strain (Bulfield et al., 1984) introducing a premature stop codon in exon 23. This leads to a shorter version of dystrophin, which is unstable and results in the absence of detectable dystrophin protein (Hoffman et al., 1987; Sicinski et al., 1989). These mice have a reduced life span compared to control mice. Particularly, life expectancy is reduced by 17% for female and 19% for the male *mdx* mice (Chamberlain et al., 2007). Muscular deficits are not equal in all *mdx* muscles. Diaphragms are the most affected muscle in *mdx* mice with progressive necrosis, companied by fibrous and fatty infiltration, as found in DMD limb muscles (Pastoret and Sebille, 1995). Besides the diaphragm, tongues are also severely affected in *mdx* mice (Chamberlain et al., 2007). Interestingly, tongues are composed of mostly fast twitch muscles in both rats and mice (Cobos et al., 2001; Abe et al., 2002). It is suggested that *mdx* mice have milder disease

phenotypes due to the expression of utrophin and the presence of revertant fibers (Connolly et al., 2001). Moreover, *mdx* mice have better regeneration capacity as a benefit from other genetic factors, especially longer telomeres (Sacco et al., 2010).

There is a substantial difference in the developmental timeline between humans and mice. Thus, when designing and evaluating pre-clinical trials in *mdx* mice, a time wise equivalence should be stressed. A comparable milestone in the case of mice that 3, 4, 6, and 8 weeks are approximately equal to humans at 6 months, 10 years, 10-18 years and 20 years old, respectively (Grounds, 2008).

As DMD is a progressive muscle wasting disease, it is important to detail progress of the pathology in animal models. *mdx* mice initially displayed muscle abnormalities at 2 weeks of age with signs of inflammation (Nakamura and Takeda, 2011) and central nuclei denoting the signs of the degeneration and regeneration cycle in several muscles. This defect then spreads to most of the studied muscles at 3 weeks of age with a peak of muscle degeneration/necrosis at around 1 month old. Necrosis continued throughout the *mdx* mouse lifespan with slower speed after 12 weeks (Nakamura and Takeda, 2011). Between 2-8 weeks, the muscle pathology is most pronounced. The muscle fibers have acquired a splitting morphology and show variation in muscle size, denoting various maturation stages at 8 weeks of age. By 26 weeks, non-peripheral nuclei were detected in up to 80-90% muscle cells. The pronounced sign of DMD in humans, the fibrosis and fat infiltration, could be observed in *mdx* mice at the age of 52 weeks with much less severity than in DMD patients. At around 72 weeks, *mdx* mice start to exhibit signs of skeletal

muscle weakness (Lefaucheur et al., 1995). From 78 weeks on, the mice had difficulty in getting food and water themselves and died by 91 weeks of age (Pastoret and Sebille, 1995).

The diaphragm is the most affected organ in *mdx* mice and the diaphragm pathology timeline is clearly demonstrated in the literature. Having regeneration that is not as high as in limb muscles, the diaphragm experiences extensively progressive degeneration. These muscles show patterns resembling DMD limb muscles in degeneration, fibrosis and malfunction (Stedman et al., 1991). Before 25 days of age, diaphragms show sporadic changes in histopathology. At 30 days of age, degeneration, necrosis and regeneration occur, but are not prevalent. At 6 months, necrosis along with fibrosis, central nuclei and varied sizes of muscle fibers are observed. At 16 months of age, extensive myofiber loss and fibrosis occur. The density of collagen rises to at least 7 fold higher than that of the control diaphragm and 10 times that of *mdx* hind-limb muscles (Stedman et al., 1991).

Besides *mdx* mice, we also used mdx^{4CV} mice in our experiments. This dystrophic mouse has a point mutation in the dystrophin gene in the C57BL/6J genetic background, changing a C to T in exon 53 at position 7916 causing a premature stop codon (Im et al., 1996). mdx^{4CV} mice also exhibited progressive abnormality in muscle histopathologies (degeneration, regeneration, necrosis, central nuclei position) and suffered severe defects in the diaphragm like *mdx* mice (Danko et al., 1992).

1.2.4 Treatment status

Currently, there is no effective treatment available for DMD (Fairclough et al., 2013). However, researchers have been trying two main approaches by - (1) replacing the dystrophy protein, or (2) reducing the dystropathologies.

1.2.4.1 Dystrophin protein replacement therapy

Previous research has shown that just 30% of dystrophin is enough to rescue the muscle dystrophy in humans (Neri et al., 2007). Thus, treating the disease on its primary defect by restoring the dystrophin protein level in skeletal and heart muscles permanently is the best approach to follow.

1.2.4.1.1 Gene therapy

Traditional gene therapy to deliver a normal dystrophin gene with a viral vector was first initiated to pursue this method. However, dystrophin is too large to be packed into viral vectors. To make dystrophin fit into the vectors, researchers use an in-frame-deletion to remove most of the rod domain of the dystrophin gene, creating a "mini dystrophin". Adeno-associate viral vector (AAV) is a well-studied vector that maintains persistently and does not cause any pathogenicity when administered to healthy muscles (Mendell et al., 2010). AAV was used to deliver this mini gene. Although no immune response in mice was discovered against the AAV vector and the mini gene (Fairclough et al., 2013), clinical trials in DMD patients showed various degrees of immune response to the transgene products (Mendell et al., 2010). Immune response can be reduced in future clinical tests by a transient immune-suppression (that has been shown to work in the DMD dog model) (Wang, Z. et al., 2012), but the persistence expression of the transgenes and gene delivery capacity to all muscles that make up 40% of the body mass is still a challenging problem.

1.2.4.1.2 Targeted Gene Correction (TGC)

While traditional gene therapy techniques struggled with the large size of the dystrophin transgene, they ended up using a mini gene that still results in a milder disease. Targeted gene correction techniques (TGC) attempt to correct the gene itself, aiming at producing normal full functional proteins. TGC delivers two elements to the cells: (1) an endonuclease called meganuclease, and (2) a small DNA sequence that corresponds to the mutated dystrophin sequence. Inside the cell, the meganuclease cuts the dystrophin sequence near the mutation sites and homologous recombination takes place with the corrected sequence. This results in fixing the mutated dystrophin DNA. Though being the best option for any treatment, TGC faces some obstacles such as off-target cleavage, micro-insertions or micro-deletion (results of non-homologous end-joining), transgene delivery efficiency, transgene expression, and immune response to the viral vectors. Current research shows promising results in using meganuclease to restore the reading frame of a model-mutated dystrophin (Chapdelaine et al., 2010). However, to successfully transform the result in a favorable condition model to the real and numerous types of mutations *in vivo* is still a hurdle and requires more time.

1.2.4.1.3 Cell-based therapy

Cell-based therapy aims at injecting myoblast or stem cells with myogenic potential into the body so they will fuse with locally damaged muscle fibers to create hybrid muscle fibers. This strategy is expected to repair the muscle damage with a healthy or corrected DMD gene. The approach with myoblasts have failed due to the poor cell survival and limited ability to extravagate into the muscle tissue. Regarding satellite cell therapy, there has been no functional or clinical improvement observed yet (Spitali and Aartsma-Rus, 2012). One of the most promising cell-base therapies is the approach using mesoangioblasts, the blood-vessel associated

stem cells that can differentiate into multiple mesoderm cell types, including skeletal muscle (Tedesco et al., 2011). Systemic delivery of wild-type mesoangioblasts into GRMD dogs resulted in a recovery of 10-70% dystrophin expression compared to control wild-type muscles. This translated into improved muscle function, as evidenced by increased contraction force, and preserved walking capacity (Sampaolesi et al., 2006). In 2011, Tedesco at al. used a human artificial chromosome to transfer full-length dystrophin to mesoangioblasts isolated from *mdx* mice, and delivered these cells into another group of *mdx* mice using intra-muscular or intra-arterial injection. In the intra-muscular injection, transplanted muscles produced 20% of the amount of dystrophin produced by muscles of healthy control mice. The gene expression of dystrophin was maintained up to 8 months after the transplantation of corrected *mdx* mesoangioblasts. In transplanted muscles subjected to intra-arterial delivery, dystrophin proteins were detected at 13% of those in control muscles. Both delivery methods resulted in more than 50% improvement in motor capacity (Tedesco et al., 2011). In conclusion, cell-based therapy is a good approach to tackle DMD. However, it needs more time to become a practical treatment.

1.2.4.1.4 Exon skipping (Antisense oligonucleotides)

If one exon is deleted, it can leave the adjunction exons out of the reading frame, resulting in unstable mRNA or non-functional proteins. Since out-of-frame deletion is the most common mutation that occurs in the dystrophin gene of DMD patients (about 83% of total mutations) (Muntoni and Wood, 2011), restoring the exon reading frame is a good approach to tackle DMD. Exon skipping aims at splicing one or more exons out of the mRNA to restore the reading frame and rescue protein function. RNaseH-independent antisense oligonucletotides (AONs) is an exon skipping agent that binds to a complementary sequence within or next to the target exon, interfering in the association of the mRNA with the spliceosome, whose function is to splice out

introns. This results in the skipping of the targeted exon, restoring the reading frame for the adjunction exons, and producing a truncated dystrophin protein with partial functions.

Two types of oligomers have been used in clinical trials to skip exon 51, applicable to about 13% of patients: the 2'-O-methyl-phosphrothioate (2'OMe) and morpholino phosphorodiamidate oligonucleotide (PMO). Even though this approach is promising due to being well-tolerated and producing different levels of dystrophin protein restoration, as evidenced by novel dystrophin expression in roughly 60-100% of muscle fibers in 10 of 12 patients that were subjected to a 6-minute walk test (Mendell et al., 2012), exon-skipping methods have some major limitations. First, they have low efficiency due to poor cellular uptake, leading to less restored dystrophin. Second, the restored protein is truncated, leading to only a semi-functional dystrophin. Third, this exon skipping method is mutation specific and a highly personalized approach that cannot be used widely, hence, it is costly, and the patients with low frequency mutations have less chances to be cured (Fairclough et al., 2013).

1.2.4.1.5 Stop codon read through

Fifteen percent of DMD mutations are premature termination codons. To overcome this problem, the stop-codon read-through method was invented. This method uses a molecule to interact with a ribosomal sub-unit when it recognizes a stop codon, and introduces an amino acid for the stop codon, allowing the translation to continue. Clinical trials in DMD patients using gentamicin, an aminoglycoside antibiotic showed increased dystrophin protein levels with stable muscle strength (Mendell et al., 2012). However, safety reasons made gentamicin not suitable for further use.

Besides gentamicine, Ataluren (PTC124) was also tried. It proved to be relatively safe compared to gentamicine, and helped in elevating dystrophin levels in clinical tests. Unfortunately, it failed to demonstrate an improved effect in the 6-minute walk test (Pichavant et al., 2011; Mendell et al., 2012). Therefore, until now, stop codon read through is not a very promising approach.

1.2.4.1.6 Utrophin up-regulation therapy

Utrophin can compensate dystrophin function because of its highly similar DNA sequence and protein structure to dystrophin (Fairclough et al., 2013). In normal adult muscles, utrophin is only expressed in neuromuscular synapse and myotendinous junctions. In DMD patients, utrophin is seen at the sarcolemma, and even just a slight increase in utrophin level can delay the onset of being wheelchair-bound for DMD patients (Fairclough et al., 2013). Upregulating utrophin in all tissues has been shown to be safe and provides a beneficial effect in the muscle pathologies (Fairclough et al., 2013). Therefore, increasing utrophin should be applicable in all DMD patients, regardless of their different mutations. However, utrophin does not have binding sites for nNOS, and none of the recently used utrophin methods could increase this protein level by 2 or 4 fold, which is the benchmark for preclinical rescue (Tinsley et al., 1998). In conclusion, utrophin therapy is highly promising, but more work is required before it can be available as an effective treatment for DMD patients.

1.2.4.2 Ameliorative therapy

Tackling DMD on its primary defects is still a hurdle. Thus, to delay DMD symptoms and lengthen the patients' lifespan, steroids such as glucocorticoids are used as an ameliorative therapy to treat the secondary effects of DMD. The treated patients show partly rescued phenotypes, for example in muscle strength, respiratory function, walk and climb capacity. However, the side effects are also pronounced. The DMD patients experience abnormal weight

gain with a cushingoid-like appearance and other behavioral problems. In addition, they are at risk of defects in bone density and structures, hypertension, vertebral compression, and cataract formation (Mendell et al., 2012). Because using glucocorticoids addresses only the secondary effects of the DMD and produces numerous side effects, there is a strong demand for a better ameliorative therapy for DMD.

In 2012, the Lynch group suggested increasing heat shock protein 72 (Hsp72) to ameliorate DMD pathologies. Hsp72 tackles the abnormal high intracellular Ca^{2+} concentration in DMD patients that leads to muscle degeneration. To exert this function, Hsp72 interacts with the sarcoplasmic/endoplasmic reticulum Ca^{2+}-ATPase (SERCA) to preserve its function in pumping Ca^{2+} back to the sarcoplasmic reticulum. SERCA function is severely affected in *mdx* mice. Administration of BGF-15, a drug in use for clinical trials for diabetes, to induce Hsp72 in *mdx* mice has been shown to increase SERCA function, muscle force and reduce DMD hallmarks, such as fibrosis, and muscle membrane damage. BGF-15 that is used in clinical trials for insulin-resistant patients has been shown to be safe. This gives a hope to make BGF-15 an ameliorative treatment for DMD patients (Gehrig et al., 2012).

Another approach for DMD ameliorative treatment was proposed using Wnt7a (von Maltzahn et al., 2012b). Wnt7a is a secreted protein that belongs to the Wnt signaling pathway. Wnt signaling pathway has been known to be involved in muscle regeneration (Kuroda et al., 2013). Particularly, Wnt7a can induce the symmetric expansion of satellite cells through the non-canonical Wnt signaling pathway (Le Grand et al., 2009). Moreover, Wnt7a also promotes muscle hypertrophy by activating the AKT/mTOR pathway (von Maltzahn et al., 2012a). Up

regulation of Wnt7a in *mdx* muscles has shown to increase satellite cell expansion, myofiber hypertrophy and muscle strength. Interestingly, the benefit actions of Wnt7a on dystrophic muscles are concomitant with a shift toward slow twitch fibers as evident in an increase in slow MHC in *mdx* muscles and human primary myotubes that have Wnt7a up regulated (von Maltzahn et al., 2012b).

In summary, though gene or cell based therapies should give the ultimate cure for DMD, ameliorative treatments are required to delay the disease progression in waiting for the safe and successful treatments to approach the patients. The more ameliorative approaches we have, the more hope to prolong the patients' lives, and the more hints we get toward developing a successful treatment for DMD.

1.2.5. Relationship between muscle types and muscle stability

Previous studies revealed an interesting correlation between muscle types (oxidative and glycolytic muscles) and muscle stability: slow twitch muscles are less susceptible to injury than fast twitch muscles. First, in 1988, Webster et al. pointed out that regeneration occurred earlier in fast twitch than in slow twitch muscles in DMD patients (Webster et al., 1988). Second, in addition to diaphragms, tongue muscles are highly damaged in *mdx* mice, the dystrophic animal model that has milder clinical phenotypes in limb muscles than DMD patients due to their high regeneration rate (Chamberlain et al., 2007). Surprisingly, tongue muscles are mainly fast twitch muscles (Cobos et al., 2001; Abe et al., 2002), suggesting that fast twitch muscles are more vulnerable to injury in a dystrophic context (Webster et al., 1988). Third, overexpression of PGC-1α in neonatal *mdx* mice has been shown to benefit skeletal muscles, and this involves a shift from fast to slow twitch muscles (Selsby et al., 2012). These findings imply an increased

susceptibility to injury of fast twitch over slow twitch muscles in the dystrophic context. There have been a number of publications pointing the switch from fast to slow twitch fibers as beneficial effects on reducing the severity of DMD (Chakkalakal et al., 2004; Stupka et al., 2006; Selsby et al., 2012; von Maltzahn et al., 2012b).

1.3. Sphingosine-1-Phosphate (S1P)

1.3.1 S1P overview

S1P is a bioactive lipid, meaning that any changes in the levels of these types of lipids will have functional consequences (Hannun and Obeid, 2008). The sphingosine lipid plays important roles in cell survival, proliferation, migration, differentiation, cell-cell interaction, angiogenesis, inflammation, lymphocyte trafficking and development (Neri et al., 2007; Neubauer and Pitson, 2013). It has a high concentration in blood (in 200-900nM concentration) (Murata et al., 2000), and a low concentration within the cells (Neubauer and Pitson, 2013). S1P has been shown to benefit dystrophic muscles (Loh et al., 2012; Ieronimakis et al., 2013; Pantoja et al., 2013).

1.3.1.1 The sphingolipid biosynthetic pathway

S1P is synthesized in a part of the sphingolipid biosynthetic pathway. There are two biosynthesis pathways for sphingolipid: (1) the sphingomyelinase pathway, and (2) the *de novo* biosynthesis pathway. In the sphingomyellinase pathway, sphingomyellin, a sphingolipid in the animal cell membrane, is hydrolyzed into ceramide. Ceramidase then converts ceramide into sphingosine. Sphingosine is phosphorylated by sphingosine kinases (SphKs) into S1P. S1P can be reversibly processed into sphingosine by Sphingsosine phosphatase or irreversibly degraded into phosphoethanolamine and exadecenal (Bruni and Donati, 2008).

The *de novo* biosynthesis of sphingolipids is initiated at the endoplasmic reticulum (ER) with the formation of Keto by the combination of Ser and Palm-CoA. Next, Keto is reduced into Dihydrosphingosine (DHSph) that is acetylated to form DH-Ser. Under the catalyst of the desaturase, ceramide is produced. Ceramide and DH-Cer are translocated to the Golgi to finally become Glycosphingolipids (GSLs). GSLs become a component of the plasma membrane and are later degraded into sphingosine in the endosome. SphK in the cytoplasm phosphorylates Sphingosine to S1P, which is dephosphorylated back to Sphingosine by sphingosine phosphatase 1 at the ER. Sphingosine is then converted to ceramide (Spiegel and Milstien, 2003). DHSph is also formed in the ER by the de-phosphorylation of DHS1P.

1.3.1.2 S1P synthesis and degradation

S1P remains at a relatively small level within the cells under normal conditions because of the balance between its synthesis and degradation. S1P is synthesized by the phosphorylation of sphingosine, catalyzed by Sphingosine kinases (SphK1 and SphK2). S1P is degraded through two distinct pathways. The reversible pathway is mediated by S1P phosphatase in which S1P is dephosphorylated back to sphingosine. The irreversible degradation pathway is mediated by S1P lyase (Spl), which degrades S1P into hexadecenal and phosphoethanolamine.

1.3.1.2.1 Sphingosine kinase (SphK)

The enzyme in charge of S1P production is sphingosine kinase. There are two isozymes of SphK in mammals: SphK1 and SphK2. SphK2 protein is larger and harbors most regions of SphK1, for example the C1-C5 domains, including the catalytic site. These two proteins are 80% similar to each other, and their DNA sequences share 45% identity (Neubauer and Pitson, 2013). SphK2 has several more domains that are not harbored in SphK1, for example, the nuclear localization (NLS) and export (NES) signals that help SphK2 shuttle between the cytosol and nucleus while

SphK1 stays in the cytosol (Igarashi et al., 2003; Ding et al., 2007). Moreover, SphK2 can also localize to the mitochondria and ER (Neubauer and Pitson, 2013). Regarding organ location, human SphK1 mRNA is highly detected in liver, kidney, heart and skeletal muscle (Nava et al., 2000), whereas human SphK2 is mainly expressed in the kidney liver, and lower in skeletal muscles (Liu et al., 2000; Neubauer and Pitson, 2013). SphK2 has more substrates than SphK1. Both DHSphingosine and sphingosine are phosphorylated by SphK2 in the nucleus (Hait et al., 2009). Additionally, SphK2 can phosphorylate FTY720 (an immunosuppressive drug), phytosphingosine, and omega-bioinyl D-erythro-sphingosine (Neubauer and Pitson, 2013). SphK1 and SphK2 are activated via ERK1/2-mediated phosphorylation (Hait et al., 2007; Neubauer and Pitson, 2013), leading to a 14-fold and 2 to 6-fold increase in catalytic activity, respectively (Neubauer and Pitson, 2013). Stimuli for SphK1 are tumor necrosis factor α, platelet-derived growth factor, and the potent angiogenic vascular endothelial growth factor (Olivera et al., 1999; Pitson et al., 2000; Shu et al., 2002). SphK2 is activated by growth factors and cytokines (Neubauer and Pitson, 2013).

SphK1 has been shown to promote cell growth, protect cells from apoptosis, and induce muscle fiber regeneration after acute injury (Alvarez et al., 2010; Strub et al., 2010; Loh et al., 2012). On the contrary, SphK2 induces growth arrest and cell death in some cell types, but protects cell apoptosis in other cells, for example, MCF-7 (breast cancer cells) and HCT116 (colon cancer cells) (Strub et al., 2010). In SphK2-devoid cells, acetylation of H4K5, H3K9, and H2B-K12 are decreased (Hait et al., 2009).

1.3.1.2.2 S1P lyase (SPL)

S1P lyase accounts for the irreversible catabolism of S1P. It locates at the membrane of the endoplasmic reticulum (Saba and de la Garza-Rodea, 2013) and promotes apoptosis under stress conditions. SPL plays a role in the regulation of immunity, lipid homeostasis and development. The *Sgpl1* gene that is located on chromosome 10 of the human and mouse genomes encodes for SPL. SPL null mutant mice have elevated circulating and tissue S1P level, and die before reaching one month of age (Borowsky et al., 2012).

1.3.1.3 S1P responses in injured mice and *mdx* mice

In acute injured C57BL/6 mice, plasma S1P is increased by 50%. The gene expression of SphKs, S1P receptors and *Sgpl1p* (coding for S1P lyase) are up regulated. Among S1P receptors, the increase in gene expression of S1PR1 and 2 are more pronounced, and reduced to a baseline level after 10 days post injury (Loh et al., 2012). In *mdx* mice, S1P level is decreased along with an increase of S1P lyase, which denotes an increase of S1P catabolism (Loh et al., 2012). A reduction in gene expression of all three S1PRs (1-3) has been observed in mdx^{4CV} mice. The down regulated gene expression is most pronounced in S1PR1 with a five fold reduction in relative mRNA levels (Ieronimakis et al., 2013).

1.3.1.4 Related molecules

Dihydro-S1P (DHS1P) is a saturated form of S1P. DHS1P is almost identical to S1P, except it does not possess a trans 4,5 double bond (Giussani et al., 2006). Both DHS1P and S1P can bind and activate S1PRs with similar affinities, but DH-S1P is unable to confer all the effects of S1P, especially those related to cell survival and anti-apoptosis (Giussani et al., 2006; Strub et al., 2010). DHS1P is formed by the phosphorylation of dihydroshingosine (DHSph) and is catalyzed by both SphK1 and SphK2 (Hait et al., 2006). Like S1P, DHS1P is also degraded by S1P lyase (Gorshkova et al., 2013). When S1P-phosphatase 1 (SPP1) removes the phosphate group from

DHS1P, DHSph is formed (Spiegel and Milstien, 2003). DHS1P has been shown to have inhibitory effects on HDAC1 and HDAC2 (Hait et al., 2009).

FTY720 is an immunosuppressant, also known as Fingolimod. FTY720 is phosphorylated mostly by SphK2 into FTY720-P, which is a S1P receptor agonist (Strub et al., 2010). FTY720-P can bind and activate most S1P receptors, except for S1PR2 (Pyne and Pyne, 2011). Therefore, FTY720-P can exert some of S1P functions, for example, controlling lymphocyte egress from the thymus and the secondary lymphoid organs (Chiba, 2005). It is unknown if FTY-720-P has inhibitory effect on HDAC1 and HDAC2 as S1P does. Similar to S1P, FTY720-P is dephosphorylated by lipid phosphate phosphatase 3 (LPP3) (Mechtcheriakova et al., 2007).

Lysophosphatidic acid (LPA) is also a bioactive lipid that belongs to the phospholipid group and has a similar structure to S1P. LPA is the simplest glycerophospholipid and is a precursor of phospholipid biosynthesis in both eukaryotic and prokaryotic cells. LPA has a special role in cell growth and wound repair (Moolenaar, 1995). LPA also exerts several overlapping functions with S1P in regulating cell proliferation, migration, survival and differentiation (Okudaira et al., 2010; Maceyka et al., 2012).

1.3.2. S1P functions

1.3.2.1 S1P extracellular functions

SphKs have been proposed to be able to be secreted out of the cells where they play a role as an extracellular S1P producer (Venkataraman et al., 2006). It has been known for a while that S1P has extracellular functions, acting through S1P receptors (S1PRs). There are five S1P receptors identified in mammals (S1PR1-5) (Chun et al., 2002)

S1PRs couple with different G proteins. All five receptors can couple through Gi/o. In addition, S1P receptors, except S1PR1 also couple through G12/13. In particular, S1PR2 and S1PR3 have an additional coupler, the Gq protein (Brinkmann, 2007).

The phospholipase C (PLC) pathway is the common signaling through Gi/o and Gq. Activation of PLC and protein kinase C leads to an increase of intracellular Calcium. Additionally, signaling through Gi/o is also involved in the Ras (the small guanosine triphosphatase) and ERK (the extracellular signal-regulated kinase) pathway to enhance proliferation. Being one of the downstream signaling targets of Gi/o, the phosphatidylinositol 3-kinase (Pi3K), when collaborating with protein kinase B (PKB/Akt), can increase cell survival, while having positive effects on migration, the endothelial barrier and vasodilation when being induced along with the small GTPase, Rac. The negative regulation of Gi/o signaling is mediated through the inhibition of adenylyl cyclase (AC) activity to reduce cyclic adenosine monophosphate (cAMP). Signaling through G12/13 acts mainly via the small GTPase Rho and the Rho-associated kinase (ROCK) to inhibit cell migration, decrease endothelial barrier function, and induce vasoconstriction (Brinkmann, 2007).

Specifically, although S1PR1 is known to be ubiquitously expressed in many cell types, it remains especially high in brain, heart, spleen, liver, lung, thymus, kidney, lymphoid and skeletal muscle (Brinkmann, 2007). S1PR1 and S1PR3 have been proved to mediate cardioprotection from ischemia/reperfusion injury using knockout mice studies (Means and Brown, 2009). S1PR1 is a key player in angiogenesis and increases vascular integrity, mediated by Akt and Rac signaling molecules (Singleton et al., 2006). In particular, S1P is involved in immune cell

circulation by controlling the egress of lymphocytes from the secondary lymphoid organs and the thymus (Matloubian et al., 2004).

S1PR2 is highly expressed in brain, heart, spleen, liver, lung, thymus, kidney, and skeletal muscle (Brinkmann, 2007). S1PR2 functions in promoting skeletal muscle regeneration, and S1PR2-null mice have delayed muscle regeneration (Germinario et al., 2012). S1PR2 is also required for proper ear development (Herr and Chun, 2007; Kono et al., 2007) and mast cell degranulation. Furthermore, activated S1PR2 increases vascular permeability via ROCK/Rho (Sanchez, T. G. et al., 2007) and promotes healing in liver after injury (Serriere-Lanneau et al., 2007). While S1PR1 and S1PR3 activation promotes cell migration, activation of S1PR2 prevents this process (Strub et al., 2010).

S1PR3 localizes to the brain, heart, spleen, liver, lung, thymus, kidney, testis and skeletal muscle (Brinkmann, 2007). It reduces heart rate in mice by evoking bradycardia (Forrest et al., 2004) and promotes monocyte/macrophages migration during inflammation and atherosclerosis (Keul et al., 2011). Similar to S1PR2, S1PR3 regulates vascular permeability via ROCK and Rho (Sanchez, T. et al., 2007).

S1PR4 is found in lymphoid tissue and lungs (Brinkmann, 2007). Activated S1PR4 controls intracellular calcium through the mitogen activated-protein kinase ERK1/2 and phospholipase C (Van Brocklyn et al., 2000; Yamazaki et al., 2000).

S1PR5 is distributed in brain, skin and spleen (Brinkmann, 2007) and assists natural killer cells in trafficking to inflamed organs (Walzer et al., 2007).

1.3.2.2 S1P intracellular function

In mammals a number of intracellular functions of S1P have been elucidated recently. First, S1P produced by SphK2 in the nucleus was shown to inhibit HDAC1 and HDAC2 activity (Hait et al., 2009). Using a modeling method, S1P has been predicted to dock well into the active sites of a homolog for HDAC1 from the hyperthemophilic bacterium *Aquifex aeolicus* (Hait et al., 2009). Second, S1P has a regulatory role in mitochondria respiration (Strub et al., 2011). SphK2 localizes to the inner mitochondrial membrane and produces S1P that then binds to prohibitin 2 (PHB2). The interaction of S1P and PHB2 is important for the assembly of cytochrome-c oxidase (COX). Intact mitochondria isolated from SphK2-null mice have reduced mitochondrial respiration. Moreover, acute down regulation of either SphK2 or PHB2 in Hela cells also led to a decrease in oxidative phosphorylation. Third, intracellular S1P involves in the NF-κB signaling pathway by playing the role of a cofactor for TRAF2, an associate factor of the tumor-necrosis factor (TNFα) (Alvarez et al., 2010). When TNFα activates its receptors, TRAF2 polyubiquitinates RIP1 (a receptor interacting protein) at lysine 63, which then recruits and activates IκB kinase (IKK). IKK, in turn, phosphorylates IκBα, which results in its ubiquitination and finally, its degradation and releases NF-κB, leaving it free to translocate to the nucleus and activate gene expression. The mechanism underlining TRAF2 action is the S1P produced by SphK1. TRAF2 binds to SphK1, and also S1P. This interaction is important for TRAF2 E3 ligase activity (Alvarez et al., 2010).

1.3.2.3. S1P function in skeletal muscle

One known role of S1P in skeletal muscle is to promote regeneration via the activation of satellite cells (SC) (Danieli-Betto et al., 2010; Loh et al., 2012; Ieronimakis et al., 2013). In 2012, the Saba group proposed that S1P promoted SC activation through a S1PR2/STAT3 signaling pathway, in which STAT3 (signal transducer and activator of transcription) is a transcription factor that is involved in cell proliferation, survival and differentiation (Loh et al., 2012). Treating *mdx* mice with THI (2-acetyl-5-tetrahydrosybutylimidazole), a S1P lyase inhibitor to increase muscle S1P level, they saw an up regulation of STAT3 phosphorylation along with an increase in the number of satellite cells and regenerating cells. Inhibiting STAT3 with WP1066 sabotaged the THI effect on SC differentiation. Furthermore, they elucidated the role of S1PR2 in this pathway when observing a reduction in STAT3 phosphorylation as an effect of S1PR2 being knocked down. SC differentiation was also reduced when treated with JTE-013, a S1PR2 antagonist. Moreover, the downstream targets of STAT3, the cell cycle inhibitors p21 and p27 were also down regulated, supporting the hypothesis that S1P promotes muscle regeneration by activating the STAT3 pathway, in which STAT3 inhibits the cell cycle inhibitors, making the quiescent SC enter the cell cycle, proliferate and then differentiate. Interestingly, SphK1, but not SphK2, mediates muscle regeneration and SC activation after injury. SCs isolated from SphK1 KO mice post acute injured had reduced proliferation and differentiation, and the phenotype was reversed when culturing KO SCs in WT serum (Loh et al., 2012).

In 2013, publications from the Ruohola-Baker laboratory demonstrated that S1P functions beyond the SC scope. Treating dystrophic *Drosophila* with THI shows S1P function in rescuing muscle degeneration, muscle structure integrity, and muscle function, as observed in the

climbing or activity assays (Kucherenko et al., 2008; Pantoja et al., 2013). Since there is no known S1P receptor in flies, and S1P lyase is localized in the ER, the beneficial action of S1P lyase inhibitor THI in the muscle function is likely to be mediated through intracellular S1Ps (Pantoja et al., 2013; Pantoja and Ruohola-Baker, 2013). S1P's role in ameliorating dystrophic phenotypes is also seen in the *mdx* mouse model. Treating acute injured *mdx* mice led not only to increased muscle regeneration, muscle size, but also improved muscle integrity and function, and reduced other dystrophic pathologies, such as fibrosis and fat infiltration. The beneficial effects of S1P correlated with an increased level of phosphorylated ribosomal protein S6 (P-rpS6), suggesting the AKT-mTOR-S6 Kinase pathway as a potential mechanism S1P employs to elevate protein synthesis, and thus increasing muscle mass in targeting DMD phenotypes (Ieronimakis et al., 2013).

1.4. Histone deacetylase (HDAC)

The nucleosome is the basic unit of a chromosome that consists of DNA and proteins. It includes around 146bp of DNA, which wraps around four core histone proteins, a H3/H4 tetramer and two H2A/H2B dimers (de Ruijter et al., 2003). The tails and globular domain of histones can go through post-translational modifications at specific amino acids. This causes changes in the structure of chromatin resulting in gene expression changes (Singh et al., 2010). The post-translational modification of histones includes acetylation, phosphorylation, methylation, ubiquitination and sumoylation (Dokmanovic et al., 2007). Phosphorylation occurs on different amino acids, such as tyrosine, threonine, and serine. Ubiquitination, sumoylation and acetylation target only lysine. Because acetylation and deacetylation have been shown to be involved in muscle function, metabolism, differentiation and fiber type components, (Puri and Sartorelli,

2000; Colussi et al., 2008; Ferrari et al., 2012; Galmozzi et al., 2013) the next few sections will focus on the acetylation aspect of the post-translational modifications.

1.4.1. HDAC overview

Acetylation was first discovered in 1968 (Yang and Seto, 2007). Histone acetylation occurs when histone acetyltransferases (HAT) acetylate conserved lysine amino acids by adding an acetyl group onto the lysine residue of proteins. Since acetyl groups are negatively charged, the addition of an acetyl group to histones makes the negatively charged DNA loosen up its wrapping, leaving the chromatin accessible to transcriptional factors, inducing more gene expression. In histones, acetylation that can be found robustly at the transcription start site (TSS) of active and poised genes are H2AK9ac, H2BK5ac, H3K9ac, H3K18ac, H3K27ac, H3K36ac and H4K91. In other TSS sites and along the gene bodies we can find H2BK12ac, H2BK20ac, H2BK120ac, H3K4ac, H4K5ac, H4K8ac, H4K12ac, and H4K16ac (Wang et al., 2008). In a recent publication, Alamdari et al. pointed out that hyperacetylation in proteins may lead to protein degradation as several HATs have ubiquitination activities in addition to their acetyltransferase activity (Caron et al., 2005; Sadoul et al., 2008; Alamdari et al., 2013). Acetyl moieties can be removed by histone deacetylase (HDAC) - an enzyme that catalyzes the deacetylation of acetyl groups from the lysine amino acid of proteins. Some examples of the non-histone proteins that can be deacetylated by HDACs are p53, E2F, alpha-tubulin, and MyoD (de Ruijter et al., 2003).

The eighteen known HDACs in human are classified into four classes based on their homology with yeast HDACs (Ferrari et al., 2012). Class I HDAC includes HDAC1, HDAC2, HDAC3 and HDAC8. Class II consists of HDAC4, HDAC5, HDAC7, HDAC9 (class IIa), HDAC6, and

HDAC10 (class IIb). HDAC11 is the only member of class IV HDACs. Class III HDACs, also known as Sirtuins, consist of SIRTS 1-7. While the three other classes depend on zinc for their catalytic activity, class III HDACs required NAD+ as a cofactor (Ferrari et al., 2012). HDAC activity can be regulated at different levels: (1) protein-protein interaction, (2) posttranslational modification, (3) subcellular localization, and (4) metabolic cofactors availability (Dokmanovic et al., 2007). The next section will discuss the different classes of HDACs in more detail.

In addition to targeting the same proteins, HATs and HDACs also interact through a complex cross talk, in which, for example p300 can acetylate SIRTs, thereby inactivating this HDAC and thus increasing acetylation (Alamdari et al., 2013). To exert their functions, HDACs must be able to travel at some point to the nucleus where most of their substrates localize. Even though not all HDACs have nuclear localization signals (NLS), they can still translocate to the nucleus by co-transporting with other proteins that contain NLS in their sequences (de Ruijter et al., 2003). Similar to HAT, HDAC does not bind directly to DNA sequences, but through a complex of proteins that help exert their deacetylase catalytic function (Hayakawa and Nakayama, 2011).

1.4.1.1 Class I HDACs

Class I HDACs consist of HDAC1, HDAC2, HDAC3 and HDAC8. They are responsible for controlling cell survival and proliferation (Dokmanovic et al., 2007). HDAC1 and HDAC2 lack nuclear export signals (NES) and are thus predominantly found in the cell nucleus. HDAC3 has both NLS and NES, but is always seen in the nucleus. HDAC8 also resides in the nucleus. Class I HDACs are found primarily in a multi-protein complex consisting of Sin3, NuRD, CoREST, and NCoR/SMRT (Hayakawa and Nakayama, 2011). They have been shown to play an important role in regulating insulin sensitivity and energy metabolism (Ferrari et al., 2012).

Further, in skeletal muscles, class I HDACs help to regulate follistatin gene expression (Colussi et al., 2008). Follistatin is important for regulation of muscle growth and strength. In particular, chromatin immunoprecipitation analysis in C2C12 cells revealed the enrichment of HDAC1 and HDAC2 on the follistatin promoter (Minetti et al., 2006). Follistatin is not the only target of class I HDACs, microRNAs are also interesting targets. miR-29 and miR-1 are known to be regulated by class I HDACs (HDAC2) (Cacchiarelli et al., 2010). Both miR-29 and miR-1 have been shown to positively regulate skeletal muscle regeneration, particularly myogenic differentiation (Chen et al., 2006; Wang, L. et al., 2012). Furthermore, miR-29 can reduce fibrosis by targeting the mRNA transcripts of fibrotic genes. In *mdx* mouse muscles, a significant down-regulation of miR-29 was observed (Wang, L. et al., 2012). HDAC3 has been suggested to regulate oxidative metabolism. Silencing HDAC3 in C2C12 cells led to increased expression of oxidative genes (*PGC-1α, TFAM, TFB1M*). Furthermore, HDAC3 binds to *PGC-1α* promoter, and treating the mice with class I HDAC inhibitors resulted in reduced recruitment of HDAC3 to *PGC-1α* promoter (Galmozzi et al., 2013).

HDAC1 and HDAC2

HDAC1 and HDAC2 are 85% similar in amino acid sequence with the same catalytic core and C-terminal tail (Dovey et al., 2010). They need to be in a protein complex to exert their functions (de Ruijter et al., 2003). Even though HDAC1 and HDAC2 are found together in a complex, their independent functions are evident (Yang and Seto, 2007). For example, an HDAC1, but not HDAC2, knockout (KO) leads to embryonic lethality in mouse (Dovey et al., 2010). HDAC1 KO results in a 1.6-fold increase in H3K56 acetylation in ES cells (Dovey et al., 2010). Furthermore, the HDAC1 knockout has been shown to reduce general cell proliferation and survival (Dokmanovic et al., 2007). While other Class I HDACs contain a NLS, HDAC2 does not possess

one (de Ruijter et al., 2003). In the context of Alzheimer disease, aging and stress, HDAC2 expression is upregulated in brain, accompanied by decreased acetylation of H3K9 and H4K12, suggesting these are informative target lysines to examine in other systems. HDAC2 binds to the promoter regions, reducing acetylation and repressing the expression of memory-sustained genes, e.g., synaptophysin and brain-derived neurotrophic factor (BDNF) (Graff and Tsai, 2013). In the negative-feedback loop, lack of BDNF leads to reduced nitric oxide that can inhibit HDAC2 activity. This makes HDAC2 activity uncontrollable (Graff and Tsai, 2013). In the mouse hippocampus, HDAC2 was seen to act upon the acetyl group of H4K12, H2B, but not on H3K14 (Guan et al., 2009). HDAC2 also regulates p53 binding activity, thereby controlling transcriptional activity (Harms and Chen, 2007) and is important for heart function (Trivedi et al., 2007). Furthermore, HDAC2 down regulates PPP2R4 (protein phosphatase 2A activator, regulatory subunit 4), PPP2R1B (protein phosphatase 2, regulatory subunit A, beta), RBPMS (RNA Binding Protein With Multiple Splicing), NCOA4 (nuclear receptor coactivator 4), CORO1C (coronin, actin binding protein 1C) and EPHA2 (EPH receptor A2), and the acetylation of H3, H4 (investigated in colorectal cancer cell lines) (Ropero et al., 2008). In addition to histones, HDAC2 protein substrates are Stat3 and Smad7 (signaling mediators), and Bcl-6 and YY1 (DNA binding transcription factor) (Dokmanovic et al., 2007).

HDAC3 and HDAC8

HDAC3 has 34% sequence similarity to HDAC8 (de Ruijter et al., 2003). Similar to HDAC1, HDAC3 shows an effect on increasing HIF1α stability (Dokmanovic et al., 2007). In contrast to other class I HDACs, HDAC3 has a nuclear export sequence (NES) in addition to a NLS. HDAC3 needs SMRT (silencing mediator for retinoic acid and thyroid hormone receptors) and N-CoR (nuclear receptor co-repressor) for its activity (de Ruijter et al., 2003). The NLS of

HDAC8 is located in the middle of the protein. Besides the size of its two different transcripts, not much is known about HDAC8 because it has only recently been discovered (de Ruijter et al., 2003).

1.4.1.2. Class II HDACs

Class II HDACs have a more restricted and tissue-specific distribution in mammalian cells (Riccio, 2010), suggesting their function in cellular differentiation and developmental processes (de Ruijter et al., 2003). They are localized in the cytosol, and shuttle into the nucleus in response to specific signals. The shuttling of class IIa HDACs between the cytosol and nuclear compartment is regulated by its phosphorylation. Phosphorylated HDACs are determined to stay in the cytosol while dephosphorylation releases them back to the nucleus (Ferrari et al., 2012). Class II HDACs are especially up regulated in fast twitch muscle where they inhibit myocyte enhancer factor-2 (MEF2) gene expression. Sumoylation enhances repression activity of class II HDACs (Potthoff et al., 2007).

Class IIa HDACs have modest catalytic activity and act mainly as a scaffold to recruit class I HDACs. Class IIb HDACs reside in the cytoplasm and have non-histones, such as transmembrane and cytoskeletal proteins, as their main substrates (Haberland et al., 2009). HDAC4, HDAC5 and HDAC7 are in the same region of the phylogenetic tree (de Ruijter et al., 2003). They all have NLS at the N terminal and HDAC5 is the only one in this group having a NES. These class IIa HDACs change their cellular localization in response to specific signals and thus, regulate gene expression during differentiation in a sequence of changes (de Ruijter et al., 2003). Their N-termini interact with and repress the expression of MEF2 (de Ruijter et al., 2003). MEF2 can then be dissociated out of the HDAC4,5,7 complex by the phosphorylation

action of CaMK on HDAC4/5/7. An HDAC4 knockout showed defects in chondrocyte differentiation (Dokmanovic et al., 2007). HDAC5 and HDAC9 knockouts displayed cardiac abnormalities (Dokmanovic et al., 2007). The HDAC7 knockout had defects in maintenance of vascular integrity (Dokmanovic et al., 2007). HDAC7 targets onco-proteins PLAG1 and FLAG2 (Dokmanovic et al., 2007). Previous studies demonstrated the regulatory role of HDAC4 and HDAC5 in the expression of metabolic genes in skeletal muscles (Czubryt et al., 2003; Potthoff et al., 2007; McGee et al., 2008). HDAC9 has been shown to interact with MEF2, which hints at a role for HDAC9 function in muscle differentiation (de Ruijter et al., 2003).

Class IIb HDACs have two catalytic domains instead of one (Riccio, 2010), making it harder for HDACi (HDAC inhibitors) to inhibit their deacetylase function. HDAC6 is reversibly inhibited by TSA, but not by trapoxin. All other HDACs are thought to be equally sensitive to different HDACi (Riccio, 2010). HDAC6 has a role in cell migration as it interacts with and deacetylates tubulin (Dokmanovic et al., 2007). Also, knocking down or inhibiting HDAC6 results in an increase of acetylation in heat shock protein 90 (hsp90), reducing its chaperon activity (Dokmanovic et al., 2007). Although HDAC6 localizes predominantly in the cytosolic compartment, it is found in a complex with HDAC11, which is known to reside in the nucleus (de Ruijter et al., 2003). HDAC10 is the most recently discovered member of class II HDACs.

1.4.1.3 Class III HDACs

Class III HDACs (SIRTs) localize in the nucleus (SIRT1, SIRT6, SIRT7), cytoplasm (SIRT2) or mitochondria (SIRT3, SIRT4, SIRT5) (Michishita et al., 2005; Michan and Sinclair, 2007) and do not share any homology with class I, II, IV HDACs (Riccio, 2010). They regulate from cellular stress to energy metabolism (Ferrari et al., 2012), especially, SIRT1s control metabolic

adaptation through PGC-1 dependent mechanism (Ferrari et al., 2012). Particularly, under fasting condition, SIRT1 deficiency results in decreased production of glucose and reduced oxidation of fatty acid in the liver (Rodgers and Puigserver, 2007).

1.4.1.4 Class IV HDAC

Class IV HDAC (HDAC11) localizes in the nuclear compartment (Riccio, 2010). Its function is poorly understood. HDAC11 activity can be inhibited by an analogue of TSA, trapoxin. Surprisingly, it is not in any known HDAC co-repressor complex, such as Sin3, N-CoR/SMRT (de Ruijter et al., 2003).

1.4.2 HDAC regulation

HDAC deacetylase activity is inhibited by HDAC inhibitors (HDACi). Most HDACi are currently thought to exert their function by reversibly or irreversibly blocking HDAC active sites. Among the many known HDAC inhibitors, Trichostatin A (TSA) is one of the most powerful inhibitors discovered thus far. While other HDACi inhibit HDAC in a reversible manner, trapoxin and depudecin inhibit the HDACs irreversibly through a different mechanism, principally through covalent binding to the epoxyketone group (de Ruijter et al., 2003). Even though HDACs are widely distributed in chromatin, HDACi only affect a small fraction of expressed genes (2-10%) in transformed cells (Dokmanovic et al., 2007). For example, the most powerful HDACi, TSA, alters only 2% of 340 examined genes in lymphoid cell lines (Dokmanovic et al., 2007).

HDACi classification

HDACi are divided into four classes: hydroxamates, cyclic peptides, aliphatic acids, and benzamides (Dokmanovic et al., 2007).

Hydroxamates

TSA, suberoylanilide hydroxamic acid (SAHA), ITF2357 target class I and II HDACs at nanomolar (nM), micromolar (μM), and nanomolar (nM) concentrations, respectively (Dokmanovic et al., 2007)

Cyclic peptides

PCI-24781 that targets class I and II HDACs is a member of cyclic peptide class of HDACi (Dokmanovic et al., 2007).

Aliphatic acids

Valproic acid, phenyl butyrate and butyrate inhibit class I and IIa HDAC at millimolar concentration (Dokmanovic et al., 2007), and are less efficient than TSA (mM compared to nM range) (de Ruijter et al., 2003). Class II HDACs are five times less sensitive to valproic acid than are class I HDACs. HDAC4 is less susceptible to butyrate inhibition. Tailored use of HDACi may be possible through the development of new HDAC inhibitors that are targeted to a particular HDAC, together with elucidation of the tissue distributions of the HDAC subtypes (de Ruijter et al., 2003). Sodium butyrate has been reported to up regulate the number of slow twitch fibers and enhances mitochondrial function, biogenesis, and fatty acid oxidation in skeletal muscle (Gao et al., 2009; Ferrari et al., 2012). In addition, butyrate can activate PGC-1 (Peroxisome proliferator-activated receptor-gamma coactivator 1), which plays an important role in regulating mitochondrial function (Ferrari et al., 2012).

Benzamides

MS-275 and MGCD0103 both target class I HDACs at micromolar concentrations (Dokmanovic et al., 2007).

1.4.3. HDAC inhibitors in disease treatment

The potential of HDACi to treat certain diseases in humans has been suggested, and some HDACi have entered clinical trials. They are butyrate, phenylbutyrate, desipeptide, pyroxamide, suberoyl anilide bishydroxamide (SAHA), valproic acid, CI-994, etc. (de Ruijter et al., 2003; Dong et al., 2013; Fredly et al., 2013; Hajek et al., 2013).

Recently, another molecule was found to inhibit HDAC activity *in vitro*. That molecule is S1P. The Spiegel group came up with the idea of testing whether S1P inhibits HDAC activity (HDAC1 and HDAC2) when observing three facts. First, one of S1P producers, SphK2 was associated with isolated chromatin, especially histone H3. Second, the expression of SphK2 led to an increased acetylation in several histone marks (H3K9, H4K5, H2BK12), while the down regulation of SphK2 resulted in decreased acetylation of the same histone marks. This decrease in acetylation was reversed by the addition of S1P. Third, SphK2 was found to bind to HDAC1 and HDAC2, but not other class I HDACs, class II HDACs or SIRT1 of class III HDACs. By testing the deacetylase activity of HDAC1 and HDAC2 in Hela nuclear extract or recombinant protein incubated with S1P, the research group saw a significant decrease in their HDAC activities (Hait et al., 2009). It has not been tested yet whether S1P can inhibit the deacetylase activity of other HDACs. Several research groups have been testing on the potential ameliorative effects of S1P in DMD lately (Loh et al., 2012; Ieronimakis et al., 2013; Pantoja et al., 2013; Saba and de la Garza-Rodea, 2013)

1.4.4. HDACs in skeletal muscle function

Previous studies have illustrated that HDACs regulate the differentiation of muscle satellite cells by regulating the transcription of muscle specific genes and the activity of myogenic bHLH proteins (MyoD, Myf5, myogenin and MRF4) and MEF2 family factors (MEF2A, MEF2B, MEF2C and MEF2D) (Puri and Sartorelli, 2000). In undifferentiated myoblasts, HDACs are recruited to the MyoD and MEF2 complex and repress the expression of genes required for differentiation. In differentiating cells, HDACs are dissociated out of the chromatin, leading to hyperacetylation at muscle loci and up regulation of muscle gene expression (Consalvi et al., 2011). Treating myoblasts with TSA has been shown to increase expression of genes involved in differentiation (Consalvi et al., 2011). Thus, the balance between acetylation and deacetylation is an important factor in muscle regeneration.

In finding a cure for DMD, a number of HDAC inhibitors, such as TSA, VPA and phenylbutyrate have been tried on *mdx* mice and demonstrated beneficial effects on countering disease progression (Consalvi et al., 2011). Particularly, these HDAC inhibitors (1) increased the size of myofibers, (2) reduced inflammation infiltration, and (3) decreased fibrosis (Consalvi et al., 2011). These beneficial effects are similar for the three-tested HDACi, but the extent of rescue is different, with TSA as the most effective drug. This might be due to the difference in pharmacological profile and bioavailability of different HDACi. In 2006, Minetti et al. showed that prolonged treatment with TSA rescued not only the histological and morphological aspects in *mdx* mouse muscles, but also their function, represented as increased muscle force and activity (Minetti et al., 2006). The authors then narrowed down the contribution of individual classes of HDACs in contributing to muscular dystrophic pathogenesis by showing that selectively

inhibiting class I HDACs with MS27-275 had beneficial effects on muscles, both on morphology (increased muscle fiber size) and muscle function (exercise time) along with increased follistatin expression (Minetti et al., 2006). In 2008, Colussi et al. screened individual HDACs (from HDAC1 to HDAC11) and observed a pronounced morphological rescue in HDAC2 knockdown *mdx* muscles compared to other HDACs (Colussi et al., 2008). Furthermore, they found an increase in HDAC activity of both *mdx* adductor muscles and *mdx* differentiating satellite cells. Interestingly, an elevated protein level of HDAC2 was observed in both *mdx* adductors and differentiating satellite cells compared to wild-type ones. Using both *in vivo* and *in vitro* approaches, they showed that reduced HDAC2 levels rescue dystrophic pathologies in not only morphology, but also function. Particularly, after three days of transfection with siRNA, *mdx* satellite cells exhibited improved differentiation capacity, marked by an increased fusion index. In adductor muscles of *mdx* mice treated with HDAC2 siRNA (5mg/kg) for 30 days (i.p. 3 times/week), the variation in muscle size was reduced, along with decreases in inflammation infiltration and increases in exercise function (Colussi et al., 2008).

In a recent paper, Galmozzi et al. pointed out the negative effects of class I HDACs on mitochondrial biogenesis and oxidative metabolism (Galmozzi et al., 2013). Treating C2C12 cells with class I (MS275), but not class II specific HDAC inhibitors exhibited an increased expression of genes associated with mitochondrial biogenesis (*PGC-1α*, *TFAM*, *TFB1M*), mitochondrial density, DNA and activity. These up regulations translated into an increase in oxidative metabolism, as evidenced by elevated oxygen consumption in MS275 treated C2C12 cells. The changes in the metabolic mechanism of class I selective HDAC inhibitors is recapitulated in muscle tissues from MS275 treated mice. This is observed as not only an

increase in biogenesis-associated and metabolic pathway-associated gene expression and protein levels, but also an increase in the slow twitch fibers component, which was revealed by succinate dehydrogenase staining. The authors also suggested HDAC3 as the primary member of the class I HDACs that regulates oxidative metabolism mediated by PGC-1α.

Due to its beneficial effects on *mdx* mice, HDACi should be used in clinical trials to treat DMD. However, the lack of information on critical pharmacological parameters in children obstructs the administration of these drugs to DMD boys (Colussi et al., 2008). ITF2357 is an HDACi that is in phase I clinical trials for safety tests in children affected by Systemic Onset Juvenile Arthritis (SOJIA) (Vojinovic and Damjanov, 2011). The prolonged treatment of ITF2357 has shown an effect in preventing disease progression in *mdx* mice (Colussi et al., 2008).

Chapter 2: Materials and methods

2.1 Animal procedure

Experiments involving animals were performed in accordance with the guidelines and ethical approval from the University of Washington Institutional Animal Care and Use Committee. The mouse dystrophin mutant strains used were *mdx* (C-to-T transition at position 3185, resulting in a premature stop codon) and *mdx*^{4CV} (C-to-T transition in exon 53 at position 7916 resulting in a premature stop codon).

Mice used for HDAC activity assay

Wild type control *C57BL/10ScSn* (control) mice were compared to *mdx* on a *C57BL/10ScSn* background *(C57BL/10ScSn-Dmd*$^{mdx/J}$, referred as *mdx* from now on; both groups 4.5MO males, n=3). Triceps were harvested and snap frozen in liquid nitrogen and total protein lysate was extracted for the HDAC2 activity assay.

Wild type control *C57BL/6J* (control) mice were compared to *mdx*^{4CV} on a *C57BL/6J* background (*B8Ros.Cg-Dmd*$^{mdx\text{-}4CV}$*/J*, referred as *mdx*^{4CV} from now on; both groups 5MO males, n=5). Adductors, TA, triceps, heart and brain were harvested and snap frozen and nuclear extracts were prepared for the total HDAC and HDAC2 activity assay.

Mice used for Titin pattern assay

3.5MO *mdx*^{4CV} and controls (n=3 males in each group) were used, along with 4MO and 2MO vehicle and THI-treated *mdx* (n=3 males in each group). Gastrocnemius (gastro) muscles were harvested and used for Titin staining.

Three day 2-Acetyl-5-tetrahydroxybutyl Imidazole (THI) treatment for *mdx* in CTX-injury model

In *mdx*^{4CV} mice (4MO males, n=8) the left tibialis anterior (TA) were injured with 10μM cardiotoxin (CTX) (Calbiochem, Darmstadt, Germany) from *Naja nigrcollis.* Immediately after injury, the mice were injected intraperitoneally (IP) with 2-acetyl-5 tetrahydroxybutyl Imidazole (THI; 250ml of 0.15mg/ml) in PBS (n=4) or just PBS for vehicle control (n=4), twice daily (injections 6 hours apart) for 3 days. On day 4 post injury, the animals were euthanized and the muscles were dissected for analysis. Dissected TAs were snap frozen and utilized for nuclear extraction for S1P quantification and HDAC activity assay.

One month THI treatment for uninjured *mdx* mice

THI was administered to 4-week-old male *mdx* mice (Jackson Laboratory) as described previously (Schwab et al., 2005). Briefly, the mice were treated with THI (n=5) 50mg/L in 10g/L glucose, pH 2.8 or vehicle (n=5) 10g/L glucose, pH 2.8 as drinking water for one month. The THI and vehicle solutions were made fresh and replaced twice a week. The blood collections were done the last day of THI treatment and a day after the withdrawal. The mice were euthanized two days after withdrawal of THI from the drinking water using avertin and the cervical dislocation method. Adductors, gastrocnemius and diaphragm muscles were harvested. Adductors were snap frozen. The left adductors were utilized to quantify muscle and nuclear S1P levels, nuclear HDAC activity and histone acetylation profiles. RNA was extracted from right side adductors and utilized for microarrays and qPCR analysis. Diaphragms were frozen in optimal cutting temperature (OCT) compound with liquid nitrogen cooled isopentane and sectioned to 8um thick sections for Picrosirius Red, CD45 and CD68 stainings or embedded in

paraffin for H&E stainings or snap frozen for RNA extraction. Gastrocnemius muscles were kept in EGTA-Ringer solution and used for Titin pattern analysis.

Three-month-THI treatment for uninjured *mdx* mice

For the first month, THI was administered to 4-week-old male *mdx* mice with the same treatment as one-month-THI treatment above. After that, THI administration was paused for 3 days, and then THI treatment was resumed with higher dose (500mg/L) for the last two months. Gastrocnemius muscles were harvested and kept in EGTA-Ringer solution and used for Titin pattern analysis.

2.2 Peripheral blood cell analysis

Blood was collected via retro-orbital blood collection using heparinized capillaries and transferred to blood collection tubes containing 1.6mg/ml EDTA (SARDTEDT, Numbrecht, Germany) for analysis. The white blood cell and lymphocyte counts were determined with 30 µl per sample using the Hemavet 950FS system (Drew Scientific, Dallas, Texas, USA).

2.3 Mouse Histology and Immunohistochemistry

Picrosirius red with Fast Green and Hematoxylin & Eosin stainings were conducted following established protocols (Kiernan, 2008). Briefly, for Picrosirius red staining, OCT diaphragm sections were fixed in ice cold methanol for 5 minutes at 4°C, washed with water and incubated in Picro-sirius red for 1 hour. Samples were then washed in acidified water, dehydrated in ethanol and cleared with xylene. Fibrosis was quantified as percentage of area stained red within each 20x field analyzed using ImageJ v1.40. For evaluation of fibrosis, the mean value from one to two separate sections (~200µM apart in longitudinal distance) was analyzed for each muscle, five mice were examined.

For H&E staining, samples embedded in paraffin were cleared with xylene and dehydrated in ethanol. The diaphragm sections were then stained for hematoxalin for 3 minutes followed by rinsing with deionized water, developed in tap water and destained with acid ethanol. Eosin staining was then applied, followed by dehydration in ethanol and clearing in xylene.

For CD45 and CD68 stainings OCT diaphragm sections were hydrated by enclosing muscle area with a hydrophobic pen and submerging the tissue sections in 1%BSA/PBS. Primary antibodies CD45 Ab, CD68 Ab and IgG Ab (eBioScience) were then added at 1:100, 1:50 and 1:50 dilutions, respectively and incubated for 1h 30min. The muscles were washed with PBS, and incubated with secondary antibodies, Alexa Fluor 488 Donkey anti-rat IgG (H+L) (Invitrogen A21208) at 1:500 dilution for 1 hour. After three washes with PBS, sections were counterstained for 10 seconds with one drop of NucBlue Fixed Cells staining (Life technologies, R37606). Stained tissues were then mounted with 1 drop of Fluorescence Mounting media (Dako, S3023) and examined with a confocal microscope. Analysis was done by counting CD45 positive cells in total diaphragm sections (n=5 for vehicle and n=5 for THI). CD68 marker analysis was done by normalizing the number of positive CD68 cells to the number of total muscle cells in the analyzed tissues (n=3 for vehicle and n=3 for THI).

2.4 Titin pattern analysis in sarcomeres

The protocol for Titin staining was modified from a previously established method (Knight and Trinick, 1982). Briefly, freshly collected gastro muscles were incubated over night at 4^0C in EGTA-Ringer solution (1mM EGTA,100mM NaCl, 2mM KCl, 2mM MgCl2, 50mM Tris pH 7.4), and briefly minced with mini-pestles, followed by 3 washes in Rigor solution (10mM Na-

phosphate buffer pH 7.0, 100mM NaCl, 2mM MgCl2). Homogenized muscles were then treated with 1% Triton for 15 minutes at room temperature, fixed in 5% paraformaldehyde for 1 hour, and blocked in PBTB (PBT, 0.4% BSA (w/v), 5% normal goat serum (v/v)) before the staining process. Primary anti-Titin antibody (Hybridoma Bank, 9 D10) was used at 1:10 dilution followed by secondary antibody (Alexa 488 anti-mouse antibody, Invitrogen, A11029, 1:500 dilution) incubation, both at 4^0C overnight. Four washes in PBT were used after each round of antibody incubation, with 10X DAPI added in the third wash after secondary antibody incubation. Stained muscles were stored in Glycerol/Prolong (800 uL 80% glycerol/3% NPG 200 uL Prolong Gold) at 4^0C and imaging analyzed by confocal microscopy. 10 Titin bands per myofibril, 5 myofibrils per mouse and 3 mice per treatment were analyzed.

2.5 Protein extraction

Nuclear protein extraction from frozen tissues

Frozen tissues were ground into fine powder in liquid nitrogen and nuclear proteins were extracted as previously described (Hait et al., 2009). Briefly, minced tissues were homogenized in buffer A (10mM Hepes pH 7.8, 10mM KCl, 0.1mM EDTA, 1mM Na3VO4, 1mM DTT, 0.2mM PMSF, protease inhibitor (Complete Mini EDTA free, Roche) and incubated on ice for 15 min. 0.75% NP-40 was then added to the suspension and the cell plasma membranes were lysed by vortexing at high speed for 10 sec. Nuclei and cytoplasm were separated by centrifugation at 3000 rpm for 3 min at 4C. High salt buffer (20mM Hepes pH 7.8, 0.4M NaCl, 1mM EDTA, 1mM Na3VO4, 1mM DTT and protease inhibitors) was used to re-suspend the nuclei. Nuclear protein was extracted by vortexing for 15 sec and rocking for 15 min. After centrifugation at 14,000xg for 5 min at 4C, nuclear proteins were collected from the supernatant fraction.

Total protein lysate extraction

Total protein was extracted with RIPA buffer (50mM Tris pH 7.4, 150mM NaCl, 0.1% SDS, 0.5% sodium deoxycholate, 1% Triton X100, protease inhibitor (Complete Mini EDTA free, Roche). Whole muscles were ground in liquid nitrogen, 500-600ml RIPA buffer was added to lyse the cells, and the supernatant collected after centrifugation at max speed 10 minutes at 4^0C. Protein concentration was measured with the Bradford method.

2.6 Western Blot Analysis for HDAC2 protein level

Nuclear protein fractions (method described above) were separated using 4-20% linear gradient SDS-PAGE (Tris-HCl Ready Gel, BIORAD, Hercules, CA) and transferred to polyvinylidene fluoride (PVDF) membranes with a wet transfer system (BioRad). Membranes were blocked for 1 hour with Tris-buffered saline with 0.1% (v/v) Tween20 containing 5% (w/v) non-fat dry milk and incubated O/N in primary HDAC2 (H-54) antibody (Santa Cruz, sc-7899, 1:200 in blocking buffer). After the washing (3 times in TBST buffer), the blots were incubated for one hour with the secondary Ab (Goat Anti-Rabbit IgG(H+L) HRP conjugate, Biorad, #170-6515). The signals were detected using an enhanced chemiluminescense kit (Millipore, Billerica, MA, USA) and CL-XPosure Films (Thermo Scientific) and analyzed using Image J, normalized to total nuclear protein stained with coomassie blue in the stained protein gel.

2.7 Histone acetylation profile

Equal amounts of nuclear extract proteins were separated by SDS-PAGE, transferred to nitrocellulose, incubated with primary antibodies as indicated in figure legends, including rabbit polyclonal antibodies to: histone H3, and H4K5ac (Millipore); H3K9ac, H3K18ac (Upstate Biotechnology, USA), H2BK12ac (Cell Signaling); HDAC1, HDAC2 (Santa Cruz

Biotechnology). Immunopositive bands were visualized by enhanced chemiluminescence using secondary antibodies conjugated with horseradish peroxidase and Super-Signal West Pico chemiluminescent substrate (Pierce) as described (Cocco et al., 1980).

2.8 Measurement of sphingosine-1-phosphate in mouse tissues

The total lysates and nuclear preparations were isolated as described above. Nuclei were washed extensively with PBS. Internal standards were added (0.5 nmol each, Sphingolipid Mixture II/LM-6005, Avanti Polar Lipids), lipids extracted, and sphingolipids quantified by liquid chromatography, electrospray ionization-tandem mass spectrometry (LC-ESIMS/MS, 4000 QTRAP, ABI) as described previously.

2.9 Immunoprecipitation

Nuclear extracts (500µg protein) were pre-cleared with normal rabbit IgG (2.5µg) and protein A/G PLUS-Agarose beads (50µl) and incubated over night with 5µg of HDAC2 Ab (Santa Cruz, sc-7899) and incubated over night. Thereafter, protein A/G PLUS-Agarose beads (50µl) were added and incubated for 2hours at 4^0C. Beads were collected and washed with HDAC assay buffer (4 times 900µl; 50mM Tris pH8. 137mM NaCl, 2.7mM KCl and 1mM MgCls) and used for HDAC2 activity assays. Aliquots of agarose-bound immune complexes were boiled in SDS-PAGE sample buffer, and the released HDAC2 protein was analyzed by Western blotting using anti-HDAC2 as primary antibody.

2.10 HDAC activity assay

HDAC activity was determined with a Fluor-de-Lys® HDAC fluorometric activity assay kit (Enzo Life Sciences). HDAC reaction was initiated by adding *Fluor de Lys*® Substrate (100µM) to 50µg or 40µg nuclear protein (NE) for total HDAC activity. For HDAC2 activity assays,

HDAC2 was first isolated by immunoprecipitation as described above and the immunoprecipitated HDAC2 was subjected to the activity assay by adding *Fluor de Lys*® Substrate (100mM). Samples were incubated with the substrate at 37^0C for 20 minutes. The *Fluor de Lys*® Developer was added and the mixture was incubated for another 20 min at room temperature. HDAC activity levels were analyzed as AFU (arbitrary fluorescence unit) with Perkin Elmer Envision Xcite (2104 Multi-label reader) by measuring fluorescence with excitation at 360nm and emission at 460 nm.

2.11 Microarray

Adductor muscles from THI- and vehicle-treated *mdx* mice were used to extract RNA. Frozen tissues were ground into fine powder in liquid nitrogen with a mortar and pestle. Total RNA was isolated using TriZol (Invitrogen), treated with DNaseI (Thermo Scientific EN0521) and converted to cDNAs. The subsequent synthesized Cy3 labeled cRNA were amplified and purified followed by hybridization in microarray using the Agilent platform, which has 60-mer nucleotides and around 60k probes, representing around 30k genes. Hybridization and scanning were performed in the microarray facility at the Institute for Systems Biology. Any intensity-dependent biases were removed in the data using the normalize.qspline function in the affy Bioconductor package. Log2-fold-change of gene expression between THI- and vehicle-treated *mdx* samples were used and heatmaps were generated using MultiExperiment Viewer software. Density plots were generated with R studio. Gene sets were retrieved from the Broad Institute. The inflammation gene set includes Cytokines and Inflammatory Response genes, CCR3 signaling in Eosinophils and inflammation genes, which were selected from the biological database. The fatty acid oxidation gene set contains fatty acid beta oxidation, and Reactome mitochondrial fatty acid oxidation and metabolism genes, which were also acquired from the

biological database. The muscle gene set includes muscle development (GO:0007517), Biocarta IGF mTOR pathway, Reactome muscle contraction, Structural constituent of muscle (GO: 0008307), Skeletal muscle development (GO: 0007519) associated genes.

2.12 Real-Time Polymerase Chain Reaction (qPCR)

Total RNA was extracted using TriZol (Invitrogen) and treated with DNaseI (Thermo Scientific, EN0521). RNA abundance was determined using a Nanodrop ND-1000 spectrophotometer (Nanodrop Technologies, Wilmington, DE). After a reverse transcription reaction using the Omniscript RT kit (Qiagen, Valencia, CA), Mrap, Adrb3, Ccl2, Ubi, Colα1, CD4, CD8 and 18S rRNA were analyzed by qPCR with SyberGreen master mix (Applied Biosystems, Carlsbad, CA) on an Applied Biosystems 7300 Real-time PCR cycler. All data were normalized to house keeping gene transcript levels (UBC or 18S rRNA). The gene primers used are as follows: Mrap fwd and rev: AGACACTGTCGTCAAAGCCACAG and CGCTCTGTCTCCAGGCTCACCAC , respectively. Ccl2: CAGCCCAGCACCAGCACCAG and CAGCAGGTGAGTGGGGCGTTA. Adrb3: GGCCCTCTCTAGTTCCCAG and TAGCCATCAAACCTGTTGAGC. Col1α1: ACGGCTGCACGAGTCACAC and GGCAGGCGGGAGGTCTT (Kenyon et al., 2003); CD4: TGGTTCGGCATGACACTCTC and GGAAGGAGAACTCCGCTGAC; CD8: AGGAGCCGAAAGCGTGTTTG and TCCTGGCGGTGCCATTTTAC. S1PR1: ATCATGGGCTGGAACTGCATCA and CGAGTCCTGACCAAGGAGTAGAT . Ubiquitin C and 18S rRNA were used as house keeping genes, and the primers used for UBC were: CGTCGAGCCCAGTACCACCAAGAAGG for forward and CCCCCATCACACCGAACAAGCACAAG for reverse (Mamo et al., 2007), for 18S rRNA

were: TTGACGGAAGGGCACCACCAG for forward and GCACCACCACCCACGGAATCG for reverse (Au et al., 2011).

Analysis of miRNAs was performed using specific TagMan assays (Applied Biosystem). cDNAs were synthesized using Taqman MicroRNA reverse transcription kit. Primers for hsa-mir-29c (cat. number: 4427975), hsa-mir-1-2 (cat. number: 4427975) and endogenous snoRNA202 (lot. Number: 0910214-0) were purchase from AB Applied Biosystem.

2.13 THI-treated C2C12 metabolic flux assay

C2C12 cells were seeded onto SeaHorse plates at 5000 cells per XF96 well and differentiated in DMEM (Glutamax, Invitrogen), 10% horse serum (Thermo Scientific* HyClone* Donor Equine Serum), 1% insulin cocktail (insulin, transferrin, selenium solution (ITS-G), Gibco/Invitrogen) for 1 day. On day 2, 0.05mg/ml THI in 1%DMSO or 1%DMSO for control was added to fresh differentiation medium. Seahorse assays were carried out on day 3. One hour before the assay, culture media were exchanged for base media (unbuffered DMEM (Seahorse XF Assay Media) supplemented with sodium pyruvate (Gibco/Invitrogen, 1mM) and with 25mM glucose (for MitoStress assay), 25mM glucose with 0.5mM Carnitine (for Palmitate assay), or 2mM glutamine (for glucose stress assay). Injection of substrates and inhibitors was applied during the measurements to achieve final concentrations of 1μM for 4-(trifluoromethoxy)phenylhydrazone (FCCP; Seahorse Biosciences), 2.5μM for oligomycin, 2.5μM for antimycin and for 2.5μM rotenone for MitoStress assay; 200μM palmitate or 33μM BSA, and 50μM Etomoxir (ETO) for palmitate assay and 20mM glucose and 100mM 2-deaoxy-D-glucose (2-DG) for glucose stress assay. In the mitochondrial stress assay, baseline oxygen consumption rate (OCR) was first measured, then OCR changes in response to injection of oligomycin, FCCP and finally antimycin and rotenone were determined. The OCR values were further normalized to the

number of cells present in each well, quantified by the Hoechst staining (HO33342; Sigma-Aldrich) as measured using fluorescence at 355nm excitation and 460nm emission. The baseline OCR was defined as the average values measured before oligomycin injection. Changes in OCR or ECAR in response to the addition of substrates and inhibitors were defined as the maximal change after the chemical injection compared to the last OCR /ECAR value before the injection. The reagents were from Sigma, unless otherwise indicated.

2.14 S1P-treated C2C12 metabolic flux assay

C2C12 cells were treated the same way as in THI experiment, except for the medium used in the S1P treatment day: Dulbecco's modified Eagle's medium/Ham's F-12 medium (DMEM/F12) containing glutamax with 20% knockout serum replacer (SR), 1mM sodium pyruvate, 0.1mM nonessential amino acids, 50 U/mL penicillin, 50μg/mL streptomycin (all from Invitrogen, Carlsbad, CA), 0.1mM β-mercaptoethanol (Sigma-Aldrich, St. Louis, MO), and 4ng/mL basic fibroblast growth factor (FGF; Peprotech, Rocky Hill, NJ). S1P in BSA (Cayman Chemical) was used at 0.1mM final concentration. S1P was dissolved in methanol (0.5mg/ml) and aliquoted, then the solvent was evaporated with a stream of nitrogen to deposit a thin film on the inside of the tube. Prior to use, aliquots were re-suspended in PBS with 4mg/ml BSA (fatty acid free) to a concentration of 500μM.

2.15 Mitochondria copy number assay

C2C12 DNA was extracted using DNazol (Invitrogen 10503-027) following the manufacturer's protocol. Mitochondria copy number in C2C12 cells was measured as previously described (Facucho-Oliveira et al., 2007). Briefly, the primers used were mt-Co1-F 5'-CAGTCTAATGCTTACTCAGC-3' and mt-Co1-R 5'-GGGCAGTTACGATAACATTG-3' for mitochondrial DNA and Gapdh-F 5'GGGAAGCCCATCACCATCTTC-3' and Gapdh-R

5’AGAGGGGCCATCCACAGTCT-3’ for genomic DNA. The number of copies of mitochondrial DNA and genomic DNA were determined according to a standard curve with 10-fold dilutions from 10^2 to 10^7 copies, and the ratio of mtDNA to genomic DNA for each sample was calculated. A 20ul reaction with 2.0ng of DNA extract, 1X SYBR green mix, and 300nM of each primer were used. Using the 7300 realtime PCR system (Applied Biosystems), the DNAs were amplified by incubating the reaction mixture at 95°C for 10 minutes, 50 cycles at 95°C for 10 seconds, 53°C for 27 seconds for mt-Co1 or 60°C for 27 seconds for Gapdh, and then 72°C for 28 seconds.

2.16 Statistical analysis

All quantitative data were expressed as mean ± sem. The Student’s t-test with one tail was used and a p-value less than 0.05 was considered statistically significant.

Chapter 3: Result

3.1 Examining HDAC2 protein and activity in *mdx* mice

From a thorough screening of all class I HDACs in *mdx* mice, Colussi et al. observed a distinct increase of HDAC2 protein levels in 2MO *mdx* adductor muscles (2-fold increase) and differentiating satellite cells (1.75-fold increase) compared to wild-type (Colussi et al., 2008). The specific up regulation of the HDAC2 protein in *mdx* mice is a logical finding since knocking down HDAC2 has been shown to rescue DMD morphologies and function (Colussi et al., 2008). I am interested in understanding if HDAC2 has a special contribution to DMD pathologies. First, I need to confirm that HDAC2 protein levels are up regulated in *mdx* muscles. Colussi et al. only checked HDAC2 protein levels in one type of muscle (adductors) and in one type of dystrophic mutant background mice. To see if increased HDAC2 levels coincide with different dystrophic mutant backgrounds and muscles, I tested the HDAC2 protein in a different dystrophic mutant, the mdx^{4CV} line. The point mutation in the dystrophin gene is at exon 23 in *mdx* line, while it is at exon 53 for mdx^{4CV} line (Bulfield et al., 1984; Im et al., 1996). I not only checked adductors, but also the Tibialis anterior (TA) and hearts. My analyses confirmed a greater than 4-fold up regulation in HDAC protein levels in the *mdx* adductor muscles and in TAs, whereas while a trend, there was no significant increase in levels in hearts (Fig.1. A-E).

Whether the increased HDAC2 protein level translates into an increase in total HDAC activity is important to investigate. Colussi et al. showed an up regulation of around 2.7-fold and 1.8-fold of total HDAC activity in *mdx* adductors and differentiating satellite cells, respectively. I further checked if this trend was recapitulated in other muscles of mdx^{4CV} mice. Using a fluorescent-based deacetylation assay, in which a fluorophore is generated due to deacetylation, I observed a

2.67- and 1.97-fold increase in total nuclear HDAC activity in adductors and TAs, respectively (Fig. 2. A-B). These data are in agreement with the data from Colussi et al. However, total nuclear HDAC activity in the heart muscle was not significantly different between *mdx*^{4CV} and control mice (Fig. 2.C). This unexpected result impelled me to compare total nuclear HDAC activity in different muscles of control mice. Interestingly, total nuclear HDAC activity in the heart was significantly higher (around 3-fold) than it was in adductors and TAs (Fig. 2. D). This could be because heart muscle is a non-dividing tissue where not many genes are actively transcribed, leading to the need for more HDAC to repress chromatin structure. Furthermore, the high total nuclear HDAC activity in the hearts of control mice might be due to higher levels of HDAC2 protein, which has been shown to be crucial for heart function (Trivedi et al., 2007).

In a separate experiment, Colussi et al. tested the benefits of knocking down HDAC2 in dystrophic pathologies. While their main purpose was to show that HDAC2 siRNA reduces HDAC expression, and thus lowers HDAC2 activity, their experiments showed an increase of 1.7-fold on HDAC2 specific activity in *mdx* satellite cells transfected with scramble siRNA compared to wild-type untreated ones. This result cannot strongly prove a real elevation of HDAC2 activity in *mdx* satellite cells because transfected cells might have some artifacts that interfere with their HDAC2 activity. Here, I tested HDAC2 activity in different muscles of not only *mdx*, but also *mdx*^{4CV} mice. To analyze the HDAC2 activity in these samples, I immunoprecipitated HDAC2 from nuclear extracts (Fig.3. A) and subjected the isolated enzyme to a deacetylation assay. An increase of HDAC2 activity was detected in all tested muscles of *mdx*^{4CV} mice, the fold increases being 2.52 (adductors), 1.95 (TAs) and 1.15 (hearts) (Fig.3. B-D). In *mdx* mice, an increase of 2.76-fold in HDAC2 activity was also observed in triceps

muscles (Fig.3. E). Therefore, total nuclear HDAC activity, HDAC2 protein levels and HDAC2 activity are increased in *mdx* muscles, even in different dystrophic mutant genetic backgrounds. This result implies a potential role of HDAC2 in contributing to the progression of disease or pathogenesis in *mdx* mice.

3.2. HDAC activity in THI-treated-injured *mdx* muscles

Using immunoprecipitated HDAC2 from Hela nuclear extract and recombinant HDAC2, Hait et al., (2009) demonstrated the inhibitory effect of S1P (0.5-5μM) on HDAC2 activity *in vitro* (Hait et al., 2009). As S1P has been shown to have morphological and functional benefits on DMD in both fly and mouse models, we wanted to test if S1P could inhibit HDAC activity *in vivo*, and if this inhibitory effect correlated with pathology suppression. Instead of delivering S1P directly to the mice, which might cause a loss of its activity when the phosphate group is removed in the digestive tract (oral delivery) or in the blood (systemic delivery), we opted to up regulate S1P in dystrophic mice by systemically delivering THI, an FDA safety approved small molecule that inhibits S1P lyase. Previous study showed beneficial effects of THI on acute injured dystrophic mice, as evidenced by increased satellite cell based regeneration, muscle fiber size and specific force (Loh et al., 2012; Ieronimakis et al., 2013). Furthermore, in these THI-treated dystrophic mice, hallmarks of DMD pathology, such as fibrotic and fat infiltration were significantly reduced (Ieronimakis et al., 2013). Following the same treatment, we aimed to reproduce THI effects on dystrophic muscles, and check if up regulated S1P can inhibit HDAC activity in this experimental paradigm as a correlation with pathology suppression. In this experiment, we treated mdx^{4CV} (4MO, males, n=8) with THI (75μg, IP) or vehicle (PBS) daily for 3 days after TA muscle cardiotoxin (CTX. 10μM) injury and sacrificed the mice thereafter to obtain TA muscles for further analysis (Fig. 4. A). First, we needed to test if THI could enrich S1P levels in

the nuclear fraction, the place where S1P exerts its action on HDAC. To determine if THI mainly increases S1P, and if THI beneficial effects on mouse muscles are from S1P, not other sphingolipids, we also tracked the changes of other sphingolipids after THI treatment. We chose to measure the nuclear sphingolipids of the S1P precursor, sphingosine, S1P derived - dihydro-S1P (DHS1P) and its precursor- dihydrosphingosine. We observed a significant increase in nuclear S1P, but not other sphingolipids (Fig.4.B). Testing deacetylation activity on the nuclear muscle samples, we revealed a significantly reduced (approximately 1.4-fold lower) level of nuclear HDAC activity on THI-treated samples (Fig. 4. C). These data indicate that increase in nuclear S1P and reduction in total HDAC activity correlate with suppressed disease pathology observed in THI-treated *mdx* mice after acute injury (Ieronimakis et al., 2013).

3.3 Examinations of uninjured THI-treated *mdx* mice

3.3.1 Validation of THI delivery efficacy

In injured mice, the inflammatory response, degeneration and regeneration processes are clearly accelerated and more pronounced (Czerwinska et al., 2012), making it easier to observe a rescue effect of a treatment on injured versus uninjured mouse models. On the very first day after CTX injury, degeneration has already taken place extensively. Regeneration is observed also very quickly, just four days after injury (Czerwinska et al., 2012). This quicker reaction in injured mice leads to shorter experimental time, providing not only a time-wise advantage but also an economical benefit as prolonged treatment and maintenance on mice is costly. These factors make CTX injury a useful experimental strategy. However, it is not a physiological representation of chronic muscle injury observed in DMD or *mdx* dystrophic muscles. We therefore followed up the effect of THI on nuclear S1P on uninjured *mdx* mice. We delivered THI (50mg/L) to *mdx* mice in drinking water for 1 month (Fig.5. A). Before sacrificing the mice

for further assays, we needed to test the efficacy of THI delivery in the experiment procedure. If THI elevates S1P levels in the mice, there will be less lymphocytes egressing from the lymphoid organs due to the changes in S1P concentration (Cyster and Schwab, 2012). Previous studies have shown that THI administered in drinking water or by intraperitoneal injection (i.p.) can reduce the white blood cell count (Schwab et al., 2005; Ieronimakis et al., 2013). Thus, we utilized this analysis to validate the efficacy of THI delivery in our experiment. We harvested blood from THI and vehicle-treated mice and counted white blood cell (WBC) and lymphocyte numbers. We observed substantial down regulation of these cells in the THI-treated samples (Fig. 5. B), thereby validating the efficacy of THI delivery. Furthermore, 24 hours after withdrawing THI, the levels of WBC and lymphocytes reverted to normal, indicating the reversibility of THI's effects on WBC and lymphocyte counts (Fig. 5.B).

3.3.2 Examining pathological rescue in THI-treated muscles

To examine the beneficial effects of THI on dystrophic pathologies in this experimental paradigm, we assessed two hallmarks of dystrophic muscle pathology: the fibrotic and sarcomere integrity. The mice in our experiment were too young (only two months old) to exhibit a pronounced dystrophic morphology. Therefore, we chose to analyze fibrosis in the diaphragm because this organ has the strongest disease phenotype, initiating after just one month of age (Niebroj Dobosz et al., 1997; Hinkle et al., 2007; Ishizaki et al., 2008). We decided to check both the gene expression and protein levels of the causal agent of fibrosis, the collagen. qPCR analysis revealed a significant reduction of pro-collagen1α1 mRNA levels in the diaphragm of THI-treated *mdx* mice compared to the control (Fig.5.C). Next, we analyzed the protein collagen level for further fibrotic study. The protein analysis was based on picrosirius red staining that specifically detects collagen (Fig. 5.D). Quantification of the collagen area showed that THI

treatment significantly reduced fibrosis in uninjured diaphragms (Fig.5.E). Taken together, these results demonstrate that *mdx* diaphragm muscles in early life benefit from THI treatment.

Next, we assessed THI effects on the second dystrophic pathology hallmark: the sarcomere molecular architecture, particularly the myofibril integrity. For this purpose, we examined Titin, a giant elastic protein of the myofibril, which spans from the Z-disk to M-line regions of the sarcomere and develops passive force when muscles are stretched, thereby giving rise to the elasticity of myofibrils (Matsumura et al., 1989; Granzier and Labeit, 2006). It has been known that mutations in Titin can cause muscular dystrophies and cardiomyopathies (Hackman et al., 2002). In addition, previous studies have revealed that DMD pathologies are correlated with significant degradation of Titin and with an abnormal sarcomere pattern of its homologue in *Drosophila*, Projectin (Matsumura et al., 1989; Pantoja et al., 2013). Matsumura et al. 1989 showed a progressive and "relentless" Titin degradation in DMD patients' biopsies after 5 years of age (Matsumura et al., 1989) using Western blot analysis with an antibody that reacts extensively with degraded Titin. Furthermore, employing immunofluorescent staining for the projectin protein, Pantoja et al. showed that the normal projectin pattern is reduced by 1.8-fold in 3-5 day old dystrophic flies, and up to 7-fold in older flies (13-15 days) (Pantoja et al., 2013). Here, we tested whether THI treatment could have a beneficial effect on the Titin sarcomere pattern in *mdx* mice. To visualize the Titin pattern, we immunostained this protein with an antibody that recognizes the epitope close to the Z-band and produces a tight banding pattern on each side of the normal Z-disk (Fig. 6.A). In *mdx* muscles, Titin bands are somewhat disrupted and dispersed (Fig.6.B). To assess the level of sarcomere integrity, we counted the number of normal Titin bands and then normalized these counts against the total number of counted bands.

These normalized counts were then represented as percentages of wild-type myofibrils. As DMD is a progressive disease (Blake et al., 2002), we analyzed the sarcomere arrangement in *mdx* mice of different ages. Our analysis revealed 76.7% of wild-type myofibrils in 2MO *mdx*, 57.8% in 3.5MO mdx^{4CV} and 44.3% in 4MO *mdx* muscles, while 3.5MO control muscles showed 92% of the wild-type pattern (Fig. 6.G). This confirms the disrupted Titin as a dystrophic phenotype, and shows a significantly high penetrance and stronger phenotype in older *mdx* mice. In gastrocnemius muscles of 2MO THI-treated uninjured *mdx* mice, 97% of myofibrils showed a wild type Titin pattern in contrast to 76.7% of the 2MO vehicle-treated *mdx* (Fig.6.C-D, G). Moreover, three months of vehicle treatment showed 44% wild type myofibrils, whereas the THI treatment showed a 48% higher in myofibril intergrity (Fig. 6.E-F, G). Taken together, these data suggest that THI has a beneficial effect on sarcomere architecture.

3.3.3 Examining S1P levels in THI-treated uninjured *mdx* mice

After validating the THI delivery efficacy and pathological rescue function on uninjured mice, we examined further its molecular mechanism on the muscle level. Similar to the experiment on injured mice, we first analyzed whether the uninjured *mdx* mice treated with THI for one month in drinking water exhibited increased S1P levels in adductor muscles and more specifically, the muscle nucleus. Here, we measured four sphingolipids: sphingosine, S1P, DHSph, and DHS1P. We observed that in the treated *mdx* adductor muscles, S1P and DHS1P levels had robustly increased but the other sphingolipid levels were unchanged (Fig.7.A). However, in the nucleus, only S1P levels were found to be significantly up regulated (Fig.7.B). This shows that THI, as a S1P lyase inhibitor, acts in the muscle to maintain and increase nuclear S1P levels, but not other sphingolipids in the biosynthetic pathway.

3.3.4 S1P receptor gene expression in THI-treated uninjured *mdx* mice

To examine the possibility of extracellular function of S1P in our THI-treated uninjured *mdx* mice, I checked the gene expression of the intra-membrane S1P receptors, using qPCR analysis. Surprisingly, the gene expression of S1P receptor 1 is significantly down regulated in THI-treated diaphragm (Fig.8). This suggests that the extracellular function of S1P is unlikely in our experimental paradigm.

3.3.5 HDAC activity in THI-treated uninjured *mdx* mice

Since S1P is specifically enriched in the nucleus of THI-treated adductor muscles in *mdx* mice, we tested whether it had an inhibitory effect on nuclear HDACs. Nuclear HDAC activity analyzed by the deacetylation assay using the nuclear fraction of *mdx* adductor muscles revealed a 1.6-fold reduction of HDAC activity in the THI-treated samples compared to controls (Fig.9.A). Next, we wanted to know whether reduced HDAC function relates to increase histone acetylation (Alamdari et al., 2013). From a thorough screen on a number of acetylation marks on 1μM S1P-treated breast cancer cells (MCF-7 cells), Hait et al, 2009 narrowed down H3K9-, H3K18, H2BK12- and H4K5-acetylation as being sensitive to S1P regulated nuclear HDAC activity. Here, we examined the changes in histone acetylation on these known acetylation marks and observed a significant increase in the acetylation on H3K9, H3K18, H2B12. Increased expression of the histone itself was not the cause for this observed acetylation because total H3 protein level remained unchanged (Fig.9.B). Importantly, HDAC1 and HDAC2 protein levels were unchanged, substantiating the fact that S1P inhibits HDAC1/2 activity, but not their expression. Surprisingly, H4K5 acetylation, which has been shown to be sensitive to S1P, was unchanged after THI treatment (Fig.9.B). This could be due to the differences between cell types and experimental conditions (*in vitro* vs. *in vivo*). To be specific, S1P was shown to up regulate

acetylation of H4K5 in MCF-7 cells, which are breast cancer cells, and cancer cells can behave differently than normal cells, in this case mouse muscle tissues. Taken together, these data support our prediction regarding the relationship between HDAC activity and acetylation in THI-treated mice: an increase in nuclear S1P correlates with decreased HDAC activity and enhanced histone acetylation.

3.3.6 Increased S1P level in THI-treated uninjured *mdx* mice correlates with an increase in gene expression of HDAC2 regulated genes

The previous section demonstrated the *in vivo* inhibitory effects of S1P on total HDAC activity. However, S1P has been shown to specifically inhibit HDAC1 and HDAC2 *in vitro* (Hait et al., 2009), so, what is the particular HDAC that got down regulated in this case? An easy method to tackle this question is to measure individual HDAC activity. But due to the limited samples, I could not apply this approach. Therefore, I employed an indirect method - measuring the expression level of HDACs targeted genes. Since HDAC2, but not HDAC1 protein and activity are particularly up regulated in *mdx* mouse muscles, I was interested in testing HDAC2 targets first. HDAC2 has been shown to increasingly bind to the promoters of miR-29b-2/29c and miR-1-2/133a-1 of *mdx* mouse gastro and human DMD myotubes. The binding of HDAC2 to these promoters resulted in a decrease in acetylation of H3K9 and down regulation of the regulated genes (Cacchiarelli et al., 2010). Moreover, by up regulating miR-29 in *mdx* gastro, Cacchiarelli et al. demonstrated miR-29 roles in down regulating the gene expression of collagen (*Col1α1*) and elastin, the two causative factors of fibrosis in *mdx* muscles. In section 3.3.2, we have seen the effect of elevated S1P in down regulating Col1α1 in *mdx* diaphragms, thus I checked if miR-29 is the mediator in this case. Applying qPCR assay with the same samples, I observed a 9 fold-up regulation of miR-29c gene expression (Fig. 10A). This implied a down regulation of HDAC2

activity in these THI-treated *mdx* muscles. In further analyzing the changes in gene expression in response to THI treatment, I saw an increase for 5.6 folds in gene expression of miR-1-2, another HDAC2 target (Fig. 10B). These data strengthened my hypothesis that elevated S1P in THI-treated *mdx* mice worked mainly on decreasing HDAC2 activity.

3.3.7 Changes in gene expression due to THI dependent S1P increase

Section 3.3.5 showed decreased HDAC activity and increased histone acetylation as an effect of THI treatment in uninjured *mdx* mice. Elevated acetylation of histone would result in a "relaxed state" of the chromatin structure, thus inducing more expression of the genes wherever these acetylations may lie. This up regulation of these genes might in turn repress the expression of other genes. I thereby was interested in examining changes in gene expression in the THI-treated samples, concerning the beneficial effects of S1P on DMD. I looked at changes in gene expression using microarray analysis. RNA was extracted from adductor muscles of THI- and vehicle-treated *mdx* mice and analyzed for gene expression differences using the Agilent platform. Being skeletal muscles, our dissected adductors might contain embedded blood vessels and adipocytes that could confound the gene expression analysis. A fairly pure muscle sample should contain an enriched muscle gene relative to a background gene set, consisting of other necessary genes for a normal cell to survive and be governed. Using density plot analysis, I revealed a significant enrichment of muscle genes in vehicle- and THI-treated adductors, validating our samples (Fig.11.A). Furthermore, based on the p-value of the log fold-change of gene expression of THI compared to vehicle-treated samples; I identified 602 genes whose expression was significantly changed after THI treatment ($p<0.5$) (Fig.11.B). To have a general idea of the functions of these up and down regulated genes, I used the GeneMANIA web-interface software program to identify gene functional groups. GeneMANIA is a free, public

resource that allows users to enter their list of interested genes, and receive a ranked list of related genes, and an interactive network demonstrating the functional link of these genes, thereby grouping the query gene list into functional groups. Analysis with GeneMANIA program revealed a remarkable decrease in gene expression of chromosome condensation genes as an effect of THI (Table 1). This supported the findings that THI treatment reduced HDAC activity and increased acetylation, "relaxing" the chromosome structure, resulting in genes for chromosomal tightening to not be needed. In addition, a considerable up regulation of fatty-acid-metabolism related genes was revealed in THI-treated adductors compared to controls (Table 1).

The increase of fatty acid metabolism-related-gene expression may be due to (1) a change in the metabolism of the myofiber itself or (2) increased adipocyte infiltration into the muscle tissue. Muscle sections were stained with Oil red O to detect fat deposits in muscle interstitium to determine if THI treatment increased the number of adipocytes in *mdx* muscles. We did not observe an increase in fat deposits within an entire cross section of the diaphragm in the THI-treated samples relative to the vehicle treated samples (Fig.12.A-C). This analysis indicates that increased fat metabolism gene expression in THI-treated samples is not due to increased adipocyte infiltration to the diaphragm.

The intriguing information obtained from the general analysis of the gene expression changes with GeneMANIA analysis inspired me to thoroughly examine the function of individual genes whose gene expression was changed after THI treatment. After mining each gene function from the biological database, I classified them into different groups based on their functions (Fig.13.A). Interestingly, genes whose functions are involved in metabolic processes in the THI-

upregulated-genes were abundant. Most of the genes in this metabolic gene group are fatty-acid-related, supporting the findings from the GeneMANIA analysis. qPCR results validated the up regulation of one representative of the metabolic gene group, the *Adrb3* gene (Fig. 13.B). In addition, insulin pathway-, Wnt signaling pathway-, and slow twitch muscle-related genes were also up regulated in *mdx* muscle after THI treatment (Fig.13.A). Interestingly, due to its long known positive function in skeletal myogenesis and muscle stem cell function (Kuroda et al., 2013), the up regulation of Wnt pathway involved genes supports the findings that THI increases muscle regeneration (Loh et al., 2012; von Maltzahn et al., 2012b; Ieronimakis et al., 2013), Wnt signaling activation has recently been shown to be restricted to the slow myofibers in adult mice (Kuroda et al., 2013). Furthermore, slow twitch muscles are insulin sensitive (Song et al., 1999) and heavily based on fatty acids for energy (Schiaffino and Reggiani, 2011). Thus, the concomitant up regulation of the four gene group suggests a shift to slow-twitch-muscle fibers as an effect of THI treatment.

Along with the prominent metabolic groups, the expressions of genes that have beneficial effects on muscles were also elevated in THI-treated adductors (Fig. 13.A). The up regulation of *Mrap* gene expression, a representative of this group was validated by qPCR (Fig.13.B). I observed a particularly remarkable sarcomere related gene in this group. The beneficial effect of sarcomere related genes is obvious as they strengthen the sarcomere architecture, thus, enhancing the firmness (support) of muscle structure. The representatives of this group are *Myh7b*, *Actg2*, *Myl10*, *AbLim*, *Nrap*, *Asap1* and *Tnnc1* (Fig.13.A) (Roof et al., 1997; Dhume et al., 2006). These data support our earlier findings that improved sarcomere structure is an effect of THI in

these mice as shown by Titin staining. Taken together, THI dependent up regulation of S1P led to elevated expression of genes supporting muscle structure, functions, and metabolic switching.

Down regulated genes

In the THI-dependent-down-regulated genes, a group of inflammation genes is particularly noticeable (Fig.13.A). I chose *Ccl2* (Chemokine(C-C motif) ligand 2), a representative gene from this inflammation group to validate my bioinformatics data. Ccl2 is a cytokine produced by a number of cells, for example endothelial, fibroblast, and smooth muscle cells, as result of oxidative stress or growth factor induction. It recruits monocytes, memory T cells and natural killer cells to inflammation sites (Deshmane et al., 2009). qPCR results showed a trend of reduced *Ccl2* gene expression after THI treatment, but this was not significant (Fig. 13.B). This variation was due to the highly different behaviors and responses between each mouse in each treatment, a known issue of experimentation when working with mice. The down regulation of inflammation-involved gene expression in muscle samples could be due to (1) the reduction in muscle damage itself or (2) the reduction in the immune cell populations migrating and infiltrating into the muscle fibers. I was interested in investigating the second possibility further. I tested for the gene expression of inflammation markers of T cells using qPCR analysis, and recorded a reduced trend in CD4, but not CD8 expression (Fig. 14.A). I further analyzed the protein level of the hematopoietic lineage (CD45) and macrophage (CD68) populations in vehicle and THI-treated *mdx* diaphragms by immunofluorescent staining. Unexpectedly, these two cell populations remained unchanged after THI treatment (Fig. 14. B-E). Taken together, even not pronounced, there was a reduction in inflammation in THI-treated muscles, in accordance with the microarray data.

Confirming the gene expression changes with density plots

To see if the changes of the above mentioned gene groups were significant, I obtained the broader and unbiased gene lists from the Broad Institute (website) for metabolism, muscle, and inflammation, and compared the fold change (THI/vehicle) data of these specific gene sets to the whole data set of adductor muscle samples. I first used R studio to visualize the fold change distribution (THI/vehicle) for these gene groups in the form of a density distribution blot. Next, I calculated the distribution changes p-values based on the Kolmogorov-Smirnov test when comparing fold changes of metabolism, muscle tissue, and inflammation genes to the total data set. The obtained p-values substantiated the significant up or down regulation in the tested groups, which were 3.221e-10, 0.01909, and 0.04793 for metabolic-, beneficial muscle- and inflammation genes, respectively (Fig.15).

3.4 The relationship between THI treatment and metabolic changes

The microarray-based gene expression analysis revealed an indication of a shifting to slow myofibers in the components of adductor muscle tissues after THI treatment. This shift was supported by the up regulation in expression of fatty acid metabolic-, insulin-pathway-, Wnt pathway-, slow twitch muscle related genes. Importantly, slow twitch muscles are less vulnerable than fast twitch muscles within the DMD context (Webster et al., 1988). We were interested in confirming our microarray data at the functional level by tracking the changes in the metabolic mechanism of THI-treated samples. We chose to start with the C2C12 cell culture, as it is easier to analyze their metabolic flux than isolated muscle fibers. In this experiment, differentiating C2C12 cells were used because their morphologies, metabolism processes, etc., are more similar to mature muscle fibers, thus better representing them. In addition, undifferentiated C2C12 are more vulnerable (sensitive) to treating chemicals.

We treated the one-day-differentiating C2C12 with either THI (0.05mg/ml) or S1P (0.1mM) for one day. At the third day of differentiation, the cells were assayed for sphingolipid levels and metabolic profiles. Cellular-sphingolipid measurement showed a similar result to muscle-sphingolipid data: S1P and DHS1P levels were increased in THI-treated samples (Fig.16). Because metabolism changes are clearly detectable in mitochondrial respiration, which is relative simple to track with the Seahorse Extracellular Flux analyzer, we chose to examine these mitochondrial changes as the first step to check the altered metabolism in THI-treated cells. To do this, we measured the oxygen consumption rate (OCR), a metabolic parameter representing the mitochondrial respiration in THI or S1P-treated C2C12 cells. To record the maximum turn over of the electron transport chain uncoupled from ATP synthesis, we first inhibited mitochondrial ATP synthase with oligomicine. Next, we stimulated maximum mitochondrial respiration by adding a proton gradient discharger, carbonyl cyanide 4-(trifluoromethoxy)phenylhydrazone (FCCP). We then calculated the maximum OCR changes after FCCP addition. We observed significantly higher OCR changes post FCCP treatment in THI- or S1P-treated C2C12 cells compared to the vehicle-treated samples (Fig.17-A-D), demonstrating an increase in mitochondrial respiration as a consequence of S1P.

Mitochondrial respiration enhancement could be due to (1) increased mitochondrial copy number or (2) increased mitochondrial activity. To check the first possibility, I measured mitochondrial copy number in THI/vehicle-treated C2C12 cells. Utilizing absolute quantification qPCR, I analyzed the amount of mitochondrial DNA by normalizing to genomic DNA content, and compared the relative number of mitochondria in C2C12 under different treatments. To examine

mitochondrial DNA content, I checked the DNA quantity of mt-Co1 (mitochondrial cytochrome c oxidase subunit 1) that encodes one subunit of the mitochondrial respiratory complex IV. To check genomic DNA, I tracked the DNA quantity of GAPDH. My data revealed no difference in the number of mitochondria between THI- and vehicle- treated cells (Fig.18). This suggests that the THI-dependent increased mitochondrial respiration is due to increases in mitochondrial activity, e.g., higher efficiency of glucose or fatty acid usage as energy substrates. To investigate if THI-treated cells utilize more glucose for their energy, we measured the extracellular acidification rate (ECAR) that mainly defines the cell glycolysis level, with and without THI treatment. We maximized the production of lactic acid by glycolysis by adding the ATP synthase inhibitor, oligomycine to inhibit the import of pyruvate into the mitochondria, and analyzed the ECAR changes with and without THI treatment. No significant difference was observed in the maximum ECAR change after adding oligomycin for THI- or S1P-treated compared to vehicle-treated C2C12 cells, suggesting that the cells used a substrate other than glucose to obtain the increased OCR observed after THI and S1P treatment (Fig. 19. A-B, E-F). To further confirm this result, we employed a more specific test, the glucose-stress assay in which the cells were first supplied with a glucose substrate and then induced to maximum glycolysis with oligomycin, and finally, glycolytic capacity was calculated. Results from the glucose stress assay did not show any significant difference between THI- and vehicle-treated cells (Fig. 19. C-D), strongly strengthening the idea that THI-treated cells use other substrates rather than glucose for their energy. We next tested if the cells oxidize more fatty acid in response to THI treatment. We used a fatty-acid-stress test, in which in the cells were supplied with exogenous fatty acid substrate, palmitate, and then fatty-acid oxidation was inhibited by carnitine palmitoyltransferase I inhibitor, etomoxir (ETO). Results from this test revealed that the THI-treated cells show

higher maximal OCR changes, as an indication of higher capacity to use palmitate as an energy source. These data demonstrated that THI-treated cells have a higher fatty acid oxidation than control samples (Fig. 20. A-B).

Chapter 4: Discussion

4.1 Summary and Conclusions

We investigated the molecular mechanism for the beneficial S1P actions in dystrophic muscles. Since HDAC2 protein levels is increased in *mdx* mouse adductors, and knocking down of this specific HDAC has been shown to benefit dystrophic pathologies (Colussi et al., 2008), I began to study the discernable protein level and enzyme activity of HDAC2 in dystrophic mice. I discovered that total nuclear HDAC activity, HDAC2 protein levels and HDAC2 activity are increased in *mdx* muscles, even in different *mdx* genetic backgrounds. Interestingly, in the *mdx* heart, total nuclear HDAC activity and HDAC2 protein levels have a slight trend of up regulation. These facts suggest a causative role of HDAC2 in dystrophic pathologies. By treating injured dystrophic mice with THI for three days, we observed a significant increase in nuclear S1P levels, and a concomitant decrease in HDAC activity. We further tested whether THI showed beneficial action on uninjured *mdx* mice, and if the disease rescue effects correlated with increased nuclear S1P and HDAC reduction. We detected reduced white blood cells, reduced fibrosis in the diaphragm, and an increased normal Titin pattern in the myofibril sarcomeres of *mdx* mice treated with THI in drinking water for one month. Moreover, these beneficial effects of THI correlate with an increase in nuclear S1P levels in the treated *mdx* muscles. This resulted in decreased HDAC activity and increased H3K9, H3K18 and H2BK12 acetylation in adductor muscles of these THI-treated *mdx* mice. I also saw an increase in gene expression of HDAC2 targets, including *miR-29c* and *miR-1-2* in THI-treated diaphragms, suggesting a down-regulation in specific HDAC2 activity. Interestingly, one of miR-29 targets, *Col1α1* was also down regulated in these muscles. Since Col1α1 is a constitutive component of collagen - the causal agent of fibrosis - these data explain how S1P can benefit degeneration and reduce

fibrosis. S1P inhibits HDAC2 activity, thereby relieves the repression of its target, miR-29. Up-regulated miR-29, in turn, binds to and inhibits its own target, Col1α1. Decreased Col1α1 expression leads to reduce muscle fibrosis in THI-treated *mdx* mice. When tracking changes in gene expression correlated to increased histone acetylation, I noticed a significant increase of fatty acid metabolic-, insulin-, wnt-, slow twitch-, sarcomere-, muscle beneficial related genes and decreases in inflammation genes. These microarray data suggested a switch to slow twitch muscles dominated by a fatty acid oxidation mechanism as a beneficial effect of S1P on dystrophic muscles. This inspired us to study the metabolic changes in response to S1P at functional level. We showed an increase in cellular S1P levels and a functional increase of mitochondrial activity, especially in fatty acid oxidation after THI treatment of differentiating C2C12 cells. Taken together, we propose that S1P inhibits HDAC activity, leading to an increased expression of beneficial muscle genes, and metabolic genes that induce a switch from fast to slow twitch muscle in *mdx* mice. This muscle type shifting, in turn, benefits *mdx* muscles.

4.2 S1P intracellular action

Experiments on fly and mouse models demonstrated S1P function on rescuing dystrophic features at both muscle pathological and functional levels (Ieronimakis et al., 2013; Pantoja et al., 2013; Pantoja and Ruohola-Baker, 2013). So, what is the underlining mechanism of S1P action in repressing dystrophic phenotypes in these cases? S1P has long been known to exert its extracellular function through its intra-membrane receptors, S1PR1-5. Once activated, the S1P receptors transmit the signal to its coupled G proteins, Gi/o, G12/13, Gq. These proteins then convey the message to the downstream signaling pathways, for example the phospholipase C (PLC), the Ras and ERK, or the PKB/Akt pathways. Ultimately, these S1P receptors and downstream pathways regulate many cellular processes, including cell survival, migration,

proliferation, intracellular calcium level, vascular permeability, and vasodilation, etc. (Brinkmann, 2007). *Drosophila* does not have orthologues for S1P receptors; however, rescuing effects of S1P on dystrophic flies were still observed (Pantoja et al., 2013). I expect that S1P actions in this case could be through another mechanism rather than extracellular functions. Besides, in *mdx* mouse experiments with THI treatment, THI up regulated the S1P level by inhibiting S1P lyase that is located at the membrane of the endoplasmic reticulum. Therefore, the elevation of intracellular levels of S1P must take place prior to export. Moreover, in THI-treated mice, the gene expression of S1P receptor 1 is significantly reduced, suggesting it is unlikely that S1P rescued *mdx* muscle function via an extracellular pathway. Recently, intracellular functions of S1P have been investigated and described. S1P has been shown to be a cofactor for TRAF2, thereby involving the NF-κB signaling pathway (Alvarez et al., 2010). In the mitochondria, S1P binds to prohibitin 2 (PHB2), and thereby regulates the assembly of cytochrome-c oxidase (COX). Thus, S1P controls mitochondrial respiration. In the nucleus, S1P has been shown to inhibit HDAC1/2 activity in Hela nuclear extract (Hait et al., 2009). Moreover, down regulating HDAC2 results in ameliorating dystrophic pathologies (Colussi et al., 2008). Here, we observed an up regulation of nuclear S1P along with decrease in nuclear HDAC activity in THI-treated *mdx* mice that showed rescued dystrophic phenotypes. I propose that S1P benefits DMD by its intra-nuclear activity, inhibiting HDAC2, releasing beneficial genes from its repressed state, thus rescuing the dystrophic pathologies. However, another possibility of intracellular S1P function is raised as an up regulation in mitochondrial respiration in THI-treated C2C12 cells was observed. As stated earlier, S1P can directly increase mitochondrial respiration. We can also hypothesize that S1P elevates mitochondria activity, enhancing energy production for the muscle, thus helping to palliate DMD disease. Even though plausible, this mechanism alone fails to explain

the many other effects of S1P on increased muscle size, regeneration induction, reduced fibrosis and fat infiltration. Therefore, enhancing mitochondrial activity might be an additional mechanism to S1P action in dystrophic mice. Taken together, the intracellular S1P function on HDAC2 should be considered the primary mechanism and as the most plausible explanation of the S1P rescuing effect on *mdx* mice that I can propose.

4.3 S1P and the dystrophin-glycoprotein complex

DMD is known to be caused by mutations in the dystrophin protein (Hoffman et al., 1987), a crucial part of the dystrophin-associated protein complex (DGC) that plays an important role in cell survival signaling (Evans et al., 2009). Does S1P benefit DMD by partly rescuing the function of DGC components? In reviewing the literature, I found an interesting connection: nNOS is a signal protein anchored to the DGC via dystrophin, and is mislocalized in DMD patients due to a defect in the DGC complex, resulting in the down regulation of its product, nitric oxide (NO). NO has been shown to inhibit HDAC2 activity by S-nitrosylating this enzyme and thereby, releasing it from the chromatin (Colussi et al., 2008). Furthermore, up regulating NO can rescue dystrophic phenotypes in *mdx* mice, e.g., decreased muscle fiber size variability, muscle injury and inflammation (Wehling et al., 2001). Therefore, I propose that S1P could suppress dystrophic phenotypes by compensating the loss of NO caused by the mislocalization of nNOS as a result of a defective DGC.

4.4 The connection of S1P, HDAC and the metabolic mechanism

Our data on C2C12 cells demonstrates the enhancement effect of S1P on the oxidative mitochondrial activity. It would be interesting to find out the underlying mechanism of this effect of S1P. A direct connection can be made as a previous study has shown that S1P generated in the

mitochondria regulates respiration. However, this can only explain the enhanced mitochondrial activity aspect, not its elevated fatty acid oxidation. Moreover, does S1P only regulate mitochondria behavior directly, or also through a mediator? Intriguingly, enhanced mitochondrial biogenesis and oxidative metabolism were also achieved by inhibiting class I HDAC activity (Galmozzi et al., 2013). Since HDAC2 belongs to class I HDACs, and S1P inhibits HDAC *in vitro* (Hait et al., 2009), I hypothesize that S1P inhibits HDAC2 activity, and the resulting decreased HDAC2 activity allows the expression of mitochondria biogenesis and oxidative metabolic genes, leading to increased mitochondria activity, especially fatty acid oxidation. Due to the limited samples, we only showed S1P inhibiting HDAC *in vivo*, but not specifically HDAC2. However, there is indeed evidence for suppressed HDAC2 activity in our THI-treated samples. A previous study revealed that HDAC2 targets miR-29 family, and the resulting up regulated miR-29b-2/29c leads to decreased expression of Col1α1 gene (Cacchiarelli et al., 2010). In our THI-treated diaphragms, I observed a significant increase of miR-29c and a reduction of Col1α1 expression. This applauds the possibility that HDAC2 activity is down regulated in THI-treated diaphragms, which results in increased miR-29 gene expression. The elevated mir-29 then inhibits the expression of Col1α1, a constitute component of collagen. Since collagen is the causal agent of fibrosis, decreased collagen means reduced fibrosis. This connection links the inhibitory effect of S1P on HDAC2 to the beneficial effect of S1P on DMD pathologies in reducing fibrosis. Furthermore, miR-1-2, another known target of HDAC2 was also increased in gene expression in the THI-treated diaphragms. Taken together, these data demonstrate the inhibitory effect of S1P on HDAC2.

4.5 The relationship between muscle types and muscle function

The two main types of myofibers are different from each other in a number of ways: slow twitch muscles use fatty acids while fast twitch ones use glucose for their energy (Schiaffino and Reggiani, 2011), slow twitch muscles are insulin sensitive while fast twitch muscles are insulin resistant (Song et al., 1999; Chen et al., 2000), and the Wnt signaling pathway is activated in mature slow twitch-, but not fast twitch muscles (Kuroda et al., 2013). I observed evidence of a shift to slow twitch metabolism, denoting in an up regulation in expression of slow twitch muscle-, fatty acid metabolic-, insulin-, Wnt pathway-related genes. The functional assay on C2C12 cells strengthens the case with evidence of significant increases in oxidation of fatty acids, but not glycolysis in THI-treated cells. What is interesting about this muscle fiber shifting and how does it benefit dystrophic muscles? Slow twitch muscles in a dystrophic context have been shown to be less prone to injury than fast twitch muscles (Webster et al., 1988). Furthermore, switching to slow twitch muscles has been viewed as beneficial for ameliorating muscular dystrophy (Selsby et al., 2012; von Maltzahn et al., 2012b). Is this muscle type switching possible in adults? There are a number of reports for muscle shifting from slow to fast twitch myofibers and vice versa after birth by altering the pattern of motor innervation or gene expression (Chin et al., 1998; Delling et al., 2000; Naya et al., 2000; Olson and Williams, 2000; Wu et al., 2000; Lin et al., 2002). Why are slow twitch muscles more stable than fast twitch ones? A number of hypotheses could explain the relative stability of slow twitch muscles. First, the injury-resistant characteristic of slow twitch muscles might be conferred by its specific gene expression. Microarray data have shown the difference in gene expression of the two main muscle types (Chemello et al., 2011). The benefit of expressed genes in slow twitch muscles could compensate the dystrophin protein, or the proteins required for the cell survival signaling

pathway, or enhance structural proteins for muscle firmness. For example, the up regulation of utrophin, a beneficial gene for dystrophic muscles, has been observed specifically in slow twitch muscles, not fast muscles (Tinsley et al., 1998; Gramolini et al., 2001; Fairclough et al., 2013). Second, slow twitch muscles are insulin sensitive, which helps them get better use of the body's energy fuel source (Song et al., 1999; Ryder et al., 2003; Guan et al., 2009). Third, slow twitch muscles generate more energy than fast twitch ones, because fatty acids are known to be a higher energy source than glucose. Oxidation of a short fatty acid (8-carbon) yields 48 ATPs, a longer fatty acid (three chains of 8-carbon) yields 144 ATPs, while anaerobic and aerobic glycolysis yield only 2 and 36 ATPs, respectively.

Our observation that S1P ameliorates DMD pathologies by increasing fatty acid metabolism, the main metabolic mechanism of slow twitch muscles is an informative hint. Insightful research on the beneficial generation of slow twitch muscles will generate more knowledge on muscle stability and lead to a better strategy to deal with DMD.

4.6 Future direction

4.6.1 Validating the metabolic changes in muscle switch in response to S1P

While experiments on C2C12 cells are a good strategy to track the changes in the metabolic mechanisms that respond to THI/S1P treatment at a functional level, several drawbacks still need to be addressed. First, what happens in cultured cells might not exactly represent the dynamics of what happens in an intact living body where the cells are interacting with the whole body, and under complex regulation of numerous signals. Second, the (many) differences between normal and dystrophic cells make it difficult to know if there is any specific metabolic reaction towards S1P in dystrophic context. The second problem is solved by our microarray data on THI-treated

mdx mice showing an up regulation of metabolic genes. To address the first problem, future studies on THI-treated *mdx* mice where isolated contact myofibers or myoblasts subjected to a fatty acid stress assay with the Seahorse analyzer are needed to further validate the data obtained from treated cultured C2C12 cells. Furthermore, the muscle fibers switch should be confirmed by examining differential gene expression and proteins in THI-treated muscle samples.

4.6.2 Examining if S1P ameliorates DMD by compensating NO

To check the connection of S1P function and the DGC, the target genes whose expressions are regulated by NO should be elucidated and compared with S1P target genes. This can be done by monitoring the changes of gene expression when NO is up or down regulated with a NO donor (SNAP or GSNO) or a NO inhibitor (L-NAME) in C2C12 cells. If there is a considerable overlap between the two gene groups, the compensation function of S1P for NO can be proposed. A functional assay where S1P is up regulated in nNOS knockout mice could be used to test if S1P can compensate NO function.

4.6.3 Determining if HDAC2 is the target of S1P in THI-treated *mdx* mice

The *in vivo* inhibitory activity of S1P on total nuclear HDAC was clearly demonstrated in our experiment. However, the specific individual HDAC that is targeted by S1P in these THI- mice has yet to be determined. HDAC2 is a likely candidate due to its particularly high expression and activity in dystrophic muscles and reducing its expression has been shown to benefit muscle function and morphologies. Our result substantiates the possibility that HDAC2 could be the main target of S1P in ameliorating dystrophic diseases by showing an increase in gene expression of two HDAC2 targets - miR29c and miR-1-2. However, to further narrow down the S1P targets in this case, future studies should address both HDAC1 and HDAC2 activities in

THI-treated *mdx* mice. Also, a ChIP-seq analysis on HDAC2 in THI- and vehicle-treated *mdx* muscles should be done to elucidate all potential HDAC2 gene targets. If gene targets of HDAC2 and S1P overlap with each other, it is possible that inhibiting HDAC2 is a beneficial effect of S1P in dystrophic muscles.

4.6.4 Examining if S1P directly up regulates mitochondria activity

To further confirm if acting directly on mitochondria is one of the beneficial actions of S1P on *mdx* mice, future experiments should measure the S1P level in the mitochondria after THI treatment. In addition, the binding of S1P to prohibitin 2 (PHB2) should also be evaluated.

Chapter 5: Appendix Chapters

5.1 Appendix chapter 1

Introduction

Reducing HDACs, specifically HDAC2, has been shown to benefit dystrophic mouse muscle (Colussi et al., 2008). In the previous chapter, I have discussed the rescuing function of S1P on dystrophic mouse muscles (Ieronimakis et al., 2013), and that this beneficial effect correlates with inhibition of HDAC activity. Since S1P has also been shown to benefit fly muscles (Pantoja et al., 2013), we are interested in checking if the beneficial effect of S1P on dystrophic flies is also mediated by reduced HDAC activity. To explore the common mechanism of S1P's beneficial action on both flies and mice, we started by testing whether reducing HDAC levels benefit dystrophic flies. To assess the rescue effect of reducing HDAC in dystrophic flies, we screened for alterations in the visible phenotype of the posterior cross vein in fly wings, which is a dystrophic hallmark (Kucherenko et al., 2008).

Material and methods

Experiments involving animals were performed in accordance with the guidelines and ethical approval from the University of Washington Institutional Animal Care and Use Committee. The fly strains used in this study were: *Rpd3*$^{12\text{-}37}$*/TM6,Tb; Rpd3*^{303}*/TM6,Tb; Rpd3*^{04556}*/TM6*; and *TubGal4:UAS-Dys*$^{C\text{-}RNAi}$*/TM6B,Tb.*

Wing vein phenotype was scored as previously described (Kucherenko et al., 2008)

Results

We reduced Rpd3, a *Drosophila* homologue of mammalian HDAC1 and HDAC2 (Tea et al.,

2010) in dystrophic flies and analyzed the potential interaction by quantifying the *dys* visual phenotype, posterior cross-vein defect (Christoforou et al., 2008; Kucherenko et al., 2008; Pantoja et al., 2013). We used three types of Rpd3 mutants to reduce HDAC2 levels in flies, $Rpd3^{12\text{-}37}$, $Rpd3^{303}$ and $Rpd3^{04556}$, which code for a non-active protein, a point mutation with a dominant negative allele and a hypomorphic allele, respectively (Tea et al., 2010). Importantly, reduction of Rpd3 in the *dys* mutant background ($Rpd3^{303}$*/tubtg6* and $Rpd3^{12\text{-}37}$*/tubtg6)* resulted in significant suppression of the dystrophic posterior cross-vein phenotypes (Fig.21.A-B). These results show that reduction of HDAC, especially HDAC1/2 activity can partially rescue *dys* mutant phenotypes in *Drosophila*.

Discussion

The fact that reducing Rpd3 rescues the wing vein phenotype of dystrophic files suggests HDAC might be a mediator of S1P action in both flies and mice. However, the test on the wing vein itself cannot strongly support rescued muscle function. Future experiments on climbing activity and sarcomere integrity should be done to address the beneficial effects of reducing HDAC in dystrophic flies. Rpd3 protein and HDAC activity should also be measured to validate the experimental conditions.

5.2 Appendix chapter 2

Introduction

FTY720, also known as Fingolimod, is a S1P analogue. When it enters cells, it becomes phosphorylated by SphK2, and then is released as a FTY720 phosphate (FTY720-P). The phosphorylated form of FTY-720 can bind to and activate most S1P receptors, except for S1PR2 (Pyne and Pyne, 2011). Particularly, FTY-720-P has a high affinity for binding with SIP1 (0.3 nM), S1PR4 (0.6 nM) and S1PR5 (0.3 nM), and with an approximately 10-fold lower affinity for binding to S1PR3 (3.1 nM), but not to S1PR2 (>10,000 nM) (Brinkmann, 2007). FTY-720 exerts most but not all functions of S1P. It would be interesting to know if the beneficial effect of S1P on dystrophic muscle overlaps with FTY720-P function because FTY720 is non-toxic, and is already licensed by the FDA as Gilenya, making it easier and faster to develop as a treatment for DMD. Moreover, it will be a valuable addition to possible drug treatments for DMD if S1P or THI somehow do not perform well in clinical testing. Chapter 3 showed that the inhibitory activity of S1P on HDAC activity correlates with dystrophic pathology suppression function. This suggests that testing FTY-720-P action on HDAC activity should give a preliminary idea if FTY-720 could rescue DMD phenotypes as well. To address this hypothesis, I started by testing FTY-720 activity on HDAC activity in a Hela nuclear extract *in vitro*.

Materials and methods

Chemical source

FTY-720-P was purchased from Cayman Chemical. FTY-720-P was dissolved in methanol (0.5 mg/ml) and the solvent was evaporated with a stream of nitrogen to deposit a thin film on the inside of the tube. Prior to use, FTY-720-P was re-suspended in PBS with 4 mg/ml BSA (fatty-

acid-free) to a concentration of 500 μM. Hela nuclear extract stock (14mg/ml) was purchased from Enzo Life Sciences. The HDAC activity assay was carried out as described in chapter 3 with 25μM FTY-720-P, 7μg Hela nuclear extract. HDAC substrate was added to a final concentration of 10μM. Hela nuclear extract without any HDAC inhibitor was used as a control.

Results

HDAC activity of 7μg Hela nuclear extract was measured with the addition of FTY-720-P (25μM), or control (nothing). Preliminary data showed that HDAC activity was decreased by the action of FTY-720-P (Fig. 22). This is suggestive of the inhibitory effect of FTY-720-P on HDAC activity.

Discussion

Since FTY-720-P can activate S1PRs, I first thought that it could only replicate S1P extracellular function. The result from this experiment suggests that FTY-720-P could also replicate intracellular function. If FTY-720-P can totally replicate the S1P beneficial effects on dystrophic muscles, it is a good candidate drug for DMD treatment if S1P does not succeed in further clinical tests. Future assays should be done to validate the *in vitro* result of FTY-720-P on HDAC activity in Hela nuclear extract with more replicates. After that, testing FTY-720-P effects on HDAC activity and muscle functions in *mdx* mice should address whether FTY-720-P can be a candidate drug for DMD.

FIGURE LEGENDS

Fig.1. HDAC2 protein levels are up regulated in *mdx* mice. Western blots of adductor, TA, and heart of *mdx*^{4CV} mice and controls (A), analyzed with anti-HDAC2 antibody and quantified by normalizing to total nuclear protein (B-D). 30μg of nuclear protein of *mdx4CV* or control muscles was run for each lane, the same amount as used in protein gels of (A), Adductors (B), TAs (C), Heart (D). Up regulation of HDAC2 protein in adductors and TAs of *mdx*^{4CV} was 4.34- and 4.6-fold, respectively, * $p<0.05$, ** $p<0.01$, *** $p<0.001$

Fig.2. Total nuclear HDAC activity is up regulated in *mdx* mice. Total nuclear HDAC activity of adductors (A), TA (B) and heart (C) were measured by a fluorescent deacetylation assay in *mdx*^{4CV} compared to controls (5-month-old males, n=5; up regulation in *mdx*^{4CV} 2.69- and 1.97-fold, respectively). (D) Total nuclear HDAC activity in control mice; * $p<0.05$, ** $p<0.01$, *** $p<0.001$

Fig.3 HDAC2 activity is up regulated in *mdx* mice. (A) Nuclear protein extract was immunoprecipitated with anti-HDAC2. The bound proteins were separated by SDS-PAGE and analyzed by western blotting with anti-HDAC2 antibody. Immunoprecipitated nuclear HDAC2 activity was determined in (B) adductor, (C) TA, and (D) heart of *mdx*^{4CV} and control mice (up regulation in *mdx*^{4CV} 2.52-, 1.95- and 1.15-fold, respectively). (E) Immunoprecipitated nuclear HDAC2 activity was also up regulated (2.76-fold) in *mdx* compared to control (4.5-month old males, n=3); * $p<0.05$, ** $p<0.01$, *** $p<0.001$

Fig.4. Increased nuclear S1P and HDAC inhibition correlates with suppressed disease pathology (Ieronimakis et al., 2013) in THI-treated *mdx* mice after acute injury. (A)

Experimental scheme. Four-month-old (4MO) male *mdx*^{4CV} mice (n=8) were injected IP with 75μg THI (THI) or PBS (vehicle) daily for 3 days after CTX injury to TA. (B) TAs were removed, lipids extracted from nuclear fractions and levels of sphingosine-1-phosphate (S1P), dihydro-sphingosine-1-phosphate (DHS1P), sphingosine (Sph) and dihydro-sphingosine (DHSph) were determined by LC-ESI-MS/MS. (C) HDAC activity in nuclear extracts was determined. * $p<0.05$, ** $p<0.01$, *** $p<0.001$

Fig.5. One month THI treatment has a beneficial effect in dystrophic pathology in uninjured *mdx* mice. (A) Experimental scheme. One-month-old male *mdx* mice were treated daily with THI (50mg/L THI in 55.5mM glucose in drinking water, n=5) or vehicle (55.5mM glucose in drinking water, n=5) for 1 month. Blood, diaphragm and gastrocnemius were tested for white blood cell count, fibrosis and Titin pattern, respectively, to assess THI primary efficacy. Adductors on left sides were used for nuclear protein extraction, sphingolipid measurements, HDAC activity assay and histone acetylation analysis. Right side adductors were used for RNA extraction and applied in subsequent microarray analysis and qPCR analysis. (B) White blood cells and lymphocyte counts were significantly reduced in THI-treated *mdx* mice, and increased back to nearly the level of vehicle-treated mice 24 hours after the withdrawal of THI. (C) Expression of collagen *Col1a1* mRNA was determined by QPCR in diaphragms from vehicle- and THI-treated *mdx* mice (normalized to 18S-rRNA). (D) H&E and Picrosirius red stainings of diaphragm from THI- and vehicle-treated *mdx* mice, the red color represents collagen protein in the muscles. (E) Quantification of collagen protein in (D). * $p<0.05$, ** $p<0.01$, *** $p<0.001$

Fig.6. One month of THI treatment has a beneficial effect in sarcomere architecture of uninjured gastro *mdx* mice. Representative pictures of the Titin sarcomere pattern in gastrocnemius of control and mdx^{4CV} (3.5MO) (A-B), and 2MO (C-D) or 4MO (E-F) *mdx* with vehicle or THI treatment for 1 month or 3 months, respectively. Titin protein was visualized with the Alexa 488 fluor, seen in green. Lower picture: high magnification of one myofibril. (J) Quantification of wild-type Titin sarcomere pattern in control, mdx^{4VC} (3.5MO), 2MO *mdx* and 4MO *mdx* with vehicle or THI treatment for 1 month or 3 months, respectively. * $p<0.05$, ** $p<0.01$, *** $p<0.001$

Fig. 7. One month of THI treatment in non-injured *mdx* mice results in the increase of muscle and nuclear S1P in adductor muscles. One-month-old male *mdx* were treated daily with THI (50mg/L THI in 55.5mM glucose in drinking water, n=5) or vehicle (55.5mM glucose in drinking water, n=5) for 1 month. (A) Sphingolipid levels in adductor muscles were determined by LC-ESI-MS/MS. (B) Nuclei were isolated and sphingolipid levels determined by mass spectrometry.

Fig.8. Gene expression of the S1P receptor 1 is significant down regulated in one-month-THI-treated diaphragms of *mdx* mice. Expression of S1PR1mRNA was determined by QPCR in diaphragms from vehicle- and THI-treated *mdx* mice (normalized to 18S-rRNA). * $p<0.05$, ** $p<0.01$, *** $p<0.001$

Fig.9. One month of THI treatment in non-injured *mdx* mice results in decrease of total nuclear HDAC activity and increase of specific histone acetylation in adductor muscles. (A)

Nuclear HDAC activity was determined in duplicate samples. (B) Histone acetylations were determined by western blotting with the indicated antibodies.

Fig.10. Increased S1P in THI-treated-uninjured *mdx* mice correlates with an upregulated expression of HDAC2 target genes. qPCR analysis were performed using specific Taqman assays with relative quantification normalized to endogenous controls snoRNA202. (A) miR-29c is up regulated by 9 folds in THI-treated compared to vehicle-treated diaphragms. (B) miR-1-2 is up regulated by 5.9 folds in THI-treated compared to vehicle-treated diaphragms.

Fig.11. Overview of changes in gene expression in adductors of *mdx* mice after THI treatment. One-month-old male *mdx* were treated daily with THI (50mg/L THI in 55.5mM glucose in drinking water, n=5) or vehicle (55.5mM glucose in drinking water, n=5) for 1 month. RNA extracted from the adductors was profiled using microarray analysis. (A) Density plots for gene expression in vehicle- or THI-treated adductor muscles showed enrichment of muscle genes ($p<2.2e-16$ for vehicle- and $p<2.2e-16$ for THI-treated samples). (B) An overview of significant gene expression changes in THI- versus vehicle-treated adductor muscles (163 genes up regulated, 439 down regulated in THI-treated samples).

Fig.12. Fat infiltration in diaphragms is not increased after one month of THI treatment compared to vehicle-treated *mdx* mice. Representatives of Oil Red O staining in (A) vehicle- and (B) THI-treated diaphragms. (C) Quantification of fat area normalized to muscle area shows a decreasing trend in fat infiltration in THI- compared to vehicle-treated samples.

Fig.13. Beneficial muscle genes slow twitch muscle genes, fatty acid metabolic-, insulin-, sarcomere-related genes are up regulated, while inflammation genes are down regulated in *mdx* mice treated with THI for one month (A) Heat map presentation of the gene ontology analysis of THI-responsive genes. Heat map was created using Multi-experiment viewer program, values presented as a subtraction of gene expression of THI for vehicle, and illustrated with green and red color, denoting down and up regulation of THI-treated genes, respectively. (B) QPCR validation for Mrap, Adrb3 and Ccl2 gene expression, normalized to the gene expression level of the house keeping gene, Ubiquitin C. * $p<0.05$, ** $p<0.01$, *** $p<0.001$.

Fig.14. Inflammation in THI-treated diaphragms. (A) qPCR analysis of inflammation (T cell) markers (CD4 and CD8). (B-C) Representatives of hematopoetic (CD45) and macrophage (CD68) immunostaining in vehicle- and THI-treated diaphragms. (D-E) Quantification of hematopoetic (D) and macrophage (E) populations, as presented in (B) and (C), respectively.

Fig.15. Density plot for THI-responsive genes (THI/vehicle gene expression). The density plot shows enrichment for beneficial muscle and metabolic genes ($p<0.01909$ and $p<3.211e-10$, respectively) and diminishment for inflammation genes ($p<0.04793$).

Fig. 16. Intracellular S1P is increased in THI treated, differentiating C2C12 cells. One-day-differentiating C2C12 cells were treated with 0.05mg/ml THI or vehicle (1% DMSO) for 1 day, and cellular sphingolipid levels were determined by LC-ESI-MS/MS. Cellular S1P and DHS1P were up regulated in THI-treated cells. * $p<0.05$, ** $p<0.01$, *** $p<0.001$

Fig.17. Oxygen consumption is increased in THI/S1P-treated, differentiating C2C12 cells. One-day-differentiating C2C12 cells were treated with 0.05mg/ml THI or vehicle (1% DMSO) or 0.1mM S1P-BSA for 1 day, and OCR was recorded with the Seahorse apparatus. (A) OCR profile of THI- and vehicle-treated cells. (B) Quantification of OCR changes after FCCP or oligomycin addition, respectively in THI- or vehicle-treated C2C12 cells, normalized to the number of cells present in each well, quantified by Hoechst staining (3 separate runs, n=12 for THI and vehicle). (C) OCR profile in S1P-treated, differentiating C2C12 cells. One-day-differentiating C2C12 cells were treated with 0.1mM S1P-BSA in serum replacer media (S1P), serum replacer media alone (vehicle) or untreated in differentiate media (control) for 1 day. (D) Quantification of OCR change after FCCP or oligomycin addition, respectively in S1P- or vehicle-treated C2C12 cells, normalized to the number of cells present in each well, quantified by Hoechst staining (2 separate runs, n=8 for THI and vehicle). The drugs used: Oligomycine (ATP synthase inhibitor), FCCP (ATP uncoupler, to stimulate maximum respiration), Antimycin A and Rotenone (mitochondrial electron transport chain inhibitors). * $p<0.05$, ** $p<0.01$, *** $p<0.001$.

Fig.18. Mitochondrial copy number is unchanged in differentiating C2C12 cells after THI treatment. Mitochondrial copy number was determined by QPCR in THI- or vehicle-treated differentiating C2C12 cells (n=3). The ratio of mtDNA to genomic DNA was calculated by dividing measured copies of mt-Co1 with copies of GADPH.

Fig.19. Extracellular acidification rates in THI- or S1P-treated, differentiating C2C12 cells show no significant increase in glycolysis. One-day-differentiating C2C12 cells were treated with 0.05mg/ml THI or vehicle (1% DMSO) or 0.1mM S1P-BSA for 1 day, and ECAR was

recorded with the Seahorse apparatus. (A) ECAR profile of THI- and vehicle-treated cells. (B) Quantification of ECAR changes after FCCP or oligomycin addition, respectively in THI- or vehicle-treated C2C12 cells, normalized to the number of cells present in each well, quantified by Hoechst staining (3 separate runs, n=12 for THI and vehicle). **Glycolytic capacity remains unchanged THI/S1P-treated, differentiating C2C12 cells** (C-D) ECAR change graph (C) and quantification (D) of glycolytic capacity test in THI- and vehicle-treated, differentiating C2C12 (n= 6 for THI; n=6 for vehicle). (E) ECAR profile in S1P-treated, differentiating C2C12 cells. One-day-differentiating C2C12 cells were treated with 0.1mM S1P-BSA in serum replacer media (S1P), serum replacer media alone (vehicle) or untreated in differentiate media (control) for 1 day. (F) Quantification of ECAR change after FCCP or oligomycin addition, respectively in S1P or vehicle-treated C2C12 cells, normalized to the number of cells present in each well, quantified by Hoechst staining (2 separate runs, n=8 for THI and vehicle). * $p<0.05$, ** $p<0.01$, *** $p<0.001$. The drugs used: Oligomycine (ATP synthase inhibitor), FCCP (ATP uncoupler, to stimulate maximum respiration), Antimycin A and Rotenone (mitochondrial electron transport chain inhibitors)

Fig.20. Higher fatty acid oxidation in THI-treated differentiating C2C12 cells. One-day-differentiating C2C12 cells were treated with 0.05mg/ml THI or vehicle (1% DMSO) for 1 day, and OCR was recorded with the Seahorse apparatus. (A) Representative graph for fatty acid oxidation assay on THI- or vehicle-treated, differentiating C2C12 cells.

(B) Fatty acid-stress reveals higher OCR increase after palmitate addition in the THI-treated but not in control cells (two separate runs, n=9 THI, n= 12 DMSO). The drugs used: Palmitate (fatty acid substrate), ETO (Carnitine palmitoyltransferase 1 inhibitor). * $p<0.05$, ** $p<0.01$, *** $p<0.001$

Fig.21. Reducing HDAC2 in dystrophic flies suppresses the dystrophic phenotype in wing vein formation. *Tubtg6*: dystrophic flies, *Rpd3*$^{12\text{-}37}$*/tubtg6, Rpd3*^{303}*/tubtg6, Rpd3*^{04556}*/tubtg6*: dystrophic flies with reduced Rpd3. (A) Percent of defective posterior cross-veins in wings of dys mutants (tubtg6) with and without Rpd3 reduction. (B) Posterior cross-vein phenotypes observed in dys KD animals (*tubtg6*) with and without reduced Rpd3 (*Rpd3*^{303}*/tubtg6*). * $p<0.05$, ** $p<0.01$, *** $p<0.001$

Fig.22. FTY-720-P recapitulates S1P function by inhibiting HDAC activity. HDAC activity was measured by a fluorescent deacetylation assay in Hela nuclear extract.

TABLE LEGENDS

Table 1. Genes that changed expression after THI treatment were analyzed with a gene ontology program, GeneMANIA and grouped according to their functions. Down regulated genes consisted mostly of chromosome-condensation-involved genes. Up regulated genes consisted of genes related to fatty acid metabolic processes.

REFERENCES

Abe, S., Maejima, M., Watanabe, H., Shibahara, T., Agematsu, H., Doi, T., Sakiyama, K., Usami, A., Gojyo, K., Hashimoto, M. et al. (2002). Muscle-fiber characteristics in adult mouse-tongue muscles. *Anatomical science international* **77**, 145-148.

Alamdari, N., Aversa, Z., Castillero, E. and Hasselgren, P. O. (2013). Acetylation and deacetylation--novel factors in muscle wasting. *Metabolism: clinical and experimental* **62**, 1-11.

Alberts, B. A., Johnson, A., Lewis, J., Raff, M., Robert, K. and Walter, P. (2002). Molecular biology of the cell: Garland Science.

Alvarez, S. E., Harikumar, K. B., Hait, N. C., Allegood, J., Strub, G. M., Kim, E. Y., Maceyka, M., Jiang, H., Luo, C., Kordula, T. et al. (2010). Sphingosine-1-phosphate is a missing cofactor for the E3 ubiquitin ligase TRAF2. *Nature* **465**, 1084-1088.

Arany, Z., Lebrasseur, N., Morris, C., Smith, E., Yang, W., Ma, Y., Chin, S. and Spiegelman, B. M. (2007). The transcriptional coactivator PGC-1beta drives the formation of oxidative type IIX fibers in skeletal muscle. *Cell metabolism* **5**, 35-46.

Au, C. G., Butler, T. L., Sherwood, M. C., Egan, J. R., North, K. N. and Winlaw, D. S. (2011). Increased connective tissue growth factor associated with cardiac fibrosis in the mdx mouse model of dystrophic cardiomyopathy. *International journal of experimental pathology* **92**, 57-65.

Bach, J. R. and Martinez, D. (2011). Duchenne muscular dystrophy: continuous noninvasive ventilatory support prolongs survival. *Respiratory care* **56**, 744-750.

Bassel-Duby, R. and Olson, E. N. (2006). Signaling pathways in skeletal muscle remodeling. *Annual review of biochemistry* **75**, 19-37.

Blake, D. J., Weir, A., Newey, S. E. and Davies, K. E. (2002). Function and genetics of dystrophin and dystrophin-related proteins in muscle. *Physiological reviews* **82**, 291-329.

Borowsky, A. D., Bandhuvula, P., Kumar, A., Yoshinaga, Y., Nefedov, M., Fong, L. G., Zhang, M., Baridon, B., Dillard, L., de Jong, P. et al. (2012). Sphingosine-1-phosphate lyase expression in embryonic and adult murine tissues. *Journal of lipid research* **53**, 1920-1931.

Brennan, J. P., Southworth, R., Medina, R. A., Davidson, S. M., Duchen, M. R. and Shattock, M. J. (2006). Mitochondrial uncoupling, with low concentration FCCP, induces ROS-dependent cardioprotection independent of KATP channel activation. *Cardiovascular research* **72**, 313-321.

Brinkmann, V. (2007). Sphingosine 1-phosphate receptors in health and disease: mechanistic insights from gene deletion studies and reverse pharmacology. *Pharmacology & therapeutics* **115**, 84-105.

Bruni, P. and Donati, C. (2008). Pleiotropic effects of sphingolipids in skeletal muscle. *Cellular and molecular life sciences : CMLS* **65**, 3725-3736.

Bulfield, G., Siller, W. G., Wight, P. A. and Moore, K. J. (1984). X chromosome-linked muscular dystrophy (mdx) in the mouse. *Proceedings of the National Academy of Sciences of the United States of America* **81**, 1189-1192.

Bushby, K. M. and Gardner-Medwin, D. (1993). The clinical, genetic and dystrophin characteristics of Becker muscular dystrophy. I. Natural history. *Journal of neurology* **240**, 98-104.

Cacchiarelli, D., Martone, J., Girardi, E., Cesana, M., Incitti, T., Morlando, M., Nicoletti, C., Santini, T., Sthandier, O., Barberi, L. et al. (2010). MicroRNAs involved in molecular circuitries relevant for the Duchenne muscular dystrophy pathogenesis are controlled by the dystrophin/nNOS pathway. *Cell metabolism* **12**, 341-351.

Campbell, N. A., Reece, J. B. and Lawrence, M. G. (1999). Biology: Addison Wesley Longman.

Caron, C., Boyault, C. and Khochbin, S. (2005). Regulatory cross-talk between lysine acetylation and ubiquitination: role in the control of protein stability. *BioEssays : news and reviews in molecular, cellular and developmental biology* **27**, 408-415.

Carpenter, J. L., Hoffman, E. P., Romanul, F. C., Kunkel, L. M., Rosales, R. K., Ma, N. S., Dasbach, J. J., Rae, J. F., Moore, F. M., McAfee, M. B. et al. (1989). Feline muscular dystrophy with dystrophin deficiency. *The American journal of pathology* **135**, 909-919.

Chakkalakal, J. V., Harrison, M. A., Carbonetto, S., Chin, E., Michel, R. N. and Jasmin, B. J. (2004). Stimulation of calcineurin signaling attenuates the dystrophic pathology in mdx mice. *Human molecular genetics* **13**, 379-388.

Chamberlain, J. S., Metzger, J., Reyes, M., Townsend, D. and Faulkner, J. A. (2007). Dystrophin-deficient mdx mice display a reduced life span and are susceptible to spontaneous rhabdomyosarcoma. *FASEB journal : official publication of the Federation of American Societies for Experimental Biology* **21**, 2195-2204.

Chapdelaine, P., Pichavant, C., Rousseau, J., Paques, F. and Tremblay, J. P. (2010). Meganucleases can restore the reading frame of a mutated dystrophin. *Gene therapy* **17**, 846-858.

Chappell, J. B. and Greville, G. D. (1961). Effects of oligomycin on respiration and swelling of isolated liver mitochondria. *Nature* **190**, 502-504.

Chemello, F., Bean, C., Cancellara, P., Laveder, P., Reggiani, C. and Lanfranchi, G. (2011). Microgenomic analysis in skeletal muscle: expression signatures of individual fast and slow myofibers. *PloS one* **6**, e16807.

Chen, J. F., Mandel, E. M., Thomson, J. M., Wu, Q., Callis, T. E., Hammond, S. M., Conlon, F. L. and Wang, D. Z. (2006). The role of microRNA-1 and microRNA-133 in skeletal muscle proliferation and differentiation. *Nature genetics* **38**, 228-233.

Chen, Y. W., Zhao, P., Borup, R. and Hoffman, E. P. (2000). Expression profiling in the muscular dystrophies: identification of novel aspects of molecular pathophysiology. *The Journal of cell biology* **151**, 1321-1336.

Chiba, K. (2005). FTY720, a new class of immunomodulator, inhibits lymphocyte egress from secondary lymphoid tissues and thymus by agonistic activity at sphingosine 1-phosphate receptors. *Pharmacology & therapeutics* **108**, 308-319.

Chin, E. R., Olson, E. N., Richardson, J. A., Yang, Q., Humphries, C., Shelton, J. M., Wu, H., Zhu, W., Bassel-Duby, R. and Williams, R. S. (1998). A calcineurin-dependent transcriptional pathway controls skeletal muscle fiber type. *Genes & development* **12**, 2499-2509.

Christoforou, C. P., Greer, C. E., Challoner, B. R., Charizanos, D. and Ray, R. P. (2008). The detached locus encodes Drosophila Dystrophin, which acts with other components of the Dystrophin Associated Protein Complex to influence intercellular signalling in developing wing veins. *Developmental biology* **313**, 519-532.

Chun, J., Goetzl, E. J., Hla, T., Igarashi, Y., Lynch, K. R., Moolenaar, W., Pyne, S. and Tigyi, G. (2002). International Union of Pharmacology. XXXIV. Lysophospholipid receptor nomenclature. *Pharmacological reviews* **54**, 265-269.

Cobos, A. R., Segade, L. A. and Fuentes, I. (2001). Muscle fibre types in the suprahyoid muscles of the rat. *Journal of anatomy* **198**, 283-294.

Cocco, L., Maraldi, N. M., Manzoli, F. A., Gilmour, R. S. and Lang, A. (1980). Phospholipid interactions in rat liver nuclear matrix. *Biochemical and biophysical research communications* **96**, 890-898.

Colussi, C., Mozzetta, C., Gurtner, A., Illi, B., Rosati, J., Straino, S., Ragone, G., Pescatori, M., Zaccagnini, G., Antonini, A. et al. (2008). HDAC2 blockade by nitric oxide and histone deacetylase inhibitors reveals a common target in Duchenne muscular dystrophy treatment. *Proceedings of the National Academy of Sciences of the United States of America* **105**, 19183-19187.

Connolly, A. M., Keeling, R. M., Mehta, S., Pestronk, A. and Sanes, J. R. (2001). Three mouse models of muscular dystrophy: the natural history of strength and fatigue in dystrophin-, dystrophin/utrophin-, and laminin alpha2-deficient mice. *Neuromuscular disorders : NMD* **11**, 703-712.

Consalvi, S., Saccone, V., Giordani, L., Minetti, G., Mozzetta, C. and Puri, P. L. (2011). Histone deacetylase inhibitors in the treatment of muscular dystrophies: epigenetic drugs for genetic diseases. *Mol Med* **17**, 457-465.

Consalvi, S., Mozzetta, C., Bettica, P., Germani, M., Fiorentini, F., Del Bene, F., Rocchetti, M., Leoni, F., Monzani, V., Mascagni, P. et al. (2013). Preclinical Studies in the mdx Mouse Model of Duchenne Muscular Dystrophy with the Histone Deacetylase Inhibitor Givinostat. *Mol Med* **19**, 79-87.

Cooper, B. J., Winand, N. J., Stedman, H., Valentine, B. A., Hoffman, E. P., Kunkel, L. M., Scott, M. O., Fischbeck, K. H., Kornegay, J. N., Avery, R. J. et al. (1988). The homologue of the Duchenne locus is defective in X-linked muscular dystrophy of dogs. *Nature* **334**, 154-156.

Cyster, J. G. and Schwab, S. R. (2012). Sphingosine-1-phosphate and lymphocyte egress from lymphoid organs. *Annual review of immunology* **30**, 69-94.

Czerwinska, A. M., Streminska, W., Ciemerych, M. A. and Grabowska, I. (2012). Mouse gastrocnemius muscle regeneration after mechanical or cardiotoxin injury. *Folia histochemica et cytobiologica / Polish Academy of Sciences, Polish Histochemical and Cytochemical Society* **50**, 144-153.

Czubryt, M. P., McAnally, J., Fishman, G. I. and Olson, E. N. (2003). Regulation of peroxisome proliferator-activated receptor gamma coactivator 1 alpha (PGC-1 alpha) and mitochondrial function by MEF2 and HDAC5. *Proceedings of the National Academy of Sciences of the United States of America* **100**, 1711-1716.

Danieli-Betto, D., Peron, S., Germinario, E., Zanin, M., Sorci, G., Franzoso, S., Sandona, D. and Betto, R. (2010). Sphingosine 1-phosphate signaling is involved in skeletal muscle regeneration. *American journal of physiology. Cell physiology* **298**, C550-558.

Danko, I., Chapman, V. and Wolff, J. A. (1992). The frequency of revertants in mdx mouse genetic models for Duchenne muscular dystrophy. *Pediatric research* **32**, 128-131.

de Ruijter, A. J., van Gennip, A. H., Caron, H. N., Kemp, S. and van Kuilenburg, A. B. (2003). Histone deacetylases (HDACs): characterization of the classical HDAC family. *The Biochemical journal* **370**, 737-749.

Delling, U., Tureckova, J., Lim, H. W., De Windt, L. J., Rotwein, P. and Molkentin, J. D. (2000). A calcineurin-NFATc3-dependent pathway regulates skeletal muscle differentiation and slow myosin heavy-chain expression. *Molecular and cellular biology* **20**, 6600-6611.

Deshmane, S. L., Kremlev, S., Amini, S. and Sawaya, B. E. (2009). Monocyte chemoattractant protein-1 (MCP-1): an overview. *Journal of interferon & cytokine research : the official journal of the International Society for Interferon and Cytokine Research* **29**, 313-326.

Dhume, A., Lu, S. and Horowits, R. (2006). Targeted disruption of N-RAP gene function by RNA interference: a role for N-RAP in myofibril organization. *Cell motility and the cytoskeleton* **63**, 493-511.

Ding, G., Sonoda, H., Yu, H., Kajimoto, T., Goparaju, S. K., Jahangeer, S., Okada, T. and Nakamura, S. (2007). Protein kinase D-mediated phosphorylation and nuclear export of sphingosine kinase 2. *The Journal of biological chemistry* **282**, 27493-27502.

Dokmanovic, M., Clarke, C. and Marks, P. A. (2007). Histone deacetylase inhibitors: overview and perspectives. *Molecular cancer research : MCR* **5**, 981-989.

Dong, L. H., Cheng, S., Zheng, Z., Wang, L., Shen, Y., Shen, Z. X., Chen, S. J. and Zhao, W. L. (2013). Histone deacetylase inhibitor potentiated the ability of MTOR inhibitor to induce autophagic cell death in Burkitt leukemia/lymphoma. *Journal of hematology & oncology* **6**, 53.

Dovey, O. M., Foster, C. T. and Cowley, S. M. (2010). Histone deacetylase 1 (HDAC1), but not HDAC2, controls embryonic stem cell differentiation. *Proceedings of the National Academy of Sciences of the United States of America* **107**, 8242-8247.

Duncan, C. J. (1978). Role of intracellular calcium in promoting muscle damage: a strategy for controlling the dystrophic condition. *Experientia* **34**, 1531-1535.

Eagle, M., Bourke, J., Bullock, R., Gibson, M., Mehta, J., Giddings, D., Straub, V. and Bushby, K. (2007). Managing Duchenne muscular dystrophy--the additive effect of spinal surgery and home nocturnal ventilation in improving survival. *Neuromuscular disorders : NMD* **17**, 470-475.

Emery, A. E. (1991). Population frequencies of inherited neuromuscular diseases--a world survey. *Neuromuscular disorders : NMD* **1**, 19-29.

Engvall, E. and Wewer, U. M. (2003). The new frontier in muscular dystrophy research: booster genes. *FASEB journal : official publication of the Federation of American Societies for Experimental Biology* **17**, 1579-1584.

Evans, N. P., Misyak, S. A., Robertson, J. L., Bassaganya-Riera, J. and Grange, R. W. (2009). Dysregulated intracellular signaling and inflammatory gene expression during initial disease onset in Duchenne muscular dystrophy. *American journal of physical medicine & rehabilitation / Association of Academic Physiatrists* **88**, 502-522.

Fairclough, R. J., Wood, M. J. and Davies, K. E. (2013). Therapy for Duchenne muscular dystrophy: renewed optimism from genetic approaches. *Nature reviews. Genetics* **14**, 373-378.

Ferrari, A., Fiorino, E., Giudici, M., Gilardi, F., Galmozzi, A., Mitro, N., Cermenati, G., Godio, C., Caruso, D., De Fabiani, E. et al. (2012). Linking epigenetics to lipid metabolism: focus on histone deacetylases. *Molecular membrane biology* **29**, 257-266.

Flanigan, K. M., von Niederhausern, A., Dunn, D. M., Alder, J., Mendell, J. R. and Weiss, R. B. (2003). Rapid direct sequence analysis of the dystrophin gene. *American journal of human genetics* **72**, 931-939.

Forrest, M., Sun, S. Y., Hajdu, R., Bergstrom, J., Card, D., Doherty, G., Hale, J., Keohane, C., Meyers, C., Milligan, J. et al. (2004). Immune cell regulation and cardiovascular effects of sphingosine 1-phosphate receptor agonists in rodents are mediated via distinct receptor subtypes. *The Journal of pharmacology and experimental therapeutics* **309**, 758-768.

Fredly, H., Gjertsen, B. T. and Bruserud, O. (2013). Histone deacetylase inhibition in the treatment of acute myeloid leukemia: the effects of valproic acid on leukemic cells, and the clinical and experimental evidence for combining valproic acid with other antileukemic agents. *Clinical epigenetics* **5**, 12.

Galmozzi, A., Mitro, N., Ferrari, A., Gers, E., Gilardi, F., Godio, C., Cermenati, G., Gualerzi, A., Donetti, E., Rotili, D. et al. (2013). Inhibition of class I histone deacetylases unveils a mitochondrial signature and enhances oxidative metabolism in skeletal muscle and adipose tissue. *Diabetes* **62**, 732-742.

Gao, Z., Yin, J., Zhang, J., Ward, R. E., Martin, R. J., Lefevre, M., Cefalu, W. T. and Ye, J. (2009). Butyrate improves insulin sensitivity and increases energy expenditure in mice. *Diabetes* **58**, 1509-1517.

Gehrig, S. M., van der Poel, C., Sayer, T. A., Schertzer, J. D., Henstridge, D. C., Church, J. E., Lamon, S., Russell, A. P., Davies, K. E., Febbraio, M. A. et al. (2012). Hsp72 preserves muscle function and slows progression of severe muscular dystrophy. *Nature* **484**, 394-398.

Germinario, E., Peron, S., Toniolo, L., Betto, R., Cencetti, F., Donati, C., Bruni, P. and Danieli-Betto, D. (2012). S1P2 receptor promotes mouse skeletal muscle regeneration. *J Appl Physiol* **113**, 707-713.

Giussani, P., Maceyka, M., Le Stunff, H., Mikami, A., Lepine, S., Wang, E., Kelly, S., Merrill, A. H., Jr., Milstien, S. and Spiegel, S. (2006). Sphingosine-1-phosphate phosphohydrolase regulates endoplasmic reticulum-to-golgi trafficking of ceramide. *Molecular and cellular biology* **26**, 5055-5069.

Gorshkova, I. A., Wang, H., Orbelyan, G. A., Goya, J., Natarajan, V., Beiser, D. G., Vanden Hoek, T. L. and Berdyshev, E. V. (2013). Inhibition of sphingosine-1-phosphate lyase rescues sphingosine kinase-1-knockout phenotype following murine cardiac arrest. *Life sciences*.

Graff, J. and Tsai, L. H. (2013). Histone acetylation: molecular mnemonics on the chromatin. *Nature reviews. Neuroscience* **14**, 97-111.

Gramolini, A. O., Belanger, G., Thompson, J. M., Chakkalakal, J. V. and Jasmin, B. J. (2001). Increased expression of utrophin in a slow vs. a fast muscle involves posttranscriptional events. *American journal of physiology. Cell physiology* **281**, C1300-1309.

Granzier, H. L. and Labeit, S. (2006). The giant muscle protein titin is an adjustable molecular spring. *Exercise and sport sciences reviews* **34**, 50-53.

Grounds, M. D. (2008). Two-tiered hypotheses for Duchenne muscular dystrophy. *Cellular and molecular life sciences : CMLS* **65**, 1621-1625.

Guan, J. S., Haggarty, S. J., Giacometti, E., Dannenberg, J. H., Joseph, N., Gao, J., Nieland, T. J., Zhou, Y., Wang, X., Mazitschek, R. et al. (2009). HDAC2 negatively regulates memory formation and synaptic plasticity. *Nature* **459**, 55-60.

Haberland, M., Montgomery, R. L. and Olson, E. N. (2009). The many roles of histone deacetylases in development and physiology: implications for disease and therapy. *Nature reviews. Genetics* **10**, 32-42.

Hackman, P., Vihola, A., Haravuori, H., Marchand, S., Sarparanta, J., De Seze, J., Labeit, S., Witt, C., Peltonen, L., Richard, I. et al. (2002). Tibial muscular dystrophy is a titinopathy caused by mutations in TTN, the gene encoding the giant skeletal-muscle protein titin. *American journal of human genetics* **71**, 492-500.

Hait, N. C., Oskeritzian, C. A., Paugh, S. W., Milstien, S. and Spiegel, S. (2006). Sphingosine kinases, sphingosine 1-phosphate, apoptosis and diseases. *Biochimica et biophysica acta* **1758**, 2016-2026.

Hait, N. C., Bellamy, A., Milstien, S., Kordula, T. and Spiegel, S. (2007). Sphingosine kinase type 2 activation by ERK-mediated phosphorylation. *The Journal of biological chemistry* **282**, 12058-12065.

Hait, N. C., Allegood, J., Maceyka, M., Strub, G. M., Harikumar, K. B., Singh, S. K., Luo, C., Marmorstein, R., Kordula, T., Milstien, S. et al. (2009). Regulation of histone acetylation in the nucleus by sphingosine-1-phosphate. *Science* **325**, 1254-1257.

Hajek, R., Siegel, D., Orlowski, R. Z., Ludwig, H., Palumbo, A. and Dimopoulos, M. A. (2013). The Role of Hdac Inhibitors in Patients with Relapsed/Refractory Multiple Myeloma. *Leukemia & lymphoma*.

Halmilton, N., Luttens, K. and Weimar, W. (2001). Kinesiology: Scientific Basic of Human Motion: McGraw-Hill.

Hannun, Y. A. and Obeid, L. M. (2008). Principles of bioactive lipid signalling: lessons from sphingolipids. *Nature reviews. Molecular cell biology* **9**, 139-150.

Harms, K. L. and Chen, X. (2007). Histone deacetylase 2 modulates p53 transcriptional activities through regulation of p53-DNA binding activity. *Cancer research* **67**, 3145-3152.

Hawke, T. J. and Garry, D. J. (2001). Myogenic satellite cells: physiology to molecular biology. *J Appl Physiol* **91**, 534-551.

Hayakawa, T. and Nakayama, J. (2011). Physiological roles of class I HDAC complex and histone demethylase. *Journal of biomedicine & biotechnology* **2011**, 129383.

Herr, D. R. and Chun, J. (2007). Effects of LPA and S1P on the nervous system and implications for their involvement in disease. *Current drug targets* **8**, 155-167.

Hinkle, R. T., Lefever, F. R., Dolan, E. T., Reichart, D. L., Dietrich, J. A., Gropp, K. E., Thacker, R. I., Demuth, J. P., Stevens, P. J., Qu, X. A. et al. (2007). Corticortophin releasing factor 2 receptor agonist treatment significantly slows disease progression in mdx mice. *BMC medicine* **5**, 18.

Hoffman, E. P., Brown, R. H., Jr. and Kunkel, L. M. (1987). Dystrophin: the protein product of the Duchenne muscular dystrophy locus. *Cell* **51**, 919-928.

Ieronimakis, N., Pantoja, M., Hays, A., Dosey, T., Qi, J., Fischer, K., Hoofnagle, A., Sadilek, M., Chamberlain, J., Ruohola-Baker, H. et al. (2013). Increased Sphingosine-1-Phosphate ameliorates disease pathology in mdx mice after acute injury. *Skeletal muscle*.

Igarashi, N., Okada, T., Hayashi, S., Fujita, T., Jahangeer, S. and Nakamura, S. (2003). Sphingosine kinase 2 is a nuclear protein and inhibits DNA synthesis. *The Journal of biological chemistry* **278**, 46832-46839.

Im, W. B., Phelps, S. F., Copen, E. H., Adams, E. G., Slightom, J. L. and Chamberlain, J. S. (1996). Differential expression of dystrophin isoforms in strains of mdx mice with different mutations. *Human molecular genetics* **5**, 1149-1153.

Ishizaki, M., Suga, T., Kimura, E., Shiota, T., Kawano, R., Uchida, Y., Uchino, K., Yamashita, S., Maeda, Y. and Uchino, M. (2008). Mdx respiratory impairment following fibrosis of the diaphragm. *Neuromuscular disorders : NMD* **18**, 342-348.

Jenkins, G. W., Kemnitz, C. P. and Tortora, G. J. (2007). Anatomy and Physiology: From Science to Life: Wiley.

Kelly, A. M. (1978). Satellite cells and myofiber growth in the rat soleus and extensor digitorum longus muscles. *Developmental biology* **65**, 1-10.

Kenyon, N. J., Ward, R. W., McGrew, G. and Last, J. A. (2003). TGF-beta1 causes airway fibrosis and increased collagen I and III mRNA in mice. *Thorax* **58**, 772-777.

Keul, P., Lucke, S., von Wnuck Lipinski, K., Bode, C., Graler, M., Heusch, G. and Levkau, B. (2011). Sphingosine-1-phosphate receptor 3 promotes recruitment of monocyte/macrophages in inflammation and atherosclerosis. *Circulation research* **108**, 314-323.

Kiernan, J. (2008). Histological and Histochemical Methods: Theory and Practice 4th edition. : Cold Springs Harbor laboratory Press.

Knight, P. J. and Trinick, J. A. (1982). Preparation of myofibrils. *Methods in enzymology* **85 Pt B**, 9-12.

Koenig, M., Monaco, A. P. and Kunkel, L. M. (1988). The complete sequence of dystrophin predicts a rod-shaped cytoskeletal protein. *Cell* **53**, 219-228.

Kono, M., Belyantseva, I. A., Skoura, A., Frolenkov, G. I., Starost, M. F., Dreier, J. L., Lidington, D., Bolz, S. S., Friedman, T. B., Hla, T. et al. (2007). Deafness and stria vascularis defects in S1P2 receptor-null mice. *The Journal of biological chemistry* **282**, 10690-10696.

Kucherenko, M. M., Pantoja, M., Yatsenko, A. S., Shcherbata, H. R., Fischer, K. A., Maksymiv, D. V., Chernyk, Y. I. and Ruohola-Baker, H. (2008). Genetic modifier screens

reveal new components that interact with the Drosophila dystroglycan-dystrophin complex. *PloS one* **3**, e2418.

Kuroda, K., Kuang, S., Taketo, M. M. and Rudnicki, M. A. (2013). Canonical Wnt signaling induces BMP-4 to specify slow myofibrogenesis of fetal myoblasts. *Skeletal muscle* **3**, 5.

Le Grand, F., Jones, A. E., Seale, V., Scime, A. and Rudnicki, M. A. (2009). Wnt7a activates the planar cell polarity pathway to drive the symmetric expansion of satellite stem cells. *Cell stem cell* **4**, 535-547.

Lefaucheur, J. P., Pastoret, C. and Sebille, A. (1995). Phenotype of dystrophinopathy in old mdx mice. *The Anatomical record* **242**, 70-76.

Lin, J., Wu, H., Tarr, P. T., Zhang, C. Y., Wu, Z., Boss, O., Michael, L. F., Puigserver, P., Isotani, E., Olson, E. N. et al. (2002). Transcriptional co-activator PGC-1 alpha drives the formation of slow-twitch muscle fibres. *Nature* **418**, 797-801.

Liu, H., Sugiura, M., Nava, V. E., Edsall, L. C., Kono, K., Poulton, S., Milstien, S., Kohama, T. and Spiegel, S. (2000). Molecular cloning and functional characterization of a novel mammalian sphingosine kinase type 2 isoform. *The Journal of biological chemistry* **275**, 19513-19520.

Lodish, Berk, Kaiser, Krieger, Scott, Bretscher, Ploegh and Matsudaira. (2007). Molecular cell biology: Freeman.

Loh, K. C., Leong, W. I., Carlson, M. E., Oskouian, B., Kumar, A., Fyrst, H., Zhang, M., Proia, R. L., Hoffman, E. P. and Saba, J. D. (2012). Sphingosine-1-phosphate enhances satellite cell activation in dystrophic muscles through a S1PR2/STAT3 signaling pathway. *PloS one* **7**, e37218.

Maceyka, M., Harikumar, K. B., Milstien, S. and Spiegel, S. (2012). Sphingosine-1-phosphate signaling and its role in disease. *Trends in cell biology* **22**, 50-60.

Mamo, S., Gal, A. B., Bodo, S. and Dinnyes, A. (2007). Quantitative evaluation and selection of reference genes in mouse oocytes and embryos cultured in vivo and in vitro. *BMC developmental biology* **7**, 14.

Mann, C. J., Perdiguero, E., Kharraz, Y., Aguilar, S., Pessina, P., Serrano, A. L. and Munoz-Canoves, P. (2011). Aberrant repair and fibrosis development in skeletal muscle. *Skeletal muscle* **1**, 21.

Matloubian, M., Lo, C. G., Cinamon, G., Lesneski, M. J., Xu, Y., Brinkmann, V., Allende, M. L., Proia, R. L. and Cyster, J. G. (2004). Lymphocyte egress from thymus and peripheral lymphoid organs is dependent on S1P receptor 1. *Nature* **427**, 355-360.

Matsumura, K. and Campbell, K. P. (1994). Dystrophin-glycoprotein complex: its role in the molecular pathogenesis of muscular dystrophies. *Muscle & nerve* **17**, 2-15.

Matsumura, K., Shimizu, T., Nonaka, I. and Mannen, T. (1989). Immunochemical study of connectin (titin) in neuromuscular diseases using a monoclonal antibody: connectin is degraded extensively in Duchenne muscular dystrophy. *Journal of the neurological sciences* **93**, 147-156.

McDonald, C. M. (2002). Physical activity, health impairments, and disability in neuromuscular disease. *American journal of physical medicine & rehabilitation / Association of Academic Physiatrists* **81**, S108-120.

McDonald, C. M., Abresch, R. T., Carter, G. T., Fowler, W. M., Jr., Johnson, E. R., Kilmer, D. D. and Sigford, B. J. (1995). Profiles of neuromuscular diseases. Duchenne muscular dystrophy. *American journal of physical medicine & rehabilitation / Association of Academic Physiatrists* **74**, S70-92.

McGee, S. L., van Denderen, B. J., Howlett, K. F., Mollica, J., Schertzer, J. D., Kemp, B. E. and Hargreaves, M. (2008). AMP-activated protein kinase regulates GLUT4 transcription by phosphorylating histone deacetylase 5. *Diabetes* **57**, 860-867.

Means, C. K. and Brown, J. H. (2009). Sphingosine-1-phosphate receptor signalling in the heart. *Cardiovascular research* **82**, 193-200.

Mechtcheriakova, D., Wlachos, A., Sobanov, J., Bornancin, F., Zlabinger, G., Baumruker, T. and Billich, A. (2007). FTY720-phosphate is dephosphorylated by lipid phosphate phosphatase 3. *FEBS letters* **581**, 3063-3068.

Mendell, J. R., Rodino-Klapac, L., Sahenk, Z., Malik, V., Kaspar, B. K., Walker, C. M. and Clark, K. R. (2012). Gene therapy for muscular dystrophy: lessons learned and path forward. *Neuroscience letters* **527**, 90-99.

Mendell, J. R., Campbell, K., Rodino-Klapac, L., Sahenk, Z., Shilling, C., Lewis, S., Bowles, D., Gray, S., Li, C., Galloway, G. et al. (2010). Dystrophin immunity in Duchenne's muscular dystrophy. *The New England journal of medicine* **363**, 1429-1437.

Michan, S. and Sinclair, D. (2007). Sirtuins in mammals: insights into their biological function. *The Biochemical journal* **404**, 1-13.

Michishita, E., Park, J. Y., Burneskis, J. M., Barrett, J. C. and Horikawa, I. (2005). Evolutionarily conserved and nonconserved cellular localizations and functions of human SIRT proteins. *Molecular biology of the cell* **16**, 4623-4635.

Minetti, G. C., Colussi, C., Adami, R., Serra, C., Mozzetta, C., Parente, V., Fortuni, S., Straino, S., Sampaolesi, M., Di Padova, M. et al. (2006). Functional and morphological recovery of dystrophic muscles in mice treated with deacetylase inhibitors. *Nature medicine* **12**, 1147-1150.

Moolenaar, W. H. (1995). Lysophosphatidic acid, a multifunctional phospholipid messenger. *The Journal of biological chemistry* **270**, 12949-12952.

Moser, H. (1984). Duchenne muscular dystrophy: pathogenetic aspects and genetic prevention. *Human genetics* **66**, 17-40.

Mozzetta, C., Minetti, G. and Puri, P. L. (2009). Regenerative pharmacology in the treatment of genetic diseases: the paradigm of muscular dystrophy. *The international journal of biochemistry & cell biology* **41**, 701-710.

Muir, A. R., Kanji, A. H. and Allbrook, D. (1965). The structure of the satellite cells in skeletal muscle. *Journal of anatomy* **99**, 435-444.

Muntoni, F. and Wood, M. J. (2011). Targeting RNA to treat neuromuscular disease. *Nature reviews. Drug discovery* **10**, 621-637.

Murata, N., Sato, K., Kon, J., Tomura, H., Yanagita, M., Kuwabara, A., Ui, M. and Okajima, F. (2000). Interaction of sphingosine 1-phosphate with plasma components, including lipoproteins, regulates the lipid receptor-mediated actions. *The Biochemical journal* **352 Pt 3**, 809-815.

Nakamura, A. and Takeda, S. (2011). Mammalian models of Duchenne Muscular Dystrophy: pathological characteristics and therapeutic applications. *Journal of biomedicine & biotechnology* **2011**, 184393.

Nava, V. E., Lacana, E., Poulton, S., Liu, H., Sugiura, M., Kono, K., Milstien, S., Kohama, T. and Spiegel, S. (2000). Functional characterization of human sphingosine kinase-1. *FEBS letters* **473**, 81-84.

Naya, F. J., Mercer, B., Shelton, J., Richardson, J. A., Williams, R. S. and Olson, E. N. (2000). Stimulation of slow skeletal muscle fiber gene expression by calcineurin in vivo. *The Journal of biological chemistry* **275**, 4545-4548.

Neri, M., Torelli, S., Brown, S., Ugo, I., Sabatelli, P., Merlini, L., Spitali, P., Rimessi, P., Gualandi, F., Sewry, C. et al. (2007). Dystrophin levels as low as 30% are sufficient to avoid muscular dystrophy in the human. *Neuromuscular disorders : NMD* **17**, 913-918.

Neubauer, H. A. and Pitson, S. M. (2013). Roles, regulation and inhibitors of sphingosine kinase 2. *The FEBS journal*.

Niebroj Dobosz, I., Fidzianska, A. and Glinka, Z. (1997). Comparative Studies of Hind Limb and Diaphragm Muscles of *mdx* Mice. *Basic Appl. Myol.* **7**, 6.

Oak, S. A., Zhou, Y. W. and Jarrett, H. W. (2003). Skeletal muscle signaling pathway through the dystrophin glycoprotein complex and Rac1. *The Journal of biological chemistry* **278**, 39287-39295.

Okudaira, S., Yukiura, H. and Aoki, J. (2010). Biological roles of lysophosphatidic acid signaling through its production by autotaxin. *Biochimie* **92**, 698-706.

Olivera, A., Kohama, T., Edsall, L., Nava, V., Cuvillier, O., Poulton, S. and Spiegel, S. (1999). Sphingosine kinase expression increases intracellular sphingosine-1-phosphate and promotes cell growth and survival. *The Journal of cell biology* **147**, 545-558.

Olson, E. N. and Williams, R. S. (2000). Calcineurin signaling and muscle remodeling. *Cell* **101**, 689-692.

Pantoja, M. and Ruohola-Baker, H. (2013). *Drosophila* as a starting point for developing therapeutics for the rare disease Dunchenne Muscular Dystrophy. *Rare Diseases* **1:324995;** http://dx.doi.org/10.4161/rdis.24995.

Pantoja, M., Fischer, K. A., Ieronimakis, N., Reyes, M. and Ruohola-Baker, H. (2013). Genetic elevation of sphingosine 1-phosphate suppresses dystrophic muscle phenotypes in Drosophila. *Development* **140**, 136-146.

Partridge, T. (1991). Animal models of muscular dystrophy--what can they teach us? *Neuropathology and applied neurobiology* **17**, 353-363.

Pastoret, C. and Sebille, A. (1995). mdx mice show progressive weakness and muscle deterioration with age. *Journal of the neurological sciences* **129**, 97-105.

Pette, D. and Staron, R. S. (2000). Myosin isoforms, muscle fiber types, and transitions. *Microscopy research and technique* **50**, 500-509.

Pichavant, C., Aartsma-Rus, A., Clemens, P. R., Davies, K. E., Dickson, G., Takeda, S., Wilton, S. D., Wolff, J. A., Wooddell, C. I., Xiao, X. et al. (2011). Current status of pharmaceutical and genetic therapeutic approaches to treat DMD. *Molecular therapy : the journal of the American Society of Gene Therapy* **19**, 830-840.

Pitson, S. M., Moretti, P. A., Zebol, J. R., Xia, P., Gamble, J. R., Vadas, M. A., D'Andrea, R. J. and Wattenberg, B. W. (2000). Expression of a catalytically inactive sphingosine kinase mutant blocks agonist-induced sphingosine kinase activation. A dominant-negative sphingosine kinase. *The Journal of biological chemistry* **275**, 33945-33950.

Potthoff, M. J., Wu, H., Arnold, M. A., Shelton, J. M., Backs, J., McAnally, J., Richardson, J. A., Bassel-Duby, R. and Olson, E. N. (2007). Histone deacetylase degradation and MEF2 activation promote the formation of slow-twitch myofibers. *The Journal of clinical investigation* **117**, 2459-2467.

Puri, P. L. and Sartorelli, V. (2000). Regulation of muscle regulatory factors by DNA-binding, interacting proteins, and post-transcriptional modifications. *Journal of cellular physiology* **185**, 155-173.

Pyne, S. and Pyne, N. J. (2011). Translational aspects of sphingosine 1-phosphate biology. *Trends in molecular medicine* **17**, 463-472.

Rando, T. A. (2001). The dystrophin-glycoprotein complex, cellular signaling, and the regulation of cell survival in the muscular dystrophies. *Muscle & nerve* **24**, 1575-1594.

Riccio, A. (2010). New endogenous regulators of class I histone deacetylases. *Science signaling* **3**, pe1.

Rodgers, J. T. and Puigserver, P. (2007). Fasting-dependent glucose and lipid metabolic response through hepatic sirtuin 1. *Proceedings of the National Academy of Sciences of the United States of America* **104**, 12861-12866.

Roof, D. J., Hayes, A., Adamian, M., Chishti, A. H. and Li, T. (1997). Molecular characterization of abLIM, a novel actin-binding and double zinc finger protein. *The Journal of cell biology* **138**, 575-588.

Ropero, S., Ballestar, E., Alaminos, M., Arango, D., Schwartz, S., Jr. and Esteller, M. (2008). Transforming pathways unleashed by a HDAC2 mutation in human cancer. *Oncogene* **27**, 4008-4012.

Ryder, J. W., Bassel-Duby, R., Olson, E. N. and Zierath, J. R. (2003). Skeletal muscle reprogramming by activation of calcineurin improves insulin action on metabolic pathways. *The Journal of biological chemistry* **278**, 44298-44304.

Saba, J. D. and de la Garza-Rodea, A. S. (2013). S1P lyase in skeletal muscle regeneration and satellite cell activation: exposing the hidden lyase. *Biochimica et biophysica acta* **1831**, 167-175.

Sacco, A., Mourkioti, F., Tran, R., Choi, J., Llewellyn, M., Kraft, P., Shkreli, M., Delp, S., Pomerantz, J. H., Artandi, S. E. et al. (2010). Short telomeres and stem cell exhaustion model Duchenne muscular dystrophy in mdx/mTR mice. *Cell* **143**, 1059-1071.

Sadoul, K., Boyault, C., Pabion, M. and Khochbin, S. (2008). Regulation of protein turnover by acetyltransferases and deacetylases. *Biochimie* **90**, 306-312.

Sampaolesi, M., Blot, S., D'Antona, G., Granger, N., Tonlorenzi, R., Innocenzi, A., Mognol, P., Thibaud, J. L., Galvez, B. G., Barthelemy, I. et al. (2006). Mesoangioblast stem cells ameliorate muscle function in dystrophic dogs. *Nature* **444**, 574-579.

Sanchez, T., Skoura, A., Wu, M. T., Casserly, B., Harrington, E. O. and Hla, T. (2007). Induction of vascular permeability by the sphingosine-1-phosphate receptor-2 (S1P2R) and its downstream effectors ROCK and PTEN. *Arteriosclerosis, thrombosis, and vascular biology* **27**, 1312-1318.

Sanchez, T. G., da Silva Lima, A., Brandao, A. L., Lorenzi, M. C. and Bento, R. F. (2007). Somatic modulation of tinnitus: test reliability and results after repetitive muscle contraction training. *The Annals of otology, rhinology, and laryngology* **116**, 30-35.

Schiaffino, S. and Reggiani, C. (1996). Molecular diversity of myofibrillar proteins: gene regulation and functional significance. *Physiological reviews* **76**, 371-423.

Schiaffino, S. and Reggiani, C. (2011). Fiber types in mammalian skeletal muscles. *Physiological reviews* **91**, 1447-1531.

Schmalbruch, H. and Hellhammer, U. (1977). The number of nuclei in adult rat muscles with special reference to satellite cells. *The Anatomical record* **189**, 169-175.

Schrauwen, P., Hinderling, V., Hesselink, M. K., Schaart, G., Kornips, E., Saris, W. H., Westerterp-Plantenga, M. and Langhans, W. (2002). Etomoxir-induced increase in UCP3 supports a role of uncoupling protein 3 as a mitochondrial fatty acid anion exporter. *FASEB journal : official publication of the Federation of American Societies for Experimental Biology* **16**, 1688-1690.

Schwab, S. R., Pereira, J. P., Matloubian, M., Xu, Y., Huang, Y. and Cyster, J. G. (2005). Lymphocyte sequestration through S1P lyase inhibition and disruption of S1P gradients. *Science* **309**, 1735-1739.

Selsby, J. T., Morine, K. J., Pendrak, K., Barton, E. R. and Sweeney, H. L. (2012). Rescue of dystrophic skeletal muscle by PGC-1alpha involves a fast to slow fiber type shift in the mdx mouse. *PloS one* **7**, e30063.

Serrano, A. L. and Munoz-Canoves, P. (2010). Regulation and dysregulation of fibrosis in skeletal muscle. *Experimental cell research* **316**, 3050-3058.

Serriere-Lanneau, V., Teixeira-Clerc, F., Li, L., Schippers, M., de Wries, W., Julien, B., Tran-Van-Nhieu, J., Manin, S., Poelstra, K., Chun, J. et al. (2007). The sphingosine 1-phosphate receptor S1P2 triggers hepatic wound healing. *FASEB journal : official publication of the Federation of American Societies for Experimental Biology* **21**, 2005-2013.

Shcherbata, H. R., Yatsenko, A. S., Patterson, L., Sood, V. D., Nudel, U., Yaffe, D., Baker, D. and Ruohola-Baker, H. (2007). Dissecting muscle and neuronal disorders in a Drosophila model of muscular dystrophy. *The EMBO journal* **26**, 481-493.

Shu, X., Wu, W., Mosteller, R. D. and Broek, D. (2002). Sphingosine kinase mediates vascular endothelial growth factor-induced activation of ras and mitogen-activated protein kinases. *Molecular and cellular biology* **22**, 7758-7768.

Sicinski, P., Geng, Y., Ryder-Cook, A. S., Barnard, E. A., Darlison, M. G. and Barnard, P. J. (1989). The molecular basis of muscular dystrophy in the mdx mouse: a point mutation. *Science* **244**, 1578-1580.

Simmons, B. J., Cohen, T. J., Bedlack, R. and Yao, T. P. (2011). HDACs in skeletal muscle remodeling and neuromuscular disease. *Handbook of experimental pharmacology* **206**, 79-101.

Singh, P., Cho, J., Tsai, S. Y., Rivas, G. E., Larson, G. P. and Szabo, P. E. (2010). Coordinated allele-specific histone acetylation at the differentially methylated regions of imprinted genes. *Nucleic acids research* **38**, 7974-7990.

Singleton, P. A., Dudek, S. M., Ma, S. F. and Garcia, J. G. (2006). Transactivation of sphingosine 1-phosphate receptors is essential for vascular barrier regulation. Novel role for hyaluronan and CD44 receptor family. *The Journal of biological chemistry* **281**, 34381-34393.

Soares, L. E., Brugnera Junior, A., Zanin, F. A., Pacheco, M. T. and Martin, A. A. (2007). Effects of treatment for manipulation of teeth and Er:YAG laser irradiation on dentin: a Raman spectroscopy analysis. *Photomedicine and laser surgery* **25**, 50-57.

Song, X. M., Ryder, J. W., Kawano, Y., Chibalin, A. V., Krook, A. and Zierath, J. R. (1999). Muscle fiber type specificity in insulin signal transduction. *The American journal of physiology* **277**, R1690-1696.

Spiegel, S. and Milstien, S. (2003). Sphingosine-1-phosphate: an enigmatic signalling lipid. *Nature reviews. Molecular cell biology* **4**, 397-407.

Spitali, P. and Aartsma-Rus, A. (2012). Muscular Dystrophy (eds M. Hegde and A. Ankala), pp. 544: InTech.

Stafstrom, C. E., Roopra, A. and Sutula, T. P. (2008). Seizure suppression via glycolysis inhibition with 2-deoxy-D-glucose (2DG). *Epilepsia* **49 Suppl 8**, 97-100.

Stedman, H. H., Sweeney, H. L., Shrager, J. B., Maguire, H. C., Panettieri, R. A., Petrof, B., Narusawa, M., Leferovich, J. M., Sladky, J. T. and Kelly, A. M. (1991). The mdx mouse diaphragm reproduces the degenerative changes of Duchenne muscular dystrophy. *Nature* **352**, 536-539.

Strub, G. M., Maceyka, M., Hait, N. C., Milstien, S. and Spiegel, S. (2010). Extracellular and intracellular actions of sphingosine-1-phosphate. *Advances in experimental medicine and biology* **688**, 141-155.

Strub, G. M., Paillard, M., Liang, J., Gomez, L., Allegood, J. C., Hait, N. C., Maceyka, M., Price, M. M., Chen, Q., Simpson, D. C. et al. (2011). Sphingosine-1-phosphate produced by sphingosine kinase 2 in mitochondria interacts with prohibitin 2 to regulate complex IV assembly and respiration. *FASEB journal : official publication of the Federation of American Societies for Experimental Biology* **25**, 600-612.

Stupka, N., Plant, D. R., Schertzer, J. D., Emerson, T. M., Bassel-Duby, R., Olson, E. N. and Lynch, G. S. (2006). Activated calcineurin ameliorates contraction-induced injury to skeletal muscles of mdx dystrophic mice. *The Journal of physiology* **575**, 645-656.

Taghli-Lamallem, O., Akasaka, T., Hogg, G., Nudel, U., Yaffe, D., Chamberlain, J. S., Ocorr, K. and Bodmer, R. (2008). Dystrophin deficiency in Drosophila reduces lifespan and causes a dilated cardiomyopathy phenotype. *Aging cell* **7**, 237-249.

Tea, J. S., Chihara, T. and Luo, L. (2010). Histone deacetylase Rpd3 regulates olfactory projection neuron dendrite targeting via the transcription factor Prospero. *The Journal of neuroscience : the official journal of the Society for Neuroscience* **30**, 9939-9946.

Tedesco, F. S., Hoshiya, H., D'Antona, G., Gerli, M. F., Messina, G., Antonini, S., Tonlorenzi, R., Benedetti, S., Berghella, L., Torrente, Y. et al. (2011). Stem cell-mediated transfer of a human artificial chromosome ameliorates muscular dystrophy. *Science translational medicine* **3**, 96ra78.

Tinsley, J., Deconinck, N., Fisher, R., Kahn, D., Phelps, S., Gillis, J. M. and Davies, K. (1998). Expression of full-length utrophin prevents muscular dystrophy in mdx mice. *Nature medicine* **4**, 1441-1444.

Trivedi, C. M., Luo, Y., Yin, Z., Zhang, M., Zhu, W., Wang, T., Floss, T., Goettlicher, M., Noppinger, P. R., Wurst, W. et al. (2007). Hdac2 regulates the cardiac hypertrophic response by modulating Gsk3 beta activity. *Nature medicine* **13**, 324-331.

Tskhovrebova, L. and Trinick, J. (2010). Roles of titin in the structure and elasticity of the sarcomere. *Journal of biomedicine & biotechnology* **2010**, 612482.

Van Brocklyn, J. R., Graler, M. H., Bernhardt, G., Hobson, J. P., Lipp, M. and Spiegel, S. (2000). Sphingosine-1-phosphate is a ligand for the G protein-coupled receptor EDG-6. *Blood* **95**, 2624-2629.

Venkataraman, K., Thangada, S., Michaud, J., Oo, M. L., Ai, Y., Lee, Y. M., Wu, M., Parikh, N. S., Khan, F., Proia, R. L. et al. (2006). Extracellular export of sphingosine kinase-1a contributes to the vascular S1P gradient. *The Biochemical journal* **397**, 461-471.

Vojinovic, J. and Damjanov, N. (2011). HDAC inhibition in rheumatoid arthritis and juvenile idiopathic arthritis. *Mol Med* **17**, 397-403.

von Maltzahn, J., Bentzinger, C. F. and Rudnicki, M. A. (2012a). Wnt7a-Fzd7 signalling directly activates the Akt/mTOR anabolic growth pathway in skeletal muscle. *Nature cell biology* **14**, 186-191.

von Maltzahn, J., Renaud, J. M., Parise, G. and Rudnicki, M. A. (2012b). Wnt7a treatment ameliorates muscular dystrophy. *Proceedings of the National Academy of Sciences of the United States of America* **109**, 20614-20619.

Walzer, T., Chiossone, L., Chaix, J., Calver, A., Carozzo, C., Garrigue-Antar, L., Jacques, Y., Baratin, M., Tomasello, E. and Vivier, E. (2007). Natural killer cell trafficking in vivo requires a dedicated sphingosine 1-phosphate receptor. *Nature immunology* **8**, 1337-1344.

Wang, L., Zhou, L., Jiang, P., Lu, L., Chen, X., Lan, H., Guttridge, D. C., Sun, H. and Wang, H. (2012). Loss of miR-29 in myoblasts contributes to dystrophic muscle pathogenesis. *Molecular therapy : the journal of the American Society of Gene Therapy* **20**, 1222-1233.

Wang, Y. and Pessin, J. E. (2013). Mechanisms for fiber-type specificity of skeletal muscle atrophy. *Current opinion in clinical nutrition and metabolic care* **16**, 243-250.

Wang, Z., Storb, R., Halbert, C. L., Banks, G. B., Butts, T. M., Finn, E. E., Allen, J. M., Miller, A. D., Chamberlain, J. S. and Tapscott, S. J. (2012). Successful regional delivery and long-term expression of a dystrophin gene in canine muscular dystrophy: a preclinical model for human therapies. *Molecular therapy : the journal of the American Society of Gene Therapy* **20**, 1501-1507.

Wang, Z., Zang, C., Rosenfeld, J. A., Schones, D. E., Barski, A., Cuddapah, S., Cui, K., Roh, T. Y., Peng, W., Zhang, M. Q. et al. (2008). Combinatorial patterns of histone acetylations and methylations in the human genome. *Nature genetics* **40**, 897-903.

Webster, C., Silberstein, L., Hays, A. P. and Blau, H. M. (1988). Fast muscle fibers are preferentially affected in Duchenne muscular dystrophy. *Cell* **52**, 503-513.

Wehling, M., Spencer, M. J. and Tidball, J. G. (2001). A nitric oxide synthase transgene ameliorates muscular dystrophy in mdx mice. *The Journal of cell biology* **155**, 123-131.

Werner, P. (2004). Color Atlas of Human Anatomy, Vol. 1, Locomotor System: Thieme.

Wu, H., Naya, F. J., McKinsey, T. A., Mercer, B., Shelton, J. M., Chin, E. R., Simard, A. R., Michel, R. N., Bassel-Duby, R., Olson, E. N. et al. (2000). MEF2 responds to multiple calcium-regulated signals in the control of skeletal muscle fiber type. *The EMBO journal* **19**, 1963-1973.

Wu, H., Rothermel, B., Kanatous, S., Rosenberg, P., Naya, F. J., Shelton, J. M., Hutcheson, K. A., DiMaio, J. M., Olson, E. N., Bassel-Duby, R. et al. (2001). Activation of MEF2 by muscle activity is mediated through a calcineurin-dependent pathway. *The EMBO journal* **20**, 6414-6423.

Wu, M., Neilson, A., Swift, A. L., Moran, R., Tamagnine, J., Parslow, D., Armistead, S., Lemire, K., Orrell, J., Teich, J. et al. (2007). Multiparameter metabolic analysis reveals a close link between attenuated mitochondrial bioenergetic function and enhanced glycolysis dependency in human tumor cells. *American journal of physiology. Cell physiology* **292**, C125-136.

Yamazaki, Y., Kon, J., Sato, K., Tomura, H., Sato, M., Yoneya, T., Okazaki, H., Okajima, F. and Ohta, H. (2000). Edg-6 as a putative sphingosine 1-phosphate receptor coupling to Ca(2+) signaling pathway. *Biochemical and biophysical research communications* **268**, 583-589.

Yang, X. J. and Seto, E. (2007). HATs and HDACs: from structure, function and regulation to novel strategies for therapy and prevention. *Oncogene* **26**, 5310-5318.

Zubrzycka-Gaarn, E. E., Bulman, D. E., Karpati, G., Burghes, A. H., Belfall, B., Klamut, H. J., Talbot, J., Hodges, R. S., Ray, P. N. and Worton, R. G. (1988). The Duchenne muscular dystrophy gene product is localized in sarcolemma of human skeletal muscle. *Nature* **333**, 466-469.

Figure 1

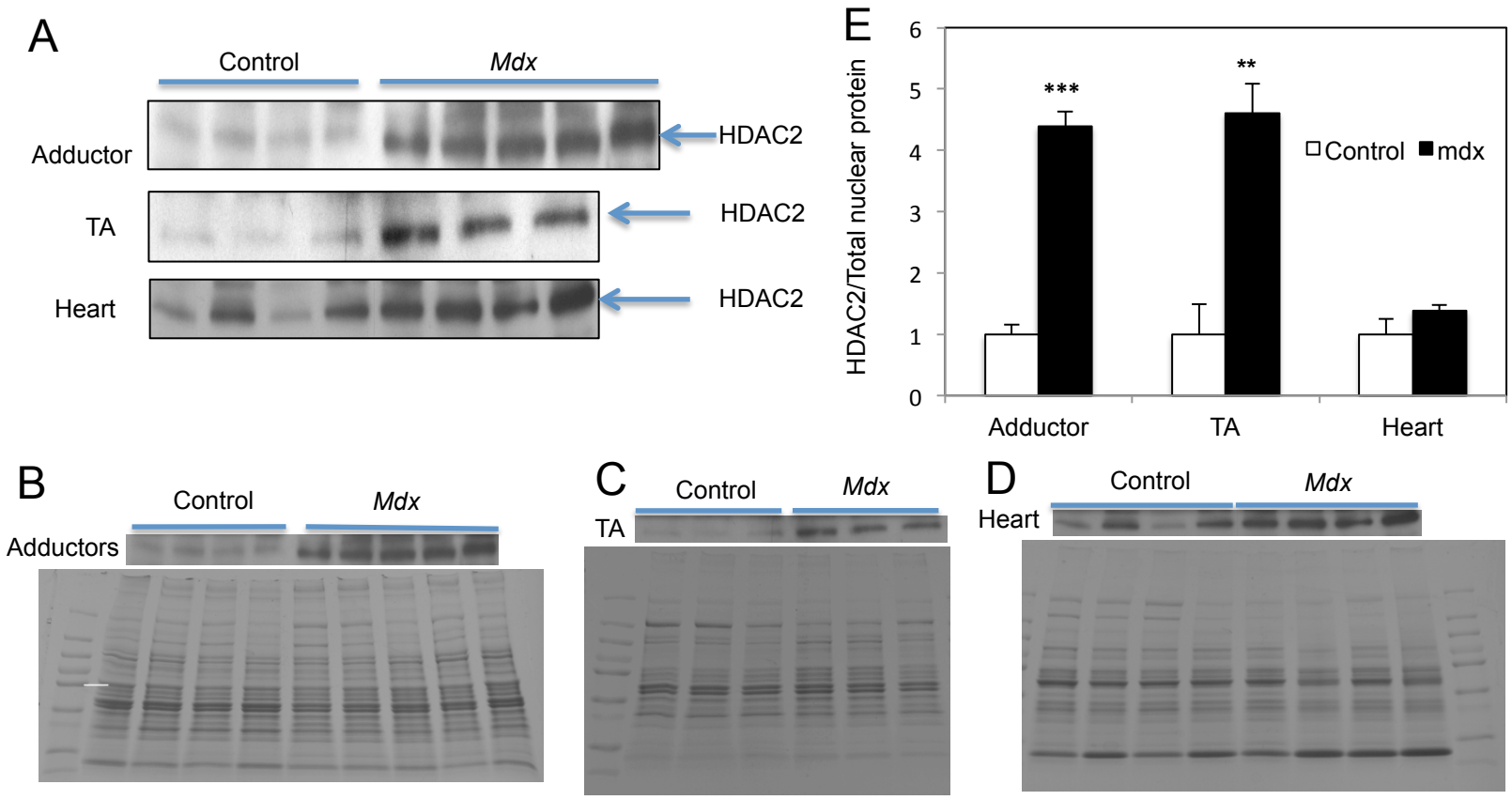
A
Control
Mdx
Adductor
TA
Heart
HDAC2
HDAC2
HDAC2
E
HDAC2/Total nuclear protein
6
5
4
3
2
1
0
***
**
Control
mdx
Adductor
TA
Heart
B
Control
Mdx
Adductors
C
Control
Mdx
TA
D
Control
Mdx
Heart

Figure 2

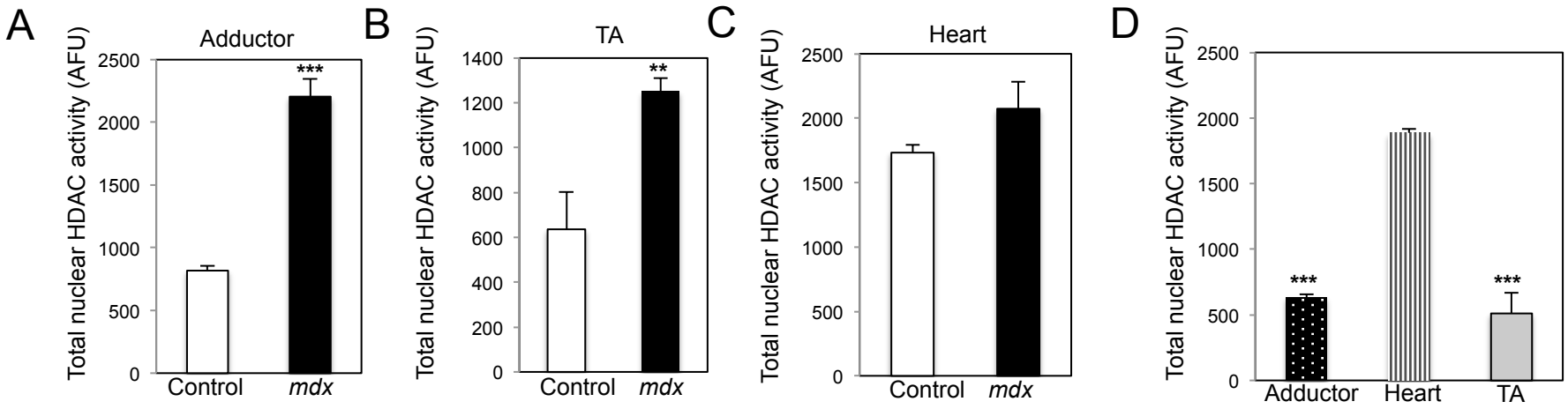
A
Adductor
Total nuclear HDAC activity (AFU)
2500
2000
1500
1000
500
0
***
Control
mdx
B
TA
Total nuclear HDAC activity (AFU)
1400
1200
1000
800
600
400
200
0
**
Control
mdx
C
Heart
Total nuclear HDAC activity (AFU)
2500
2000
1500
1000
500
0
Control
mdx
D
Total nuclear HDAC activity (AFU)
2500
2000
1500
1000
500
0
***
***
Adductor
Heart
TA

Figure 3

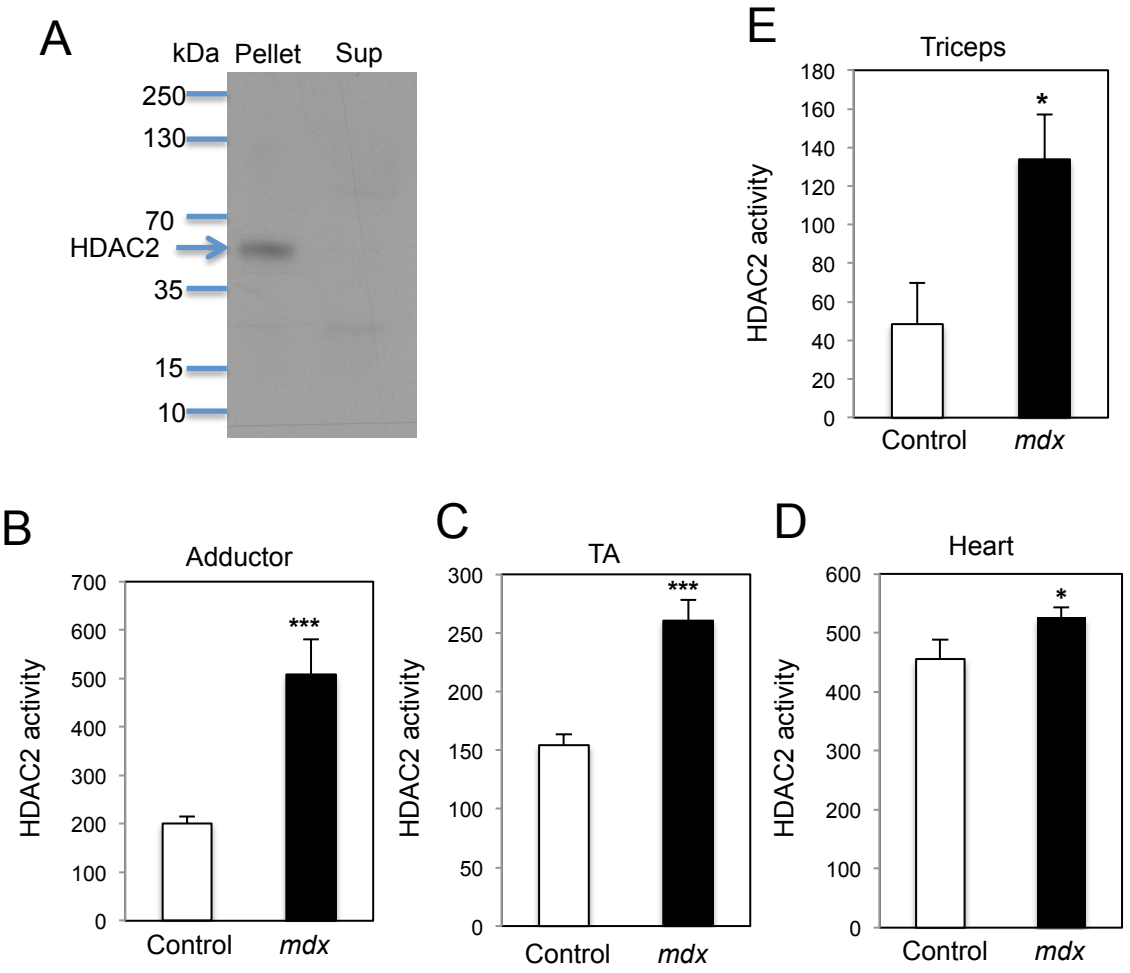
A
kDa
Pellet
Sup
250
130
70
HDAC2
35
15
10
B
Adductor
HDAC2 activity
700
600
500
400
300
200
100
0
***
Control
mdx
C
TA
HDAC2 activity
300
250
200
150
100
50
0
***
Control
mdx
D
Heart
HDAC2 activity
600
500
400
300
200
100
0
*
Control
mdx
E
Triceps
HDAC2 activity
180
160
140
120
100
80
60
40
20
0
*
Control
mdx

Figure 4

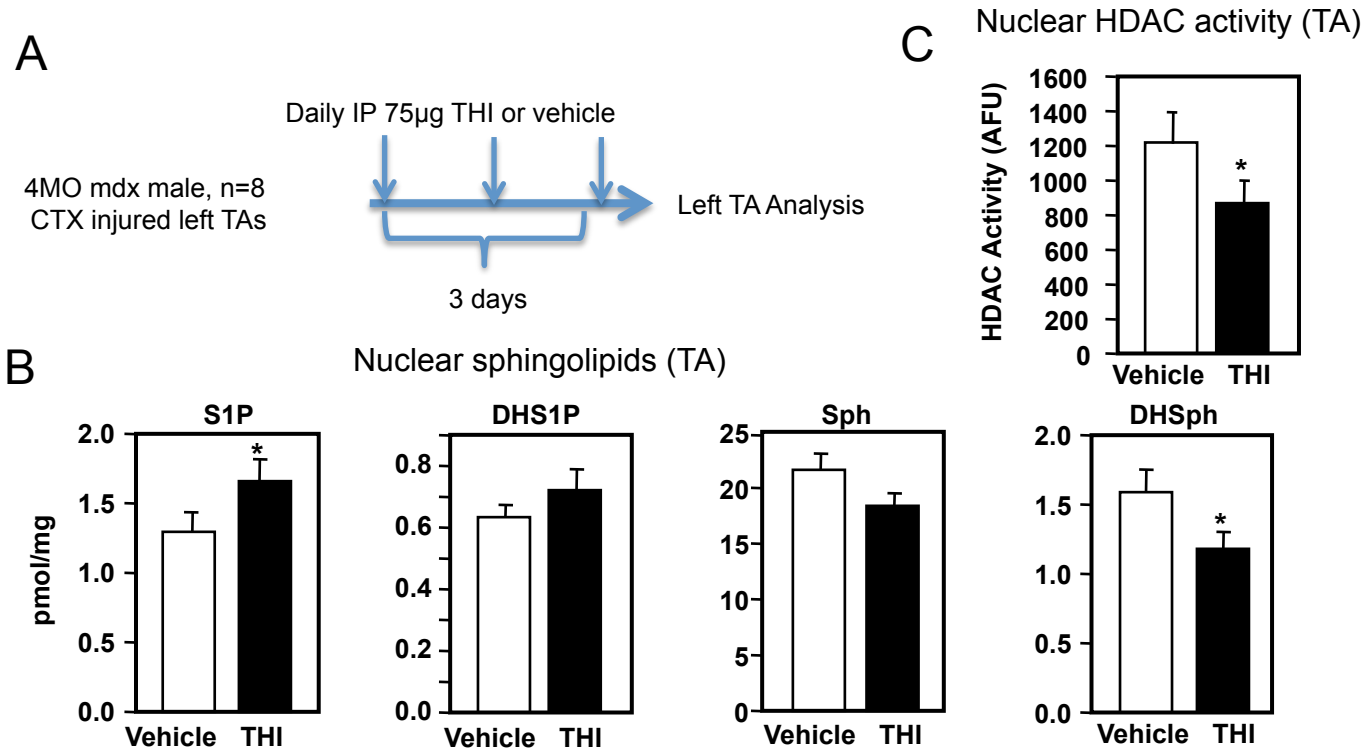
A
Daily IP 75µg THI or vehicle
4MO mdx male, n=8
CTX injured left TAs
Left TA Analysis
3 days
B
Nuclear sphingolipids (TA)
S1P
DHS1P
Sph
DHSph
pmol/mg
Vehicle
THI
C
Nuclear HDAC activity (TA)
HDAC Activity (AFU)
Vehicle
THI

Figure 5

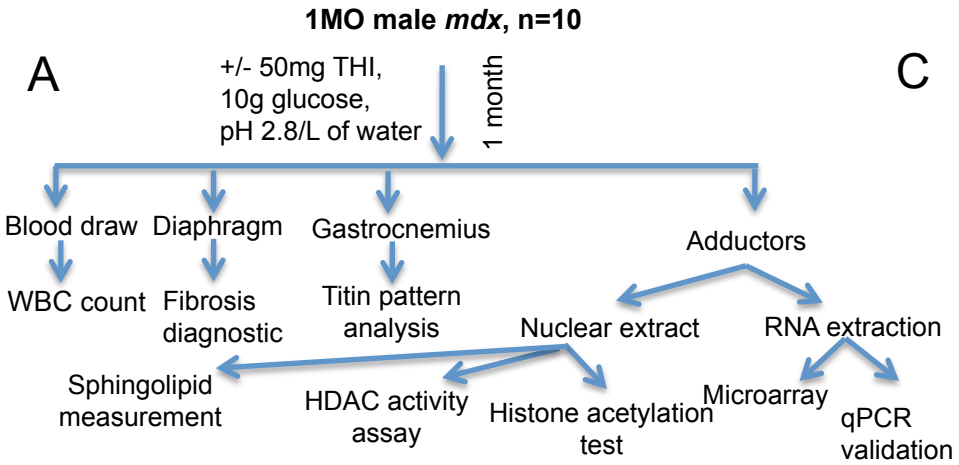
1MO male mdx, n=10
A
+/- 50mg THI,
10g glucose,
pH 2.8/L of water
1 month
Blood draw
Diaphragm
Gastrocnemius
Adductors
WBC count
Fibrosis diagnostic
Titin pattern analysis
Nuclear extract
RNA extraction
Sphingolipid measurement
HDAC activity assay
Histone acetylation test
Microarray
qPCR validation

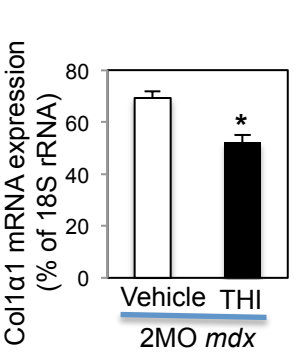
C
Col1α1 mRNA expression (% of 18S rRNA)
80
60
40
20
0
*
Vehicle
THI
2MO mdx

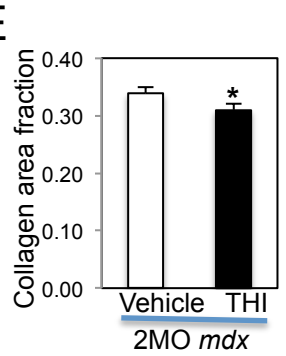
E
Collagen area fraction
0.40
0.30
0.20
0.10
0.00
*
Vehicle
THI
2MO mdx

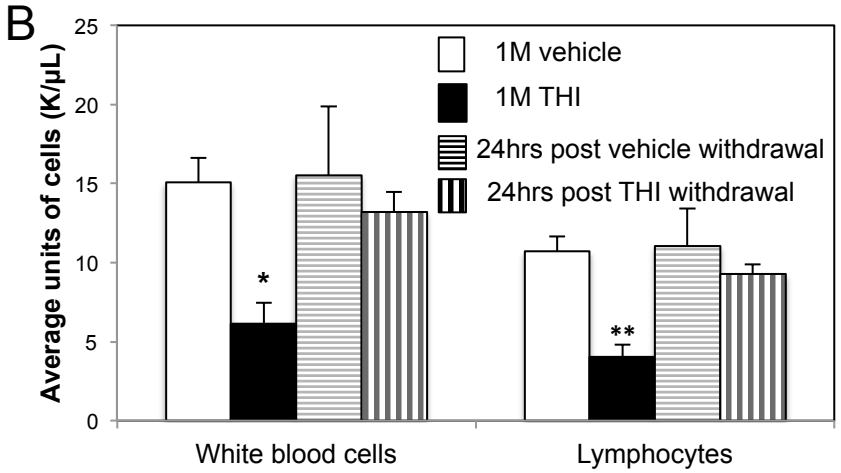
B
Average units of cells (K/μL)
25
20
15
10
5
0
1M vehicle
1M THI
24hrs post vehicle withdrawal
24hrs post THI withdrawal
*
**
White blood cells
Lymphocytes

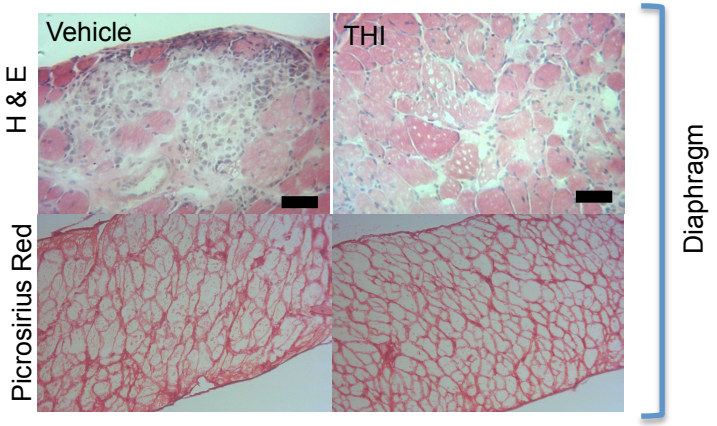
D
Vehicle
THI
H & E
Picrosirius Red
Diaphragm

Figure 6

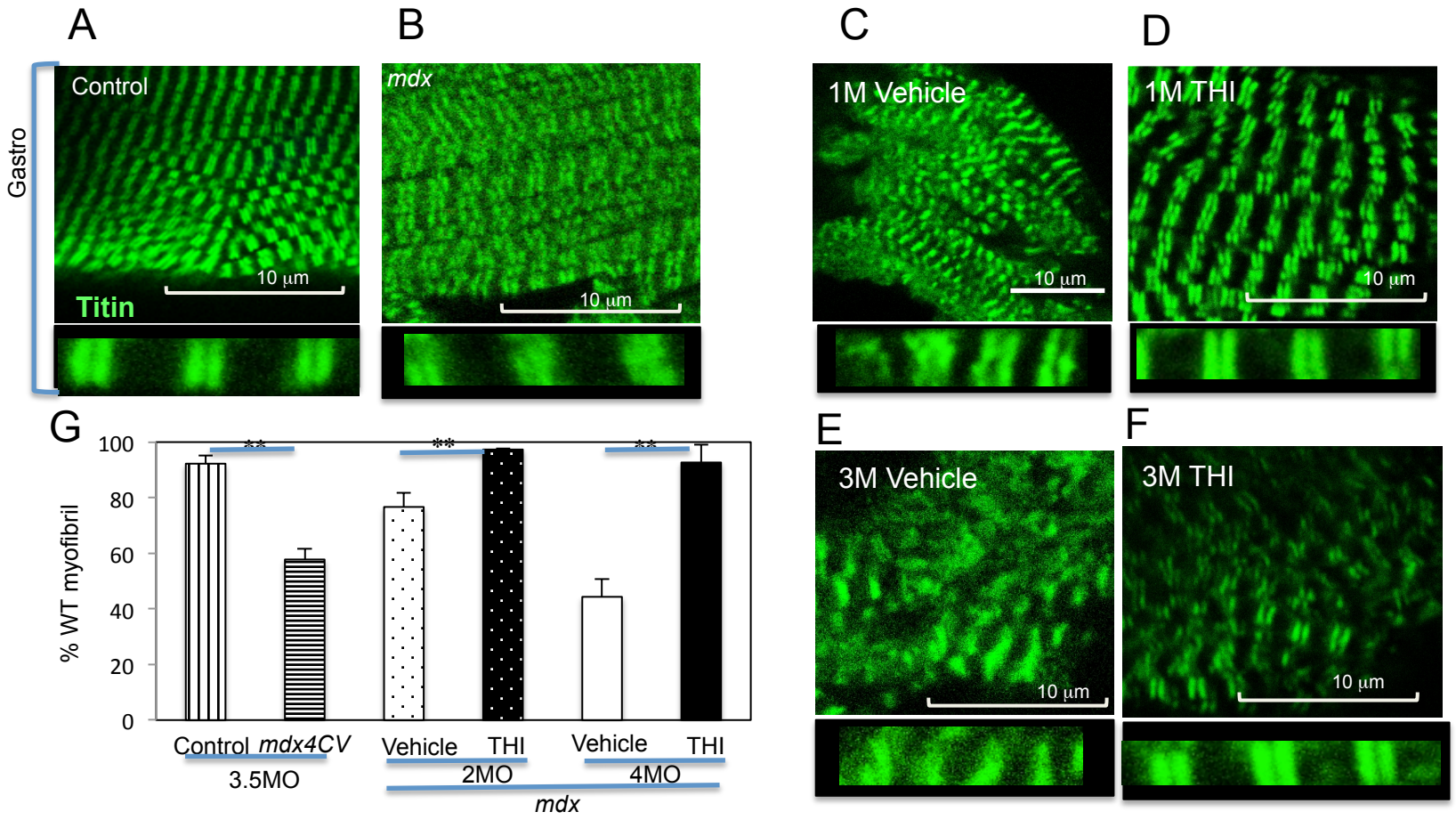
A
B
C
D
Gastro
Control
mdx
1M Vehicle
1M THI
10 μm
Titin
G
E
F
3M Vehicle
3M THI
% WT myofibril
100
80
60
40
20
0
**
Control
mdx4CV
Vehicle
THI
Vehicle
THI
3.5MO
2MO
4MO
mdx

Figure 7

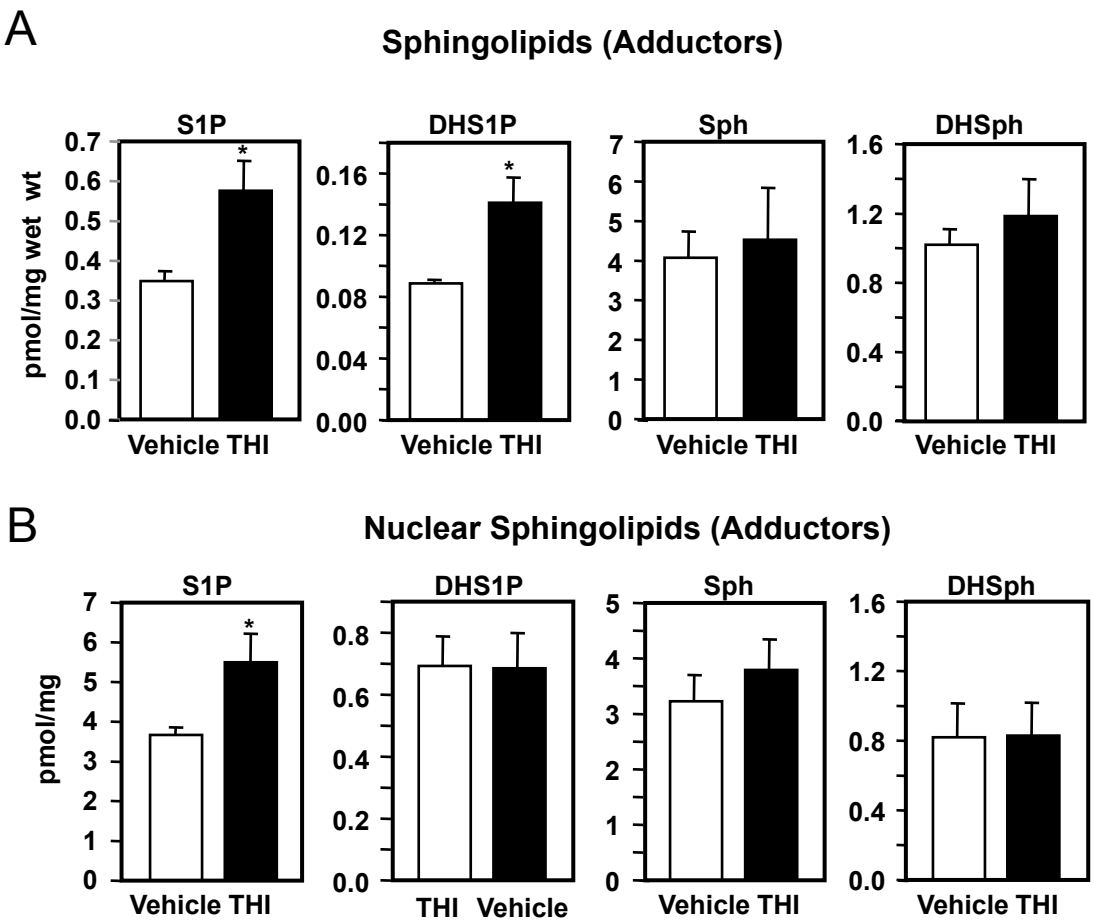
A
Sphingolipids (Adductors)
S1P
DHS1P
Sph
DHSph
pmol/mg wet wt
0.7
0.6
0.5
0.4
0.3
0.2
0.1
0.0
0.16
0.12
0.08
0.04
0.00
7
6
5
4
3
2
1
0
1.6
1.2
0.8
0.4
0.0
*
Vehicle THI
B
Nuclear Sphingolipids (Adductors)
S1P
DHS1P
Sph
DHSph
pmol/mg
7
6
5
4
3
2
1
0
0.8
0.6
0.4
0.2
0.0
1.6
1.2
0.8
0.4
0.0
*
Vehicle THI
THI Vehicle

Figure 8

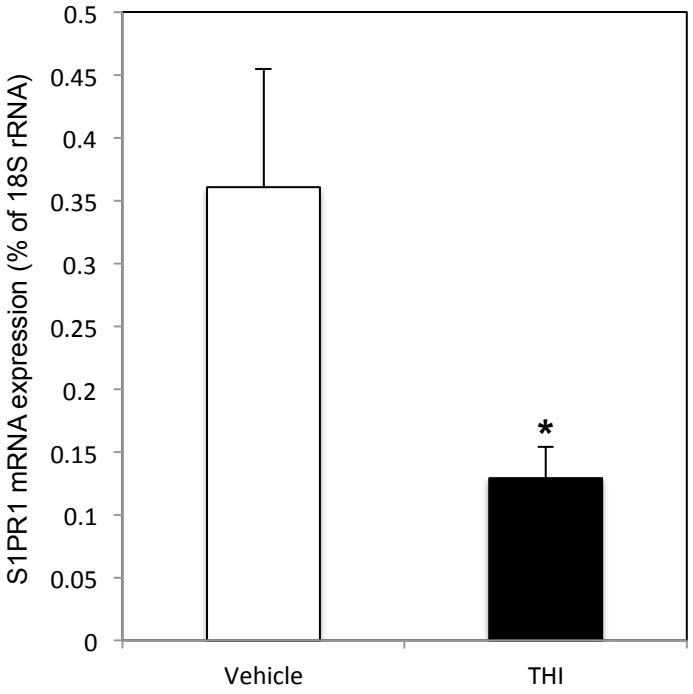
S1PR1 mRNA expression (% of 18S rRNA)
0.5
0.45
0.4
0.35
0.3
0.25
0.2
0.15
0.1
0.05
0
*
Vehicle
THI

Figure 9

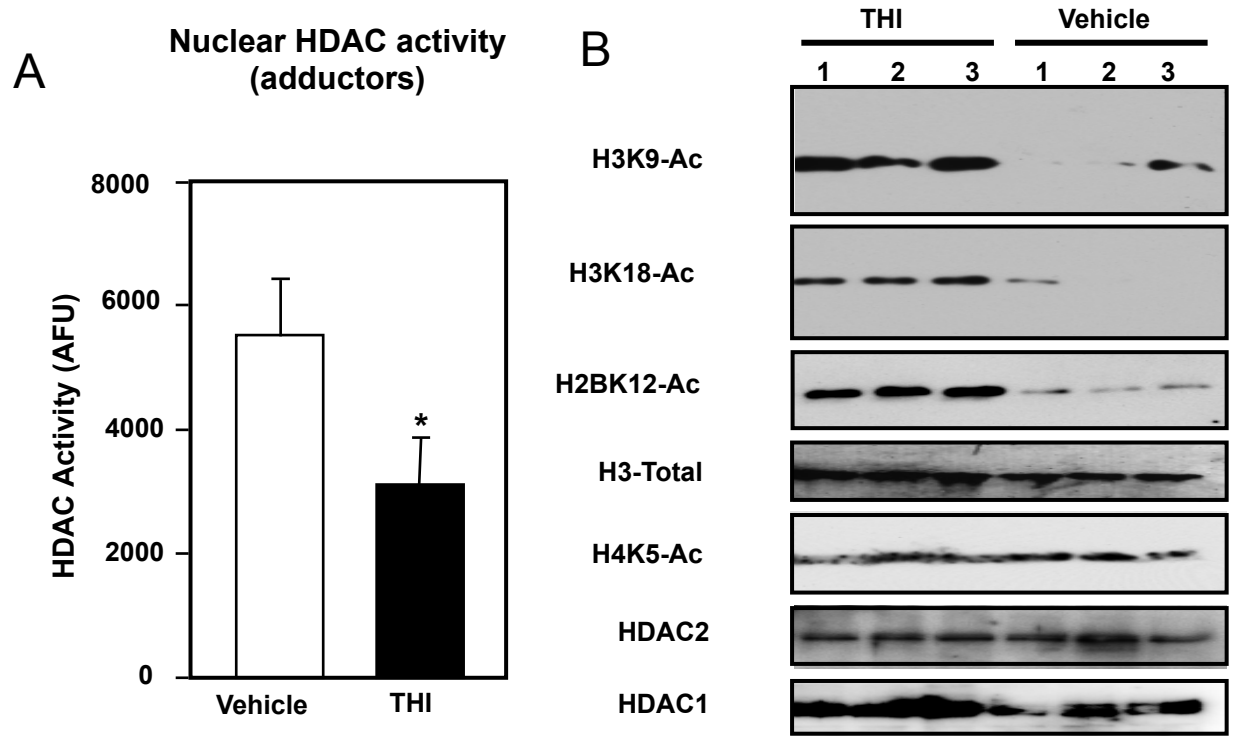
A
Nuclear HDAC activity
(adductors)
HDAC Activity (AFU)
8000
6000
4000
2000
0
*
Vehicle
THI
B
THI
Vehicle
1
2
3
1
2
3
H3K9-Ac
H3K18-Ac
H2BK12-Ac
H3-Total
H4K5-Ac
HDAC2
HDAC1

Figure 10

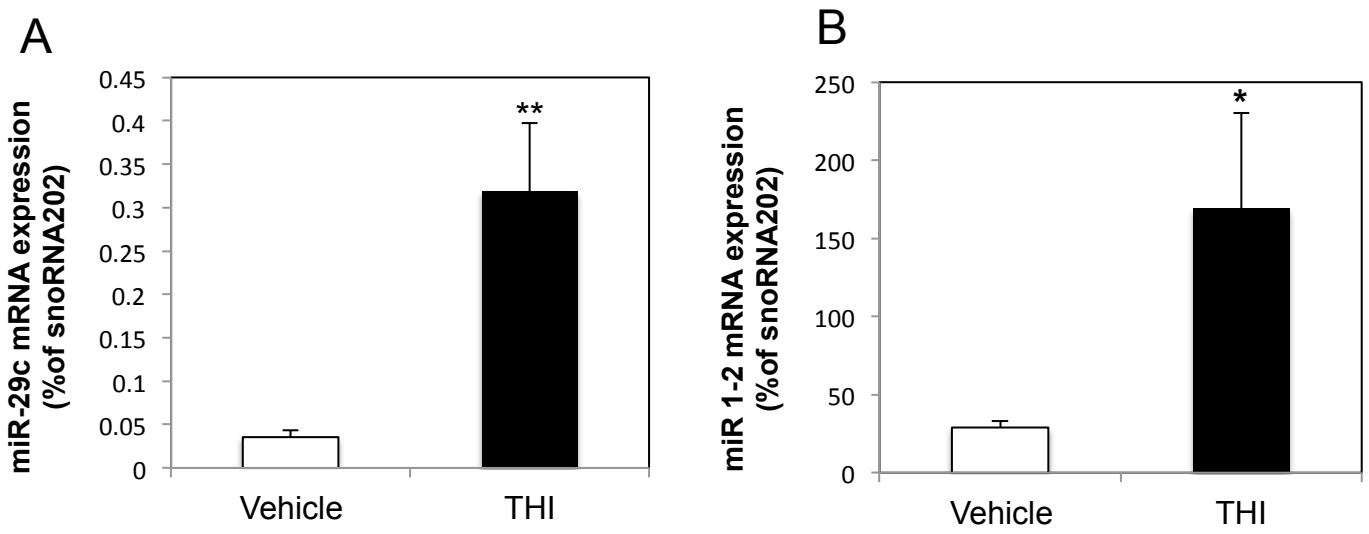
A
miR-29c mRNA expression (%of snoRNA202)
0.45
0.4
0.35
0.3
0.25
0.2
0.15
0.1
0.05
0
**
Vehicle
THI
B
miR 1-2 mRNA expression (%of snoRNA202)
250
200
150
100
50
0
*
Vehicle
THI

Figure 11

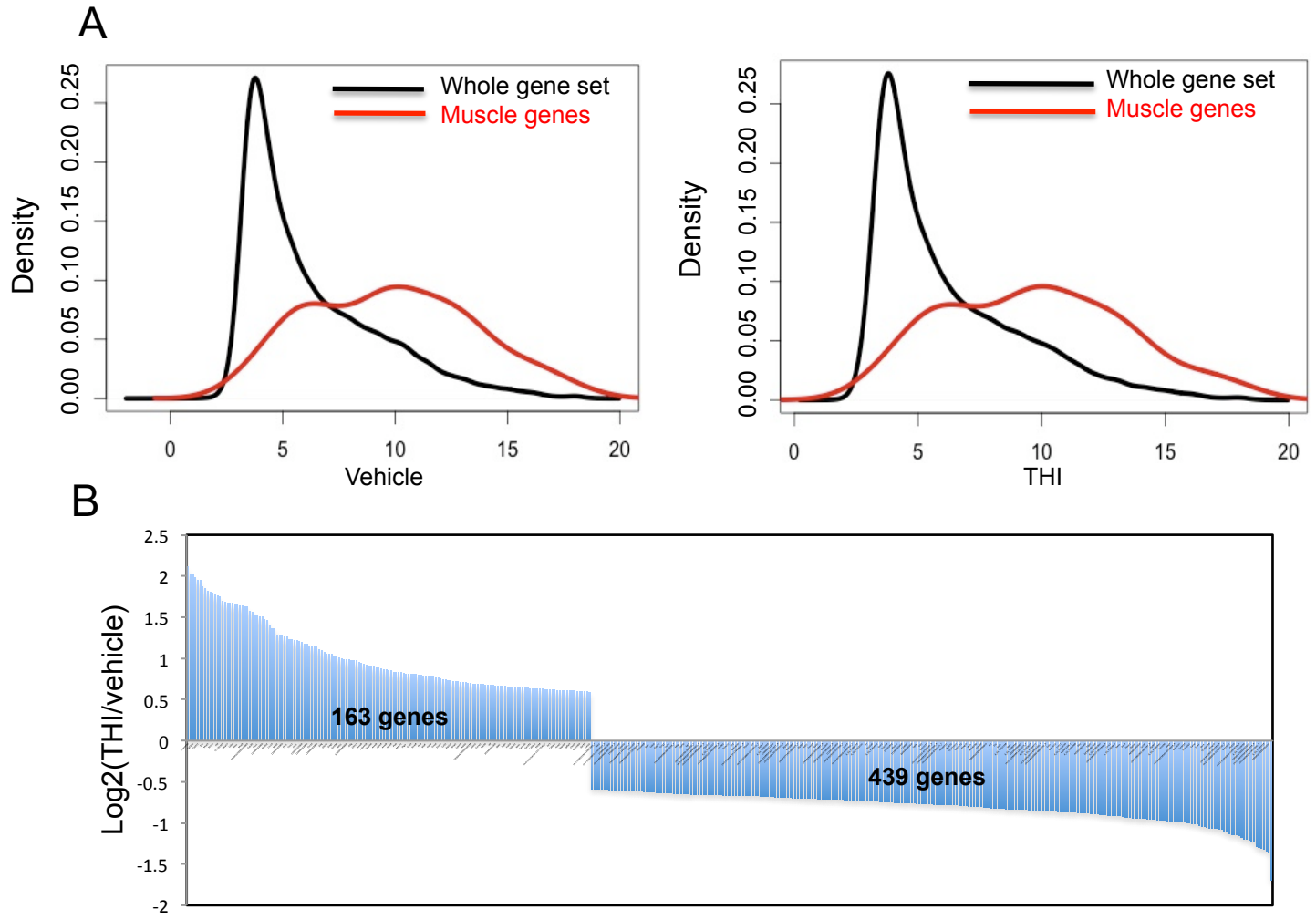
A
Density
0.00 0.05 0.10 0.15 0.20 0.25
Whole gene set
Muscle genes
0 5 10 15 20
Vehicle
Density
0.00 0.05 0.10 0.15 0.20 0.25
Whole gene set
Muscle genes
0 5 10 15 20
THI
B
Log2(THI/vehicle)
2.5 2 1.5 1 0.5 0 -0.5 -1 -1.5 -2
163 genes
439 genes

Figure 12

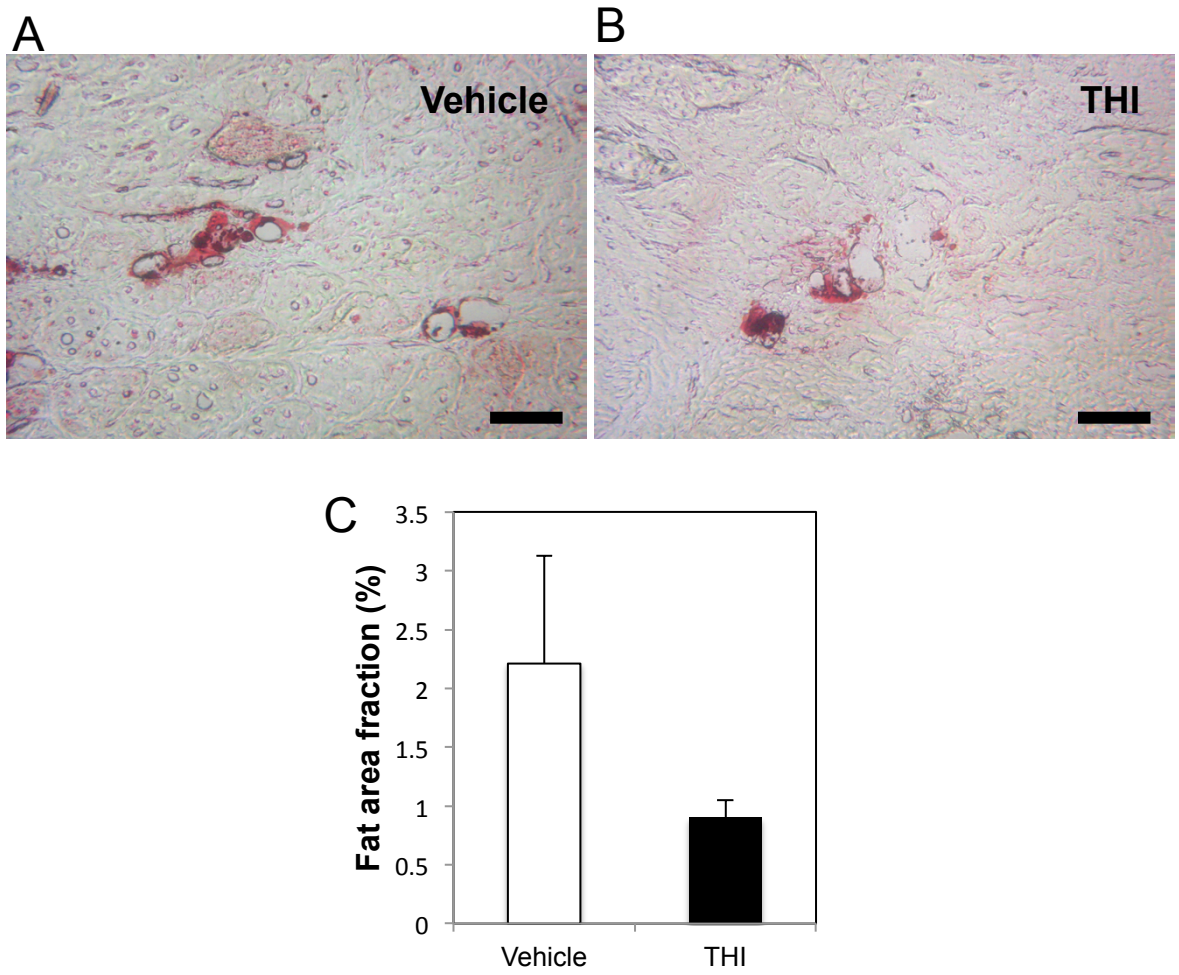
A
Vehicle
B
THI
C
Fat area fraction (%)
3.5
3
2.5
2
1.5
1
0.5
0
Vehicle
THI

Table 1: Genes down-regulated in THI treated adductor muscles

Function	FDR	Coverage
Query genes	N/A	124/124
Spindle	1.38e-4	10 / 131
Condensed chromosome	1.48e-4	9 / 105
M phase	4.04e-4	12 / 268
Cell division	4.04e-4	9 / 126
Cytokinesis	8.09e-4	7 / 69
M phase of mitotic cell cycle	8.2e-3	8 / 142
Vesicular fraction	1.69e-2	10 / 271
Chromosome Condensation	2.33e-2	4 / 22
Cell cycle cytokinesis	4.85e-2	4 / 27
Microsome	6.28e-2	9 / 262
Mitotic chromosome Condensation	6.95e-2	3 / 11
Condensed nuclear chromosome	8.21e-2	5 / 65
Chromosome segregation	8.53e-2	6 / 109

Genes over-expressed in THI treated adductor muscles

Function	FDR	Coverage
Query genes	n/a	122 / 122
Fat cell differentiation	1.8e-9	13 / 108
Brown fat cell differentiation	4.01e-8	8 / 28
Triglyceride metabolic process	9.87e-4	7 / 66
Response to peptide hormone stimulus	2.02e-3	9 / 167
Neutral lipid metabolic process	2.02e-3	7 / 79
Organic ether metabolic process	2.02e-3	7 / 83
Glycerol ether metabolic process	2.02e-3	7 / 81
Acylglycerol metabolic process	2.02e-3	7 / 77
Lipid particle	2.11e-3	4 / 13
Negative regulation of multicellular organismal process	2.27e-2	10 / 292
Negative regulation of smooth muscle cell migration	5.07e-2	3 / 10
Blood circulation	7.23e-2	9 / 279
Circulatory system process	7.23e-2	9 / 281

False discovery rate (FDR)
Coverage: (number of genes in the net work with a given function)/(all genes in the genome with the function

Figure 13

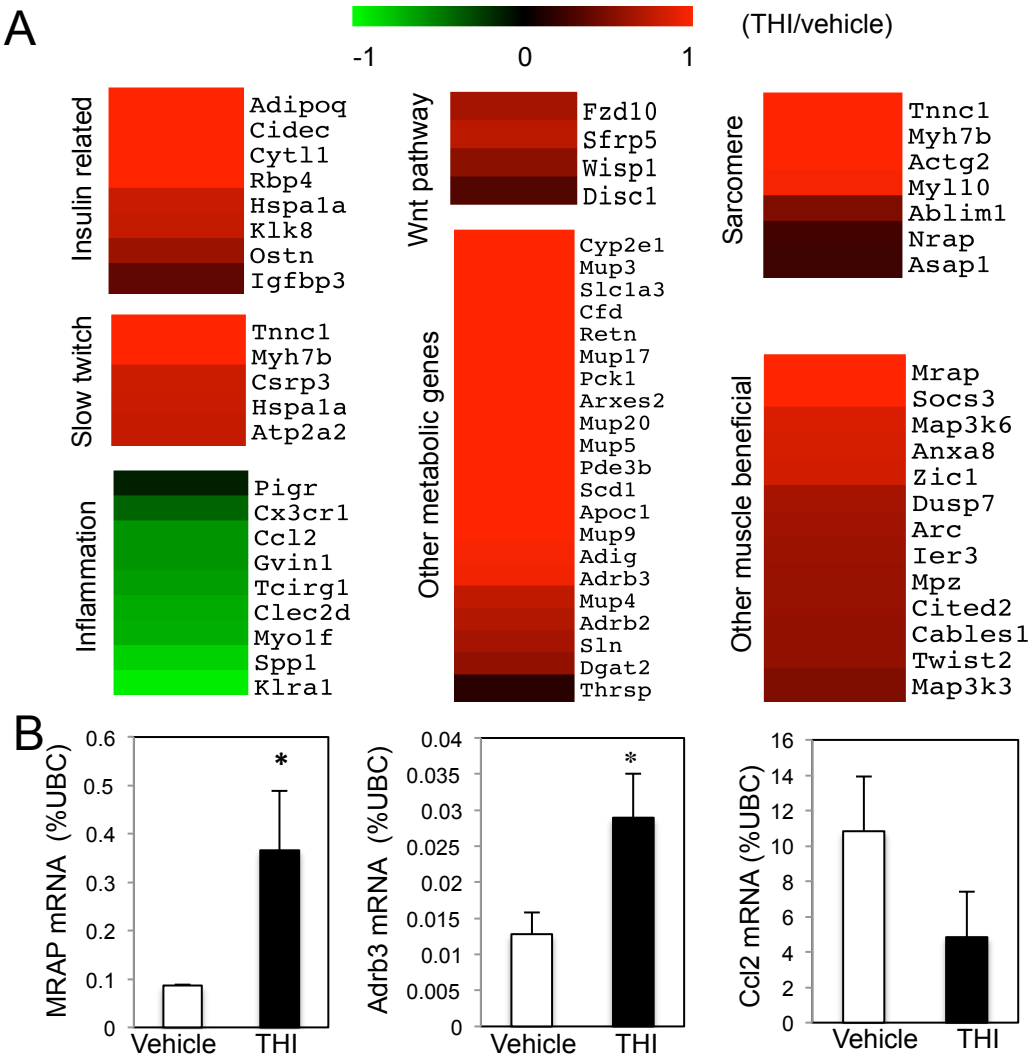
A
-1
0
1
(THI/vehicle)
Insulin related
Adipoq
Cidec
Cytl1
Rbp4
Hspa1a
Klk8
Ostn
Igfbp3
Slow twitch
Tnnc1
Myh7b
Csrp3
Hspa1a
Atp2a2
Inflammation
Pigr
Cx3cr1
Ccl2
Gvin1
Tcirg1
Clec2d
Myo1f
Spp1
Klra1
Wnt pathway
Fzd10
Sfrp5
Wisp1
Disc1
Other metabolic genes
Cyp2e1
Mup3
Slc1a3
Cfd
Retn
Mup17
Pck1
Arxes2
Mup20
Mup5
Pde3b
Scd1
Apoc1
Mup9
Adig
Adrb3
Mup4
Adrb2
Sln
Dgat2
Thrsp
Sarcomere
Tnnc1
Myh7b
Actg2
Myl10
Ablim1
Nrap
Asap1
Other muscle beneficial
Mrap
Socs3
Map3k6
Anxa8
Zic1
Dusp7
Arc
Ier3
Mpz
Cited2
Cables1
Twist2
Map3k3
B
MRAP mRNA (%UBC)
0.6
0.5
0.4
0.3
0.2
0.1
0
*
Vehicle
THI
Adrb3 mRNA (%UBC)
0.04
0.035
0.03
0.025
0.02
0.015
0.01
0.005
0
*
Vehicle
THI
Ccl2 mRNA (%UBC)
16
14
12
10
8
6
4
2
0
Vehicle
THI

Figure 14

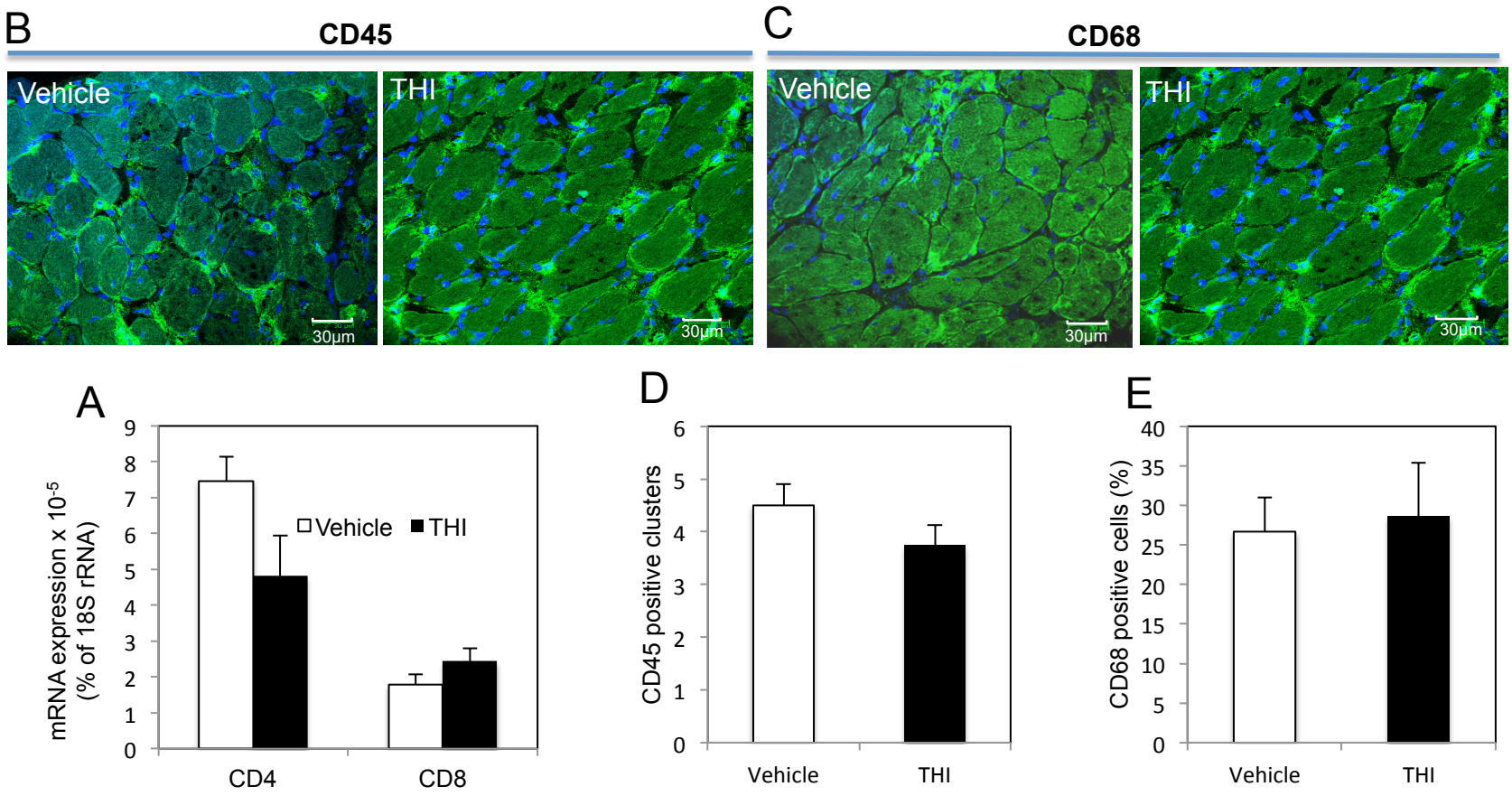
B
CD45
Vehicle
THI
30µm
C
CD68
Vehicle
THI
30µm
A
mRNA expression x 10-5 (% of 18S rRNA)
Vehicle
THI
CD4
CD8
D
CD45 positive clusters
Vehicle
THI
E
CD68 positive cells (%)
Vehicle
THI

Figure 15

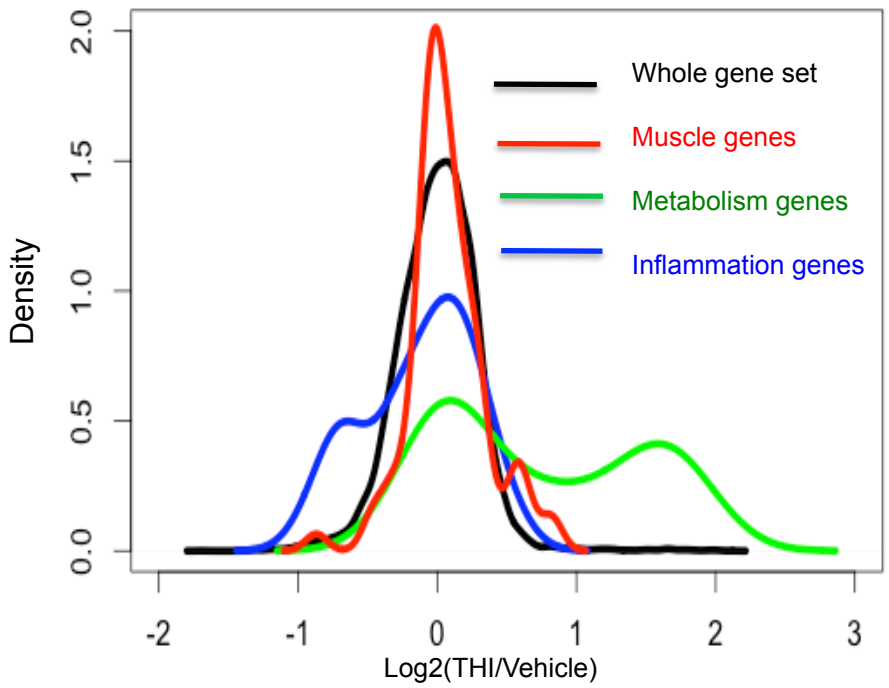
Density
0.0
0.5
1.0
1.5
2.0
-2
-1
0
1
2
3
Log2(THI/Vehicle)
Whole gene set
Muscle genes
Metabolism genes
Inflammation genes

Figure 16

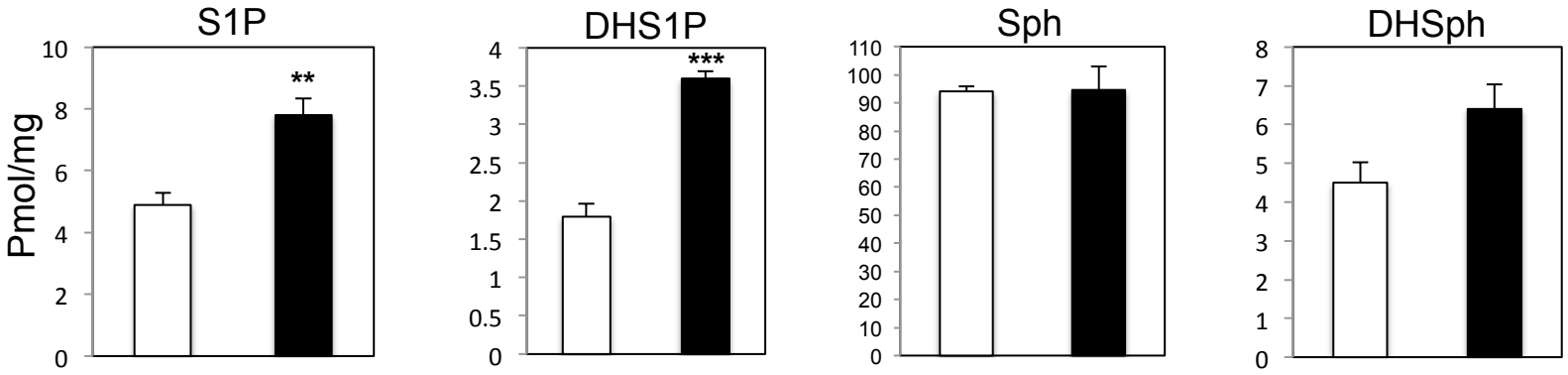
S1P
DHS1P
Sph
DHSph
Pmol/mg
**
***
0
2
4
6
8
10
0
0.5
1
1.5
2
2.5
3
3.5
4
0
10
20
30
40
50
60
70
80
90
100
110
0
1
2
3
4
5
6
7
8

Figure 17

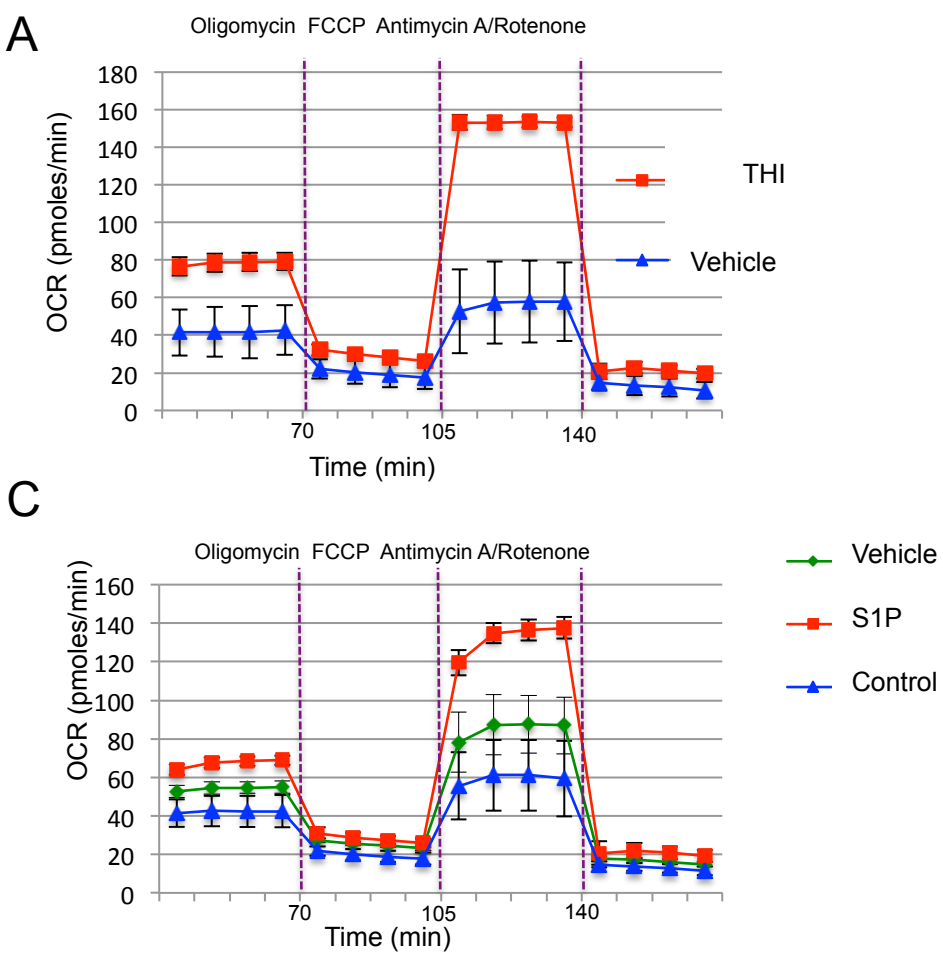
A
Oligomycin FCCP Antimycin A/Rotenone
OCR (pmoles/min)
180
160
140
120
100
80
60
40
20
0
70
105
140
Time (min)
THI
Vehicle
B
OCR (pmoles/min)
200
180
160
140
120
100
80
60
40
20
0
**
THI
Vehicle
C
Oligomycin FCCP Antimycin A/Rotenone
OCR (pmoles/min)
160
140
120
100
80
60
40
20
0
70
105
140
Time (min)
Vehicle
S1P
Control
D
OCR (pmoles/min)
140
120
100
80
60
40
20
0
*
S1P
Vehicle
Control

Figure 18

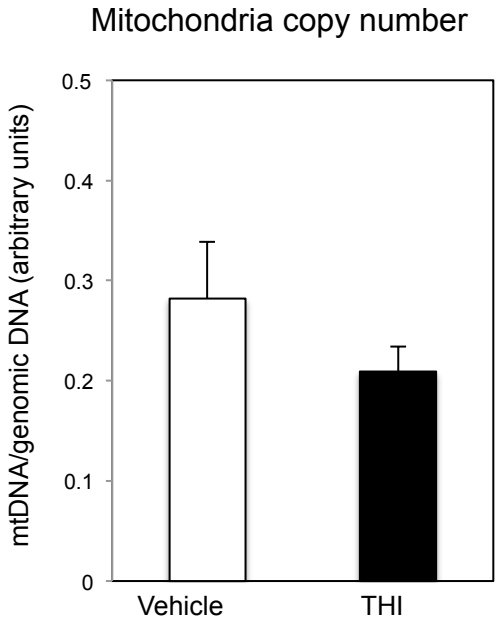
Mitochondria copy number
mtDNA/genomic DNA (arbitrary units)
0.5
0.4
0.3
0.2
0.1
0
Vehicle
THI

Figure 19

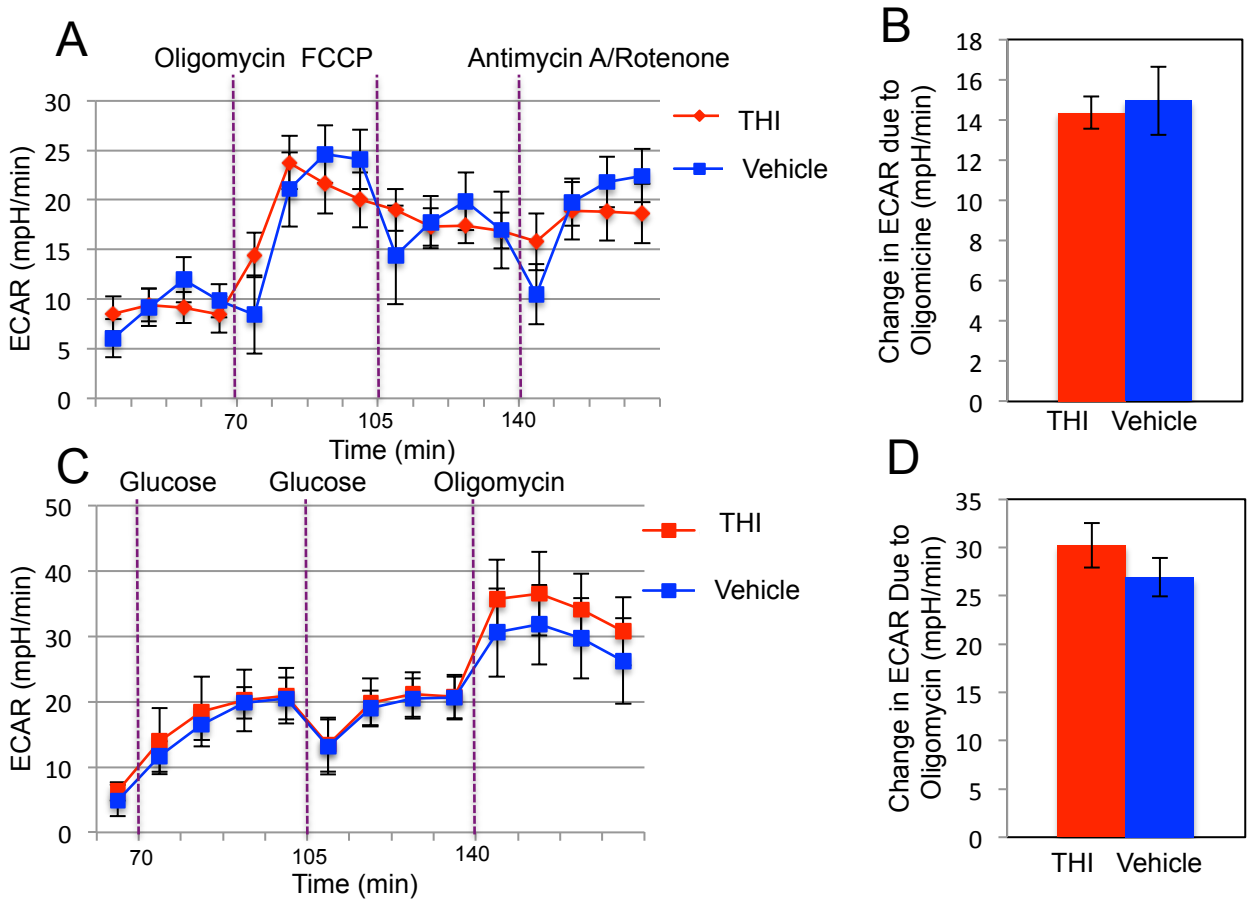
A
Oligomycin
FCCP
Antimycin A/Rotenone
ECAR (mpH/min)
Time (min)
THI
Vehicle
B
Change in ECAR due to Oligomicine (mpH/min)
THI
Vehicle
C
Glucose
Glucose
Oligomycin
ECAR (mpH/min)
Time (min)
THI
Vehicle
D
Change in ECAR Due to Oligomycin (mpH/min)
THI
Vehicle

Figure 19

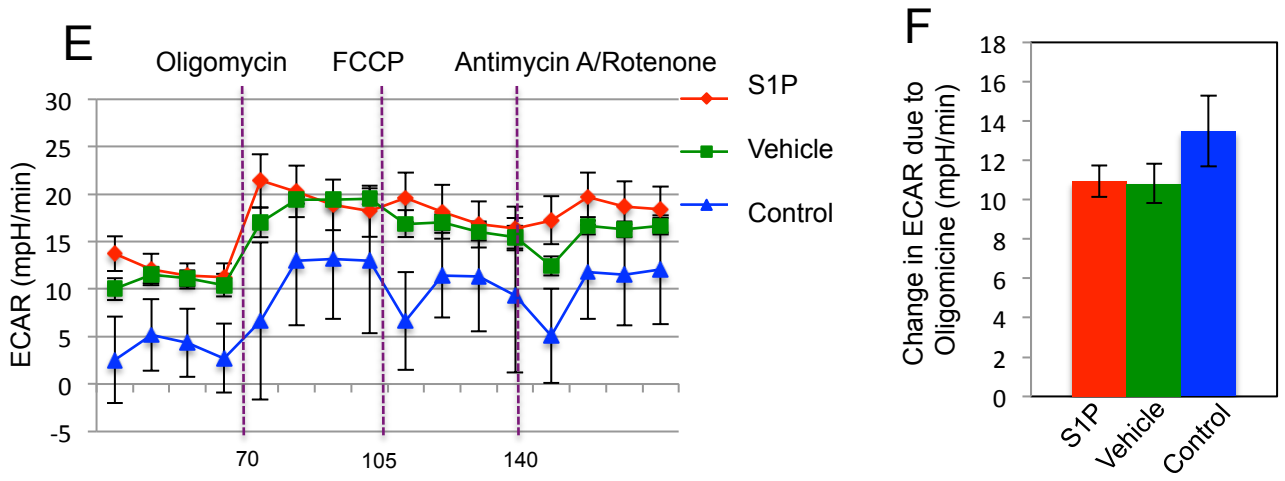
E
Oligomycin
FCCP
Antimycin A/Rotenone
S1P
Vehicle
Control
ECAR (mpH/min)
30
25
20
15
10
5
0
-5
70
105
140
F
Change in ECAR due to Oligomicine (mpH/min)
18
16
14
12
10
8
6
4
2
0
S1P
Vehicle
Control

Figure 20

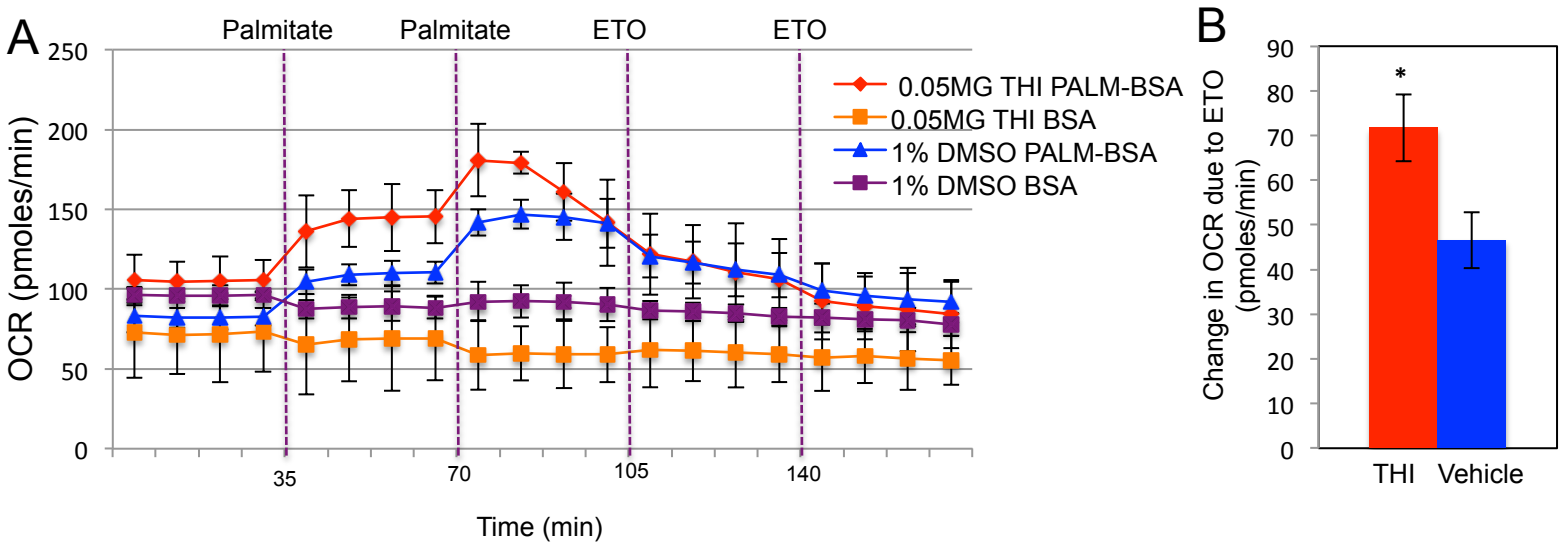
A
Palmitate
Palmitate
ETO
ETO
OCR (pmoles/min)
250
200
150
100
50
0
35
70
105
140
Time (min)
0.05MG THI PALM-BSA
0.05MG THI BSA
1% DMSO PALM-BSA
1% DMSO BSA
B
Change in OCR due to ETO (pmoles/min)
90
80
70
60
50
40
30
20
10
0
*
THI
Vehicle

Figure 21

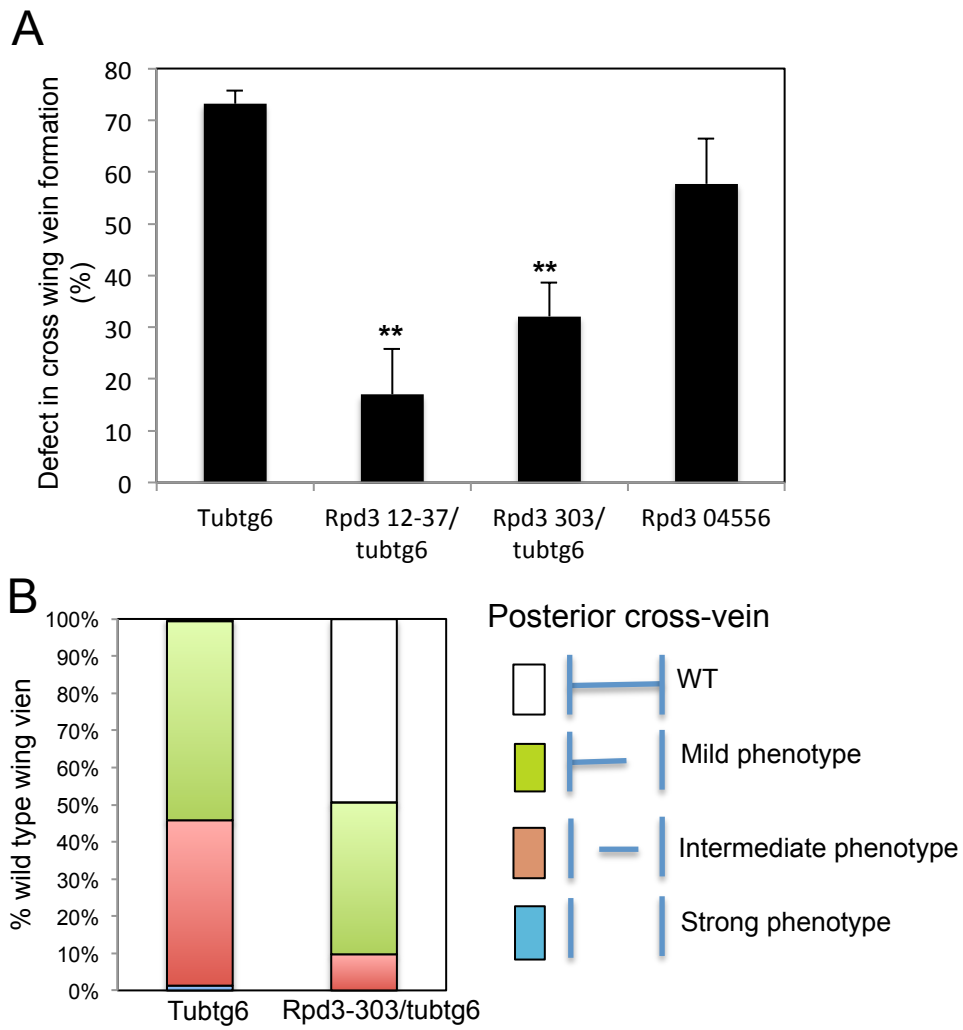
A
Defect in cross wing vein formation (%)
80
70
60
50
40
30
20
10
0
**
**
Tubtg6
Rpd3 12-37/ tubtg6
Rpd3 303/ tubtg6
Rpd3 04556
B
% wild type wing vien
100%
90%
80%
70%
60%
50%
40%
30%
20%
10%
0%
Tubtg6
Rpd3-303/tubtg6
Posterior cross-vein
WT
Mild phenotype
Intermediate phenotype
Strong phenotype

Figure 22

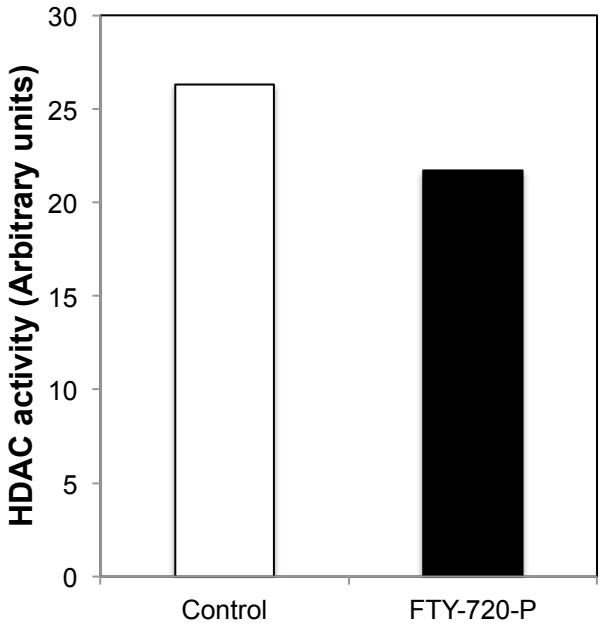
HDAC activity (Arbitrary units)
30
25
20
15
10
5
0
Control
FTY-720-P